



AN ABSTRACT OF THE DISSERTATION OF

Andrew J. Hummel for the degree of Doctor of Philosophy in Nuclear Engineering presented on December 6, 2013.

Title: Molybdenum-99 Production in the Oregon State TRIGA Reactor: Analysis of the Reactor Design using a new LEU Target as Fuel.

Abstract approved:

---

Todd S. Palmer

The most widely used and versatile medical radioisotope today is technetium-99m. Roughly 30 million people depend on this radioisotope for diagnostic procedures each year, and this demand is expected to grow.

Although there are numerous ways of procuring this isotope, the most common and most practical, for reasons to be stated later, comes from fission product molybdenum. Molybdenum is produced in all nuclear reactors as a fission fragment with a yield of around 6.1%. Molybdenum-99 has a half-life of just over 2.5 days, and it will decay to Tc-99m 87% of the time.

In 1978, the Reduced Enrichment for Research Test Reactors (RERTR) program was established at Argonne National Laboratory to investigate technology that would aid in converting High Enriched Uranium (HEU) facilities to use Low Enriched Uranium (LEU) fuel. Since the majority of all Mo-99 produced currently comes from the irradiation of HEU fuel targets, there has been a growing effort to design LEU targets that can yield comparable quantities of high Specific Activity (SA) Mo-99. Approximately three years ago the Oregon State TRIGA Reactor (OSTR) switched from HEU to LEU fuel elements in compliance with the RERTR program, and recently, a novel LEU target design has been developed for use in TRIGA reactors for production of Mo-99. Preliminary analysis has already been carried out with targets replacing several fuel elements, and it does not appear to negatively affect the reactor behavior.

The current supply capability of Tc-99m cannot keep pace with the growing demand. There are few, if any, new production facilities of Mo-99

slated for the future, and many of those presently operating will shutdown in the coming decades. Factoring in the time needed to license and construct new reactors, and the always pressing political and public wariness towards nuclear power, action must be taken immediately to ensure the future supply of this invaluable radioisotope. This research will analyze the viability of operating a low-power research reactor using the newly developed target design as the only source of fissile material. The normal TRIGA fuel will be offloaded and replaced with the new target elements for some optimal amount of time to produce molybdenum. After Mo-99 production reaches saturation, the normal fuel will be loaded back into the reactor, where normal operation can continue. MCNP5 will be the primary simulation tool used to analyze the behavior of the reactor and verify compliance with all safety limitations set forth in the OSTR Safety and Analysis Report as stated by the U.S. Nuclear Regulatory Commission

©Copyright by Andrew J. Hummel  
December 6, 2013  
All Rights Reserved

Molybdenum-99 Production in the Oregon State TRIGA Reactor: Analysis of the  
Reactor Design using a new LEU Target as Fuel

by  
Andrew J. Hummel

A DISSERTATION

submitted to

Oregon State University

in partial fulfillment of  
the requirements for the  
degree of

Doctor of Philosophy

Presented December 6, 2013

Commencement June 2014

Doctor of Philosophy dissertation of Andrew J. Hummel presented on December 6, 2013.

APPROVED:

---

Major Professor, representing Nuclear Engineering

---

Head of the Department of Nuclear Engineering and Radiation Health Physics

---

Dean of the Graduate School

I understand that my dissertation will become part of the permanent collection of Oregon State University libraries. My signature below authorizes release of my dissertation to any reader upon request.

---

Andrew J. Hummel, Author

## ACKNOWLEDGEMENTS

There have been many people who have helped me in one fashion or another as I have worked to complete my degree. Foremost, I could not have done this without the guidance and patience of my advisor, Dr. Todd Palmer. He has been instrumental in assisting me navigate through the program and has provided me with valuable help as I moved through this research. He is an extraordinary mentor as well as a friend. I would also like to thank my committee members for their time and support throughout this work.

There have been many students who have given me much needed assistance along this process. Topher Matthews and Jefferey Luitjens were constantly annoyed by my questioning, and I am truly thankful for their time and friendship. Jarvis Caffrey, Brian Gullekson, Kevin Makinson, Robert Schikler, and Rusty Williford were also eager to help when I needed it.

Finally, I would like to thank my family and parents, John and Marcia Hummel, for their never ending support throughout my educational career and life as a whole.

# TABLE OF CONTENTS

	PAGE
CHAPTER 1 INTRODUCTION .....	1
1.1 Motivation.....	1
1.2 Motivation and Present State of Mo-99 Production.....	4
1.3 Research Goal and Objectives .....	13
CHAPTER 2 BACKGROUND .....	16
2.1 Molybdenum-99 Production Techniques.....	16
2.1.1 Neutron Activation of Mo-98.....	16
2.1.2 Photoneutron Process .....	21
2.1.3 Photofission of U-238.....	22
2.1.4 Homogeneous Solution Reactors .....	23
2.1.5 Neutron Fission of U-235 .....	28
2.1.6 Other Production Methods .....	30
2.2 Target Designs .....	32
2.2.1 Uranium Foil Cylindrical Targets.....	36
2.2.2 Uranium Foil Plate Targets.....	44
2.2.3 Uranium Pin Targets.....	48
2.2.4 Other Fuel Materials .....	49

## Table of Contents (Continued)

	Page
2.3 Post Cintichem U.S. <sup>99</sup> Mo Production .....	51
CHAPTER 3 OREGON STATE TRIGA REACTOR AND LEU TARGET DESIGN .....	
3.1 OSTR.....	56
3.2 LEU Target .....	58
CHAPTER 4 REACTOR PHYSICS .....	
4.1 Reactivity Control.....	65
4.1.1 Excess Reactivity .....	65
4.1.2 Shutdown Margin .....	67
4.1.3 Rod Worth.....	68
4.2 Reactivity Coefficients.....	69
4.2.1 Prompt Temperature Coefficient of Reactivity .....	71
4.2.2 Moderator Temperature Coefficient of Reactivity .....	73
4.2.3 Void Coefficient of Reactivity .....	73
4.3 Delayed Neutron Fraction .....	74
4.4 Prompt-Neutron Lifetime .....	75
4.5 Approach to Criticality .....	75
4.6 Minimum Critical Heat Flux Ratio .....	76

## Table of Contents (Continued)

	Page
CHAPTER 5 METHODOLOGY .....	78
5.1    MCNP and Monte Carlo Methods.....	78
5.2    MCNP Input Deck .....	84
5.3    Specific Activity .....	87
5.4    Calculation of Parameters .....	89
CHAPTER 6 RESULTS.....	93
6.1    3-Ring Core .....	93
6.1.1    Power Profile and <sup>99</sup> Mo Production.....	94
6.2    4-Ring Core .....	98
6.2.1    Power Profile and <sup>99</sup> Mo Production.....	99
6.3    Reactor Physics Parameters .....	107
6.4    Minimum Critical Heat Flux Ratio .....	119
CHAPTER 7 DISCUSSION .....	122
CHAPTER 8 CONCLUSIONS AND Future Work.....	125
8.1    Conclusions.....	125
8.2    Recommendations for Future Work .....	125
BIBLIOGRAPHY .....	127

## LIST OF FIGURES

<u>Figure</u>	Page
Figure 2-1: Neutron fission of U-235. ....	28.
Figure 2-2: Mass distribution of fission products from U-235 thermal fission. ....	30.
Figure 3-1: Axial view of modeled target. ....	59.
Figure 3-2: Axial view of actual target. ....	59.
Figure 3-3: Target design specifications. ....	60.
Figure 3-4: Vertical section of OSTR. ....	61.
Figure 3-5: Horizontal section of OSTR. ....	61.
Figure 3-6: Axial view of OSTR core. ....	62.
Figure 4-1: Total rod worth, excess reactivity, and shutdown margin. ....	67.
Figure 4-2: Doppler broadening effect on self-shielding for $T_2 > T_1$ . (a) neutron flux in fuel, (b) resonance absorption cross section. ....	71.
Figure 6-1: Power profile for 3-ring core; no additional CRs. ....	93.
Figure 6-2: Power profile for 3-ring core; A1 FFCR. ....	94.
Figure 6-3: Power profile for 3-ring core; A1 AFCR. ....	94.
Figure 6-4: Power profile for 4-ring core; no additional CRs. ....	98.
Figure 6-5: Power profile for 4-ring core; A1 FFCR. ....	99.
Figure 6-6: Power profile for 4-ring core; A1 AFCR. ....	99.
Figure 6-7: Power profile for 4-ring core; A1, D12, D17 FFCRs. ....	100.

## List of Figures (Continued)

<u>Figure</u>	Page
Figure 6-8: Power profile for 4-ring core; A1, D12, D17 AFCRs.....	100.
Figure 6-9: Power profile for 4-ring core; A1, D12, D17, E4, E9 FFCRs. ....	101.
Figure 6-10: Power profile for 4-ring core; A1, D12, D17, E4, E9 AFCRs. ....	101.
Figure 6-11: Moderator COR for 3-ring cores. ....	108.
Figure 6-12: Moderator COR for 4-ring cores. ....	108.
Figure 6-13: Void COR as the void increases incrementally for the different 3-ring cores. ....	109.
Figure 6-14: Void COR as the total void increases for the different 3-ring cores.....	110.
Figure 6-15: Void COR as the void increases incrementally for the different 4-ring cores. ....	110.
Figure 6-16: Void COR as the total void increases for the different 4-ring cores.....	111.
Figure 6-17: Prompt fuel temperature COR for 3-ring cores (old library).....	115.
Figure 6-18: Prompt fuel temperature COR for 3-ring cores (new library).....	115.
Figure 6-19: Prompt fuel temperature COR for 4-ring cores (old library).....	116.
Figure 6-20: Prompt fuel temperature COR for 4-ring cores (new library).....	116.
Figure 6-2: Axial power distribution in target B3 of standard 3-ring core.....	121.

## LIST OF TABLES

<u>Table</u>	Page
Table 1.1 U.S research reactors capable of molybdenum-99 production .....	10
Table 1.2 Radionuclide production reactors.....	11
Table 1.3 Previous and projected US demand for nuclear medicine procedures ..	59
Table 2.1 Fission and activation produced Mo-99 criteria.....	115
Table 2.2 Molybdenum isotope data.....	59
Table 2.3 Photoneutron Mo-99 production quantities .....	22
Table 2.4 Solution fuel characteristics .....	25
Table 2.5 Comparison of LEU and HEU targets .....	35
Table 2.6 Characteristics of the LEU foil targets irradiated in the RSG-GAS reactor .....	39
Table 3.1 Target specifications .....	58
Table 5.1 Molybdenum isotopes present in irradiated targets .....	87
Table 6.1 Molybdenum-99 production (Ci) per pin in different 3-ring cores after five days irradiation .....	95
Table 6.2 Molybdenum-99 production in different 3-ring cores.....	96
Table 6.3 Molybdenum-99 production (Ci) in different 4-ring cores after 5 days irradiation.....	102
Table 6.4 Molybdenum-99 production in different 4-ring cores.....	104
Table 6.5 Delayed neutron fraction, mean neutron lifetime, moderator COR and void COR for different cores.....	106

## List of Tables (Continued)

<u>Table</u>	Page
Table 6.6 Prompt fuel temperature COR ( $(\Delta k/k)/^{\circ}\text{C}$ ) using old nuclear library .....	113
Table 6.7 Prompt fuel temperature COR ( $(\Delta k/k)/^{\circ}\text{C}$ ) using new nuclear library .....	114
Table 6.8 Total rod worth, excess reactivity, and shutdown margin .....	117

# **MOLYBDENUM-99 PRODUCTION IN THE OREGON STATE TRIGA REACTOR: ANALYSIS OF THE REACTOR DESIGN USING A NEW LEU TARGET AS FUEL**

## **CHAPTER 1 INTRODUCTION**

### **1.1 Motivation**

The most widely used and versatile medical radioisotope today is technetium-99m. With approximately 30 million people dependent on this radioisotope each year for diagnostic treatments, it accounts for more than 80% of all diagnostic nuclear medicine procedures in the world (IAEA-TECDOC-1065 1999). Tc-99m is the meta-stable daughter radionuclide of molybdenum-99, a fission product produced in all nuclear reactors. In the late 1950s, Brookhaven National Lab developed the first Tc-99m generators using Mo-99 (Banerjee, Pillai and Ramamoorthy 2001). The decision in 1958 to not patent their Mo-99/Tc-99m generator technology undoubtedly increased interest and research into technetium and its chemistry. Over the decades since, a wide

range of uses for this radioisotope have been discovered, making Mo-99 a radionuclide in high demand.

There are multiple ways of producing Mo-99, and hence obtaining Tc-99m, but the most practical approach with current technology comes from nuclear reactors. When uranium-235 fissions after interaction with a thermal neutron, Mo-99 is produced with a yield of around 6.1% (Baum, Knox and Miller 2002). A chemical separation process will extract the Mo-99 which can then be used to form a Tc-99m generator. Most all Mo-99 produced comes from the fission of Highly Enriched Uranium (HEU) targets. These targets typically contain around 93% U-235, and they yield Mo-99 with a high specific activity (radioactivity per unit mass) (IAEA-TECDOC-1065 1999). With the establishment of the Reduced Enrichment for Research Test Reactors (RERTR) program at Argonne National Laboratory (ANL), focus has shifted away from HEU targets towards Low Enriched Uranium (LEU) targets. The major reason for this switch is concern over the proliferation risk of the HEU material. The

amount of U-235 in LEU fuel is less than 20%, and this means that new targets, operated in the same reactor environment, will require roughly five times as much uranium in order to produce comparable amounts of Mo-99 (IAEA-TECDOC-1065 1999). This enrichment limitation could be cause for concern, but the Mo-99 production community simply cannot meet the expected demand with the current infrastructure. Currently, there is a major shortage in the production of radionuclides for medical purposes, and the Association of Imaging Producers and Equipment Suppliers (AIPES) predicts a 1.5-2.5% rate of growth in demand over the next ten years (Verbeek 2008). The motivation behind this research ultimately stems from this inability to meet the current and expected future demand of medical radioisotopes (specifically Tc-99m) while shifting away from HEU technology. A novel LEU target design has been recently developed, and this research will analyze the viability of operating a low power research reactor using the newly developed targets as the sole source of fissile material, although some control rods are followed with  $\text{UZrH}_{1.6}$  LEU fuel.

## 1.2 Motivation and Present State of Mo-99 Production

There are roughly 250 research reactors worldwide, but only five operate on an industrial scale for medically-produced radionuclides (Verbeek 2008). These include, along with their respective processing facilities, the National Research Universal (NRU) reactor in Canada (MDS-Nordion), the High Flux Reactor (HFR) in the Netherlands (Mallinckrodt), the Belgium Reactor 2 (BR2) in Mol (IRE), the OSIRIS reactor in France (IRE), and the South African Fundamental Atomic Research Installation-I (SAFARI) reactor in South Africa (NTP), and they account for over 90% of the production of Mo-99 (European Nuclear Society 2009). However, all five are approaching 50 years of operation, and temporary outages have caused supply problems in the past (Marck, Koning and Charlton 2010). Corrosion in the primary cooling system caused the HFR, which supplies between 30 and 40% of the world market, to shutdown in August 2008 according to the AIPES report.

Coincidentally, the National Institute for Radioelements (IRE) facility in Belgium ceased operation the next month because of an I-131 release. The IRE is the second largest Mo-99 processing facility in the world. Even the NRU had an unexpected safety-related shutdown for a month in 2007 (NAS 2009).

Unplanned shutdowns such as these put huge strains on the medical isotope market. In fact, leading experts believe that in order to ensure an

uninterrupted Mo-99 supply to accommodate 100% of demand, a redundancy in production capability of 250% is needed (Verbeek 2008).

Regardless of the impact of unforeseeable reactor shutdowns, many of these reactors are reaching the end of their operational lives. The Studsvik reactor in Sweden closed in July of 2005, the SILOE reactor in France in 1997, and the FRJ-II reactor in Germany stopped operating in May of 2006 (D. M. Lewis 2009, Verbeek 2008). Together these reactors produced approximately 5-10% of the world's medical radioisotopes. Additionally, the OSIRIS reactor plans to stop operation by 2015, the HFR around 2020, and the BR2 reactor has a decommissioning date in 2025. One 2008 study claimed that, "technical and licensing requirements will lead to the decommissioning of most of the production reactors within the next ten years" (Verbeek 2008). There are also very few new reactors slated for construction. Originally, the MAPLE I & II reactors were to be built at Chalk River Laboratories in Canada for the sole purpose of medical isotope production along with a New Processing Facility (NPF) to handle the irradiated targets. In June 2003, a positive coefficient of reactivity was observed in MAPLE I, and this ultimately halted operation (NAS 2009). The underlying cause could not be determined, and construction stopped in 2008. Operating just one of these reactors at its designed capacity would have yielded enough Mo-99 to almost equal the world-wide demand

(NAS 2009). With the announcement of the cancelation of these two reactors, Atomic Energy of Canada, Ltd. (AECL) sought a 5 year license extension for the NRU. There are currently 7 new research reactors around the world under construction, but none of these, or those presently operating, are dedicated to medical isotope production 100% of the time (D. M. Lewis 2009). France's Jules Horowitz Reactor (JHR), to be built in Cadarache, is the only reactor under construction whose sole purpose will be isotope production. This 100 MW pool-type reactor will start up with 27% enriched  $U_3Si_2$  fuel and then switch to a UMo fuel solution that is currently under development (CEA 2009). The goal is to commission the reactor by 2014. The Pallas reactor to be built at Petten in the Netherlands will replace the HFR, but construction is not yet underway. However, the licensing procedure for Pallas has proceeded with few hurdles, and the goal is to have it operational by 2020 (Van der Schaaf and De Jong 2010).

The United States has no reactors dedicated to Mo-99 production or any processing facilities to recover the radioisotope, and constitutes 50% of the market demand (Mirzadeh, et al. 1992, Verbeek 2008). Although Mo-99 production is an international business, one European study rightly proclaims that because "more than 50% decays away every 3 days...the responsibility for efficient and secure supply is more local, so in the case of Europe, the

responsibility is European,” and in the U.S. the responsibility is likewise our own (Alberman, et al. 2011). The two primary sources of the U.S. supply come from NRU and HFR, and all of the Mo-99 currently comes from irradiating HEU targets (NAS 2009). The Energy Policy Act (EPA) of 1992 aimed to cease the export of HEU targets by the U.S. in an attempt to reduce non-proliferation, but due to the drastic shortage of medical radioisotopes, the EPA of 2005 was passed to possibly alleviate some of these restrictions.

Section 630 states that,

“The Commission may issue a license authorizing the export (including shipment to and use at intermediate and ultimate consignees specified in the license) to a recipient country of highly enriched uranium for medical isotope production if, in addition to any other requirements of this Act (except subsection a.), the Commission determines that a recipient country that supplies an assurance letter to the United States Government in connection with the consideration by the Commission of the export license application has informed the United States Government that any intermediate consignees and the ultimate consignee specified in the application are required to use the highly enriched uranium solely to produce medical isotopes; and (B) the highly enriched uranium for medical isotope production will be irradiated only in a reactor in a recipient country that— (i) uses an alternative nuclear reactor fuel; or (ii) is the subject of an agreement with the United States Government to convert to an alternative nuclear reactor fuel when alternative nuclear reactor fuel can be used in the reactor.”

Although this act allows for the export of HEU targets under specific circumstances, the American Medical Isotopes Production Act of 2011 states that, “effective 7 years after the date of enactment of the AMIPA Act of 2011, the Commission may not issue a license for the export of highly enriched

uranium from the United States for the purposes of medical isotope production.” This act does contain waivers depending on the market demand and availability of Mo-99, but the shift towards LEU is inevitable. President Barack Obama chaired a United Nations Security Council (UNSC) meeting in 2009 in which Resolution 1887 was passed and states that all States should,

“Manage responsibly and minimize to the greatest extent that is technically and economically feasible the use of highly enriched uranium for civilian purposes, including by working to convert research reactors and radioisotope production processes to the use of low enriched uranium fuels and targets.”

The FDA has already announced that they approve the production of technetium-99m from LEU fission product Mo-99 at Mallinckrodt (which only recently split from its parent company Covidien), and NTP will provide the irradiated targets (Van Sonnenberg 2011).

The U.S. will eventually need to obtain some level of independence from foreign markets. Prior to its shutdown in 1989 due to tritium contamination, Cintichem, Inc produced Mo-99 at its 5 MW reactor in New York (NAS 2009). DOE purchased the technology rights in 1991, yet for various reasons they were never able to successfully integrate the technology into a reactor. The High Flux Isotope Reactor (HFIR) at Oak Ridge National Laboratory (ORNL), the Advanced Test Reactor (ATR) at Idaho National Laboratory (INL), and the Fast Flux Test Facility (FFTF) at the Westinghouse Hanford

Company all produce, or have had the capability to produce, medical radioisotopes. As of 2009, Babcock & Wilcox and the Missouri University Research Reactor (MURR) were the only two U.S. organizations trying to produce Mo-99 using LEU targets, and according to the NAS report, neither had obtained the financial support. The most reliable figure for the global supply and demand of Mo-99 amounted to 12,000 six-day curies per week in 2006, and the United States accounted for nearly half the demand (NNSA and ANSTO 2007). Table 1.1 gives an overall description of different U.S. reactors that could possibly be exploited for isotope production including several university research reactors, Table 1.2 has design criteria for those reactors currently contributing to the world market, and Table 1.3 gives information related to past and projected (the data comes from 2008) nuclear medicine procedures in the U.S.

Even if new reactors are built or old reactors are converted to become strict radioisotope producers, factors such as transportation and chemical processing of the targets must be taken into consideration. Aside from the National Institute for Radioelements (IRE), the major production companies include MDS Nordion in Canada, Covidien in the Netherlands, NTP in South Africa, and ANSTO in Australia. For the U.S. to become a market provider, it

**Table 1.1 US research reactors capable of molybdenum-99 production**

Reactor	Type	Operating Power	Maximum Total Flux (n/cm <sup>2</sup> /sec)	Moderator	Coolant	Fuel Type
ATR	PWR	250	1.4x10 <sup>15</sup>	H <sub>2</sub> O	H <sub>2</sub> O	UAl <sub>x</sub>
FFTF	FR	450	7.8x10 <sup>15</sup>	-	Sodium	PuO <sub>2</sub> -UO <sub>2</sub>
HFIR	PWR	85	2.5x10 <sup>15</sup>	H <sub>2</sub> O	H <sub>2</sub> O	U <sub>3</sub> O <sub>8</sub> -Al
MITR-II <sup>a</sup>	LWR	5	~1x10 <sup>14</sup>	D <sub>2</sub> O/ H <sub>2</sub> O	H <sub>2</sub> O	UAl <sub>x</sub>
MURR1 <sup>b</sup>	PWR	10	4.0x10 <sup>14</sup>	H <sub>2</sub> O	H <sub>2</sub> O	UAl <sub>x</sub>
OSTR	LWR	1	3.4x10 <sup>13</sup>	H <sub>2</sub> O	H <sub>2</sub> O	UZrH <sub>1.6</sub>

<sup>a)</sup> Massachusetts Institute of Technology Research Reactor – II

<sup>b)</sup> University of Missouri Research Reactor 1

would realistically need a processing facility within its borders. The logistics alone further limit the scope of producing medical radionuclides and the FDA approval process can be daunting. One enormous benefit to this research is that the design of the OSTR is already licensed by the U.S. Nuclear Regulatory Commission (U.S. NRC). Finally, the NAS study in 2009 claims, “To the committee’s knowledge, none of the major producers are doing much actual work on LEU targets and process...The committee views this as a missed opportunity.” This further validates the need for this and other research related to medical isotope production, particularly molybdenum-99.

The next section states the objectives of this research, and Chapter 2 contains a review of all the relevant literature. Different molybdenum production techniques are examined in Chapter 2.1 followed by a comparison of LEU target designs in Chapter 2.2. The chapter concludes with an overview of two similar analysis conducted at both Sandia National Laboratory and the University of Missouri. A description of the OSTR is given in Chapter 3, and Chapter 4 reviews the reactor physics parameters that must ultimately be analyzed in order to properly characterize a reactor design. The methodology used to carry out this work is presented in Chapter 5. The results are provided in Chapter 6. A discussion follows in Chapter 7 with a conclusion in Chapter 8.

**Table 1.2 Radionuclide production reactors.**

Reactor	Thermal Power (MW)	Thermal Flux (n/cm <sup>2</sup> /s)	Fuel	Operational Age (years)	Nominal Operating Days/Year
BR2	100	1x10 <sup>15</sup>	93% HEU	47	120
NRU	135	4x10 <sup>15</sup>	20% LEU	51	270
OSIRIS	70	2x10 <sup>14</sup>	20% LEU	42	180
HFR	45	2x10 <sup>14</sup>	20% LEU	47	270
SAFARI-1	20	2.4x10 <sup>14</sup>	20% LEU <sup>a</sup>	43	310
OPAL	20	3.0x10 <sup>14</sup>	20% LEU	2	?
LVR-15	10	1.5x10 <sup>14</sup>	36% HEU	51	200
FRM-II	20	8x10 <sup>14</sup>	93% HEU	4	250
HANARO	30	4.5x10 <sup>14</sup>	?	13	?
MARIA	30	4.5x10 <sup>14</sup>	36-80 % HEU	34	280
RA-3	5-10	1x10 <sup>14</sup>	20% LEU	40	230
RJH <sup>b</sup>	100	6x10 <sup>14</sup>	20% LEU	-	250
RBM <sup>c</sup>	30	?	< 20% LEU	?	?
TRR	5	1x10 <sup>13</sup>	20% LEU	?	7 day cycles

<sup>a)</sup> Conversion currently underway

<sup>b)</sup> Under construction

<sup>c)</sup> Currently in the conceptual design phase

Source: 2008 AIPES study

**Table 1.3 Previous and projected US demand for nuclear medicine procedures**

Year	Total Nuclear Medicine Procedure (millions)	Annual Growth Rate of Nuclear Medicine Procedures (%)	Total Tc-99m procedures (millions)	Tc-99m Procedures as % of Nuclear Medicine Procedures	Annual Growth Rate of Tc-99m Procedures (%)	Total Tc-99m Doses Utilized (millions)	Annual Growth Rate of Tc-99m Dose Utilization (%)
2002	14.1	6.7	10.2	72.2	5.4	17.7	8.7
2003	15.3	8.3	10.7	70.0	5.0	19.1	8.0
2004	16.1	5.4	11.1	68.6	3.2	20.2	5.9
2005	16.9	4.7	11.3	66.8	2.0	21.1	4.6
2006	17.7	4.7	11.7	66.0	3.5	22.1	4.5
2007	18.7	5.8	12.1	64.5	3.4	23.0	4.0
2008	19.8	6.0	12.6	63.5	4.4	24.3	5.5
2009	21.1	6.4	13.2	62.7	5.0	25.7	6.1
2010	22.4	6.1	13.8	61.5	4.2	27.1	5.3
2011	23.8	6.3	14.3	60.2	3.9	28.5	5.1
2012	25.3	6.3	14.9	59.1	4.3	30.0	5.2

Source: (Bio-Tech Systems, Inc. 2006)

### 1.3 Research Goal and Objectives

The supply for the world's most widespread and versatile radiopharmaceutical, technetium-99, does not meet the current demand.

Future projections only see this demand growing, and with current production facilities approaching the end of their engineered lifetimes, they simply cannot be relied upon to continue their current contributions to the market. This

coupled with the fact that the U.S. produces no molybdenum-99, yet consumes roughly 50% of the market, highlights the need to examine possible solutions.

The research goals are: 1) demonstrate that a small, low power research reactor such as the OSTR can produce significant quantities of the isotope molybdenum-99 and 2) perform the necessary analysis to demonstrate that such a reactor can operate safely. Attaining these goals would demonstrate a possible solution for alleviating the U.S. dependence on foreign markets; allow the U.S. to become a contributor to the global market, primarily during times of shortages; and ultimately make the most sought after radio-pharmaceutical more readily available and cheaper to those individuals who depend on it. To accomplish these goals, multiple objectives must be met, including:

- A) Examine different loading strategies in the core and their respective operating limitations.
- B) Determine the operating power, irradiation time, and cooling time for the viable core configurations.
- C) Calculate the necessary reactor physics parameters to verify the safe operation of the different core designs. These include prompt temperature, moderator, and void coefficients of reactivity, prompt neutron lifetime, delayed neutron fraction, shutdown margin, excess reactivity, and the total and integral control rod worths.

D) Show that this endeavor is worthwhile from an economic standpoint using the most up-to-date market prices.

## CHAPTER 2

### BACKGROUND

This chapter reviews all the relevant literature and background information surrounding this area. The primary aspects include Mo-99 production techniques and LEU and HEU target designs. This chapter concludes with an examination of Mo-99 production in the U.S.

#### 2.1 Molybdenum-99 Production Techniques

The most common process to produce Mo-99 is to fission HEU targets, primarily because the resulting Mo-99 is of high Specific Activity (SA). Other methods do exist, but they generally yield low SA Mo-99. These other methods will be reviewed first.

##### 2.1.1 *Neutron Activation of Mo-98*

The benefits of producing Mo-99 from activation rather than fission lie in the costs and associated wastes, but these are greatly outweighed by the small Specific Activity (SA) of the Mo-99 product. When Segre and Perrier bombarded molybdenum targets with deuterons in 1937 at the Berkeley cyclotron, the low SA made it very difficult to single out technetium (Cacciapuoti 1939). It is also possible to produce Mo-99 from bombarding natural molybdenum with neutrons, protons, and gammas, although neutron

bombardment is by far the most common method. Table 2.1 summarizes aspects of this activation method compared to fission-produced Mo-99. Activation molybdenum only becomes practically viable in countries with limited resources and without a well established nuclear infrastructure. For example, the IEA-R1 reactor at the IPEN-CNEN/SP processing facility in Brazil produced activation Mo-99 to meet the demand of the local market, but the last decade has seen a 10 % increase in demand per year (Domingos, et al. 2011). This has lead IPEN-CNEN/SP to seek a new reactor design that will replace IEA-R1 and produce fission product Mo-99.

**Table 2.1 Fission and activation produced  $^{99}\text{Mo}$  criteria**

$^{235}\text{U}(\text{n},\text{f})^{99}\text{Mo}$	$^{98}\text{Mo}(\text{n},\gamma)^{99}\text{Mo}$
High SA $^{99}\text{Mo}$	Low SA $^{99}\text{Mo}$
LEU targets require ~ 5 times more uranium than HEU targets	Highly enriched $^{98}\text{Mo}$ targets only yield ~ 4 times the SA from $^{\text{nat}}\text{Mo}$ targets
Chemical processing is complex	Chemical processing is simple
Need dedicated processing facility	Need high neutron flux source
Creates high-level waste	Creates minimal waste

**Source: (NAS 2009).**

Analytical reagent grade molybdenum trioxide ( $\text{MoO}_3$ ) is the most common target for direct neutron activation, and natural molybdenum is typically used instead of enriched Mo-98 targets due to the relatively meager increase in SA that enriched targets provide (Hetherington and Boyd 1999).

Of the seven stable isotopes of natural molybdenum, only three radioisotopes are produced from neutron activation. Due to the short half-lives and low yields of Mo-93 and Mo-101, they contribute very minimally to the overall impurities. However, Re, Sb, Cs, Co, Zn, Zr, Ag, and Ir may be present in the MoO<sub>3</sub> and lead to other activated nuclide impurities (Mirzadeh, et al. 1992). Table 2.2 gives information on the different reactions of the molybdenum isotopes.

**Table 2.2 Molybdenum isotope data**

Isotope	Thermal Cross Section (barns)	% Natural Abundance	Product	Half-Life
Mo-92	$2 \times 10^{-7}$	14.84	Mo-93m	6.9 hrs
Mo-92	0.06	14.84	Mo-93	$3.5 \times 10^3$ yrs
Mo-98	0.13	24.13	Mo-99	65 hrs
Mo-100	0.19	9.63	Mo-101	0.25 hrs

The microscopic thermal fission cross-section of U-235 is 585 barns with a corresponding Mo-99 yield of 6.1 % (Baum, Knox and Miller 2002). This amounts to a Mo-99 production cross-section of roughly 35 barns. This is 250 times greater than the thermal neutron capture cross section of Mo-98. Using the density of UZrH<sub>1.6</sub> fuel currently in the OSTR with an atomic enrichment of 19.75 % U-235, a simple comparison shows that for constant target volumes, the probability of interaction per distance traveled by a neutron is about 45

times greater for fission product Mo-99 from this LEU fuel than that produced from neutron activation of a natural molybdenum target.

$$\begin{aligned} & \frac{7.18 \text{g UZrH}_{1.6}}{\text{cm}^3} * \frac{1 \text{ mol UZrH}_{1.6}}{(.1975*235+.8025*238+91.224+1.6*1.0079)\text{g UZrH}_{1.6}} * \\ & \frac{6.022*10^{23} \text{ molecules UZrH}_{1.6}}{1 \text{ mol UZrH}_{1.6}} * \frac{.1975 \text{ atoms } ^{235}\text{U}}{1 \text{ molecule UZrH}_{1.6}} * \frac{585*10^{-24} \text{cm}^2}{\text{atom } ^{235}\text{U}} * 0.061 \\ & = 0.0923 \text{ cm}^{-1} \end{aligned} \quad (1)$$

$$\begin{aligned} & \frac{10.22 \text{g } ^{\text{nat}}\text{Mo}}{\text{cm}^3} * \frac{1 \text{ mol } ^{\text{nat}}\text{Mo}}{95.94 \text{g } ^{\text{nat}}\text{Mo}} * \frac{6.022*10^{23} \text{ atoms } ^{\text{nat}}\text{Mo}}{1 \text{ mol } ^{\text{nat}}\text{Mo}} * \frac{.2416 \text{ atoms } ^{98}\text{Mo}}{1 \text{ atom } ^{\text{nat}}\text{Mo}} * \\ & \frac{.13*10^{-24} \text{cm}^2}{\text{atom } ^{98}\text{Mo}} = 0.002012 \text{ cm}^{-1} \end{aligned} \quad (2)$$

The activation process can only yield large amounts of Mo-99 when the flux in the reactor is high enough to offset the low cross-section and the targets consist of enriched Mo-98. The NRU and HFIR reactors have fluxes on the order of  $10^{14}$  and  $10^{15}$  neutrons/cm<sup>2</sup>/s respectively, which would allow for competitive production quantities (NAS 2009). Still, fission product molybdenum has a SA roughly two to four orders of magnitude greater than that produced from neutron activation (Ottinger and Collins 1996). Other concerns include the separation process and generator technology. The technetium generator column would have to be bigger, and the liquid elution volume would need to be four to twenty times greater than for fission product

Mo-99 (TRIUMF 2008). This would lead to larger generators with shorter lifetimes since the elution of Tc-99m also releases Mo-99, and this concentration, proportional to both Mo-99 and Mo-98, must remain below a particular level. Elution is the process by which a liquid or gas is passed through a chromatography column (Harris 2007). One optimization study performed by Argonne National Laboratory (ANL) found that fission produced Mo-99 using LEU targets yielded molybdenum with a SA nearly  $10^6$  greater than that produced from neutron capture of natural MoO<sub>3</sub> targets (Mo 1993). Like most all neutron-induced reactions, the  $^{98}\text{Mo}(n,\gamma)^{99}\text{Mo}$  reaction is highly dependent on the energy of the incident neutron. The average effective resonance capture cross-section for Mo-98 was found to be  $650 \pm 30$  mbarns (Salikhbaev, et al. 2011). Samples of natural and enriched MoO<sub>3</sub> targets were irradiated in the WWR-SM research reactor in Uzbekistan and it was found that the resonance absorption accounted for nearly 70 % and 60 % of the activated Mo-98, respectively. This results because unlike neutrons in the epithermal energy range (1.0 eV to 0.1 MeV) most of the thermal neutrons interact in competing reactions with Mo-95 or Mo-97. The potential does exist to increase the SA associated with the activation of Mo-98 targets, but it was not noted in this study how one would attempt to take advantage of these neutrons.

### *2.1.2 Photoneutron Process*

Using a high energy electron accelerator, Mo-99 can be generated via the reaction  $^{100}\text{Mo}(\gamma, n)^{99}\text{Mo}$ . A converter target with a high Z such as liquid mercury or tungsten will emit bremsstrahlung as the electrons interact and lose energy in the targets (TRIUMF 2008). This bremsstrahlung radiation results because all charged particles will radiate energy when accelerated, even though these radiative losses typically only represent a small fraction of the total energy loss associated with ionization and excitation (Knoll 2000). These high energy photons can then interact with a Mo-100 target located behind the converter. Table 2.3 is adapted from the 2008 TRIUMF report and shows the estimated amounts of Mo-99 produced using a 50 MeV electron beam operating at 100 kW. Using this data, a 30 gram target subjected to a 500 kW accelerator would produce 640 six-day curies, enough to meet the current Canadian radioisotope demand (TRIUMF 2008). A six-day curie refers to the amount of radioactivity that will exist six days after the isotope has left the producer's facility, and this amount determines the Mo-99 price (NAS 2009). Like activation Mo-99, there would be a very minimal amount of waste developed and the scalability of the process is very flexible. However, the generator technology would still need to be changed, and manufacturing costs

would be relatively high due to the low percentage of Mo-100 in natural molybdenum, less than 10% (Baum, Knox and Miller 2002).

**Table 2.3 Photoneutron  $^{99}\text{Mo}$  production quantities**

Grams of Mo-100 in target	Ci/100 kW at saturation	SA (Ci Mo-99/g of Mo)	Power deposited in target (kW)
0.29	100	360	2.2
1.0	210	208	4.8
2.3	300	147	11.4
9.1	518	57	16.4
70.6	900	12.8	29

### 2.1.3 *Photofission of U-238*

A high energy photon on the order of 10 MeV could also be used to fission natural or depleted uranium targets. The reaction  $^{238}\text{U}(\gamma, f)^{99}\text{Mo}$  has a cross section similar to the photo-neutron process, with a maximum obtained with a 13 MeV gamma, and a Mo-99 fission yield of about 6%, nearly identical to that from thermal fission of U-235 (NAS 2009). A 30 MeV electron beam operating at 100 kW incident on a high Z target will produce bremsstrahlung radiation that can fission uranium targets. An optimized U-238 target subjected to these conditions can yield about  $3 \times 10^{13}$  fissions/second (Diamond 1999). This amounts to almost a 60 % smaller yield than for an enriched U-235 target, but the cost would be much less and there would be fewer regulatory concerns. The uranium carbide targets consist of hundreds of grams of uranium and are large to reduce the power density. With saturation

occurring after 14 days of irradiation, 18 six-day curies can be achieved (TRIUMF 2008). To produce 500 six-day curies, an electron beam power of about 3 MW would be needed. Caldwell et al provide much data on the photofission and photoneutron reaction thresholds, cross-sections, and yields (Caldwell, et al. 1980). The main disadvantages to this process are the small cross-section which would require an extremely high intensity beam, larger target volumes means larger amounts of waste, and the technology is new with not all the elements proven. However, the advantages lie in the fact that current generator technology and processing techniques could be used, accelerators can be turned on and off when needed, and scalability is straightforward and easy.

#### ***2.1.4 Homogeneous Solution Reactors***

One of the more novel approaches for producing Mo-99 utilizes Aqueous Homogeneous Reactors (AHRs) fueled with a uranium salt solution. These reactors have been around since the 1940s, and roughly 30 have been built and operated to date. A shielded vessel contains enriched uranium that has been dissolved in water and acid, and thus there are no targets, eliminating fabrication costs. The standard method of operation is as follows: a flow rate delivers some part of the solution fuel to a sorption column where the Mo-99 is selectively recovered and then the solution is sent back to the main tank; all

the while water radiolysis forces fission product gases into the upper plenum where they can be selectively recovered; using the same technology from target processing, these isotopes are then purified (Baranaev, et al. 2008). Some advantages to these systems include: (1) flexibility of fuel selection and geometry, (2) inherent passive safety systems, (3) less uranium waste per curie of Mo-99 produced, (4) simpler waste processing, (5) ease of processing other radioisotopes such as  $^{131}\text{Xe}$ ,  $^{89}\text{Sr}$ ,  $^{90}\text{Y}$ , and  $^{131}\text{I}$  with off-gas extraction, and (6) a lower capital cost (IAEA-TECDOC-1601 2008).

**Table 2.4 Solution fuel characteristics**

Fuel	Thermal Stability	Radiation Stability	Solubility	Neutron Absorption x-section	Isotope Extraction	Fuel Solution Purification
UO <sub>2</sub> SO <sub>4</sub>	< 280°C	Good	Pu, Ba, Sr may be deposited	Small	Difficult	Difficult
UO <sub>2</sub> (NO <sub>3</sub> ) <sub>2</sub>	< 184°C	2.5 mL N <sub>2</sub> /kW/min	Good	Slightly Larger	Easy	Easy

**Source: (Maoliang, Zuoyong and Qimin 2008)**

Solution reactors have the added benefit of operating over a range of thermal powers ranging between 50 and 300 kW, allowing for a more precise control over the Mo-99 supply needed to meet the current demand. Fuel choice is typically uranyl sulphate, UO<sub>2</sub>SO<sub>4</sub>, or uranyl nitrate, UO<sub>2</sub>(NO<sub>3</sub>)<sub>2</sub>, the former being very stable under irradiation conditions but the latter having the benefit of a higher distribution coefficient of extraction, or greater Mo-99 yield (IAEA-TECDOC-1601 2008). Table 2.4 compares the characteristics of the two fuels. These reactors typically operate at around 80°C and a pressure less than one atm. As the uranium fissions, the temperature of the fuel solution will increase. This coupled with the generation of gas bubbles from radiolysis leads to a very large negative density coefficient of reactivity. During a reactivity transient, this effect along with, “a corresponding density redistribution within the expanding volume in which the introduction of an equivalent void volume displaces fuel from regions of higher reactivity worth to regions of lower reactivity worth,” causes the reactivity excursion to terminate (IAEA-

TECDOC-1601 2008). This passive safety mechanism is inherent for all AHRs. Also, the waste generated from solution reactors, uranium consumed, and heat generated amount to only 1/100th of that from fission product Mo-99 (Ball, Pavshook and Khvostionov 1998). Rather than having to continuously dispose of or recycle uranium from an irradiated target, uranium can stay in the solution reactor for almost twenty years. The operational cost of a homogeneous reactor has the potential to be much lower than a conventional research reactor. The fuel is the target in AHRs, and as it gets depleted more LEU must be added, but the initial base fuel load could remain in the reactor over its operational lifetime. Irradiated targets must be cooled, transported, and processed, but homogeneous reactor systems can simply pump the solution to the appropriate isotope separation instrument (IAEA-TECDOC-1601 2008).

There are, however, some key challenges for this technology. It is unknown whether a solution reactor can operate long term on an industrial scale for isotope production at steady state power. Isotope separation technology would need to accommodate the continual change in the solution chemistry and the buildup of fission products (IAEA-TECDOC-1601 2008). There will also be fission and radiolytic gases in the solution that must be properly handled, possible effects due to corrosion, and these reactors would be

subjected to the licensing process, for which no regulations currently exist (for solution reactors to produce radioisotopes).

The National Power Institute of China (NPIC) has developed one such medical isotope production reactor (MIPR) design that utilizes 90 % enriched  $\text{UO}_2(\text{NO}_3)_2$  fuel. This water boiler solution reactor would operate at a thermal power of 200 kW with a projected output of 500 Ci Mo-99 and 100 Ci 131I for each 24 hour irradiation period (Song and Niu 2008). The separation process developed by the NPIC can achieve a Mo-99 recovery yield over 65% (Zuoyong, C., et al. 2008). The 20 kW ARGUS reactor at the Kurchatov Institute has been operating since 1981 using a uranyl sulphate solution. A five-day operational demonstration to produce Mo-99 yielded 708 Ci (Pavshook 2008). This reactor has successfully demonstrated the production and separation of Mo-99 to the U. S. Food and Drug Administration's standards and purity requirements (Evans 2008). In the U. S., Dr. Russell Ball developed an AHR design for the production of medical isotopes in 1997 while at Babcock & Wilcox (BWX). The current concept for this Medical Isotope Production System (MIPS) includes a 200 kW reactor that operates with LEU fuel that will yield around 1,100 six-day Ci/week of Mo-99 (Evans 2008). BWX estimates it would take 5 to 6 years to construct the reactor, but the biggest hurdle will be obtaining a license because reactors operating solely to

produce medical isotopes would not qualify as ‘Research’ facilities under Class 104 Research licensing criteria. Again the technologies for AHRs are not all proven like those which fission solid targets to produce Mo-99, but it could be possible for solution reactors to operate at a power level almost 14 times less than conventional research reactors while using about 280 times less uranium (Glenn, Heger and Hladik III 1997).

### ***2.1.5 Neutron Fission of U-235***

All reactors fueled with U-235 will produce Mo-99. It was first discovered to be a fission fragment after uranium was bombarded with neutrons at the Berkeley cyclotron (Segre and Wu 1939). Figure 2.1 shows that as a thermal neutron strikes a U-235 atom, an average of 2.43 neutrons will result along with a variety of possible fission fragments. Figure 2.2 displays the majority of these fission fragments as a function of percent yield taken from the Evaluated Nuclear Data File (ENDF) compiled from Los Alamos National Lab (LANL) (England and Rider 1994). These fission fragments are formed as pairs, and depending on the number of neutrons emitted, Mo-99 is generally produced with some isotope of tin. Because nearly all of the 40 fission product pairs lead to characteristic decay chains from beta emission, over 200 radioactive fission products will exist in a nuclear reactor (E. E. Lewis 2008). As the energy of the incident neutron increases, so does

the probability of yielding products with equal masses, and the observed dip will tend to flatten out.

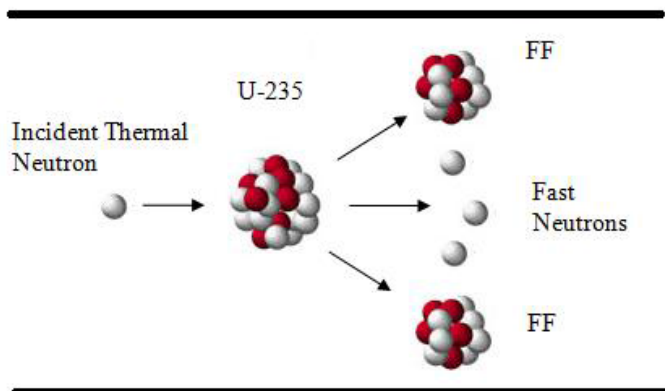


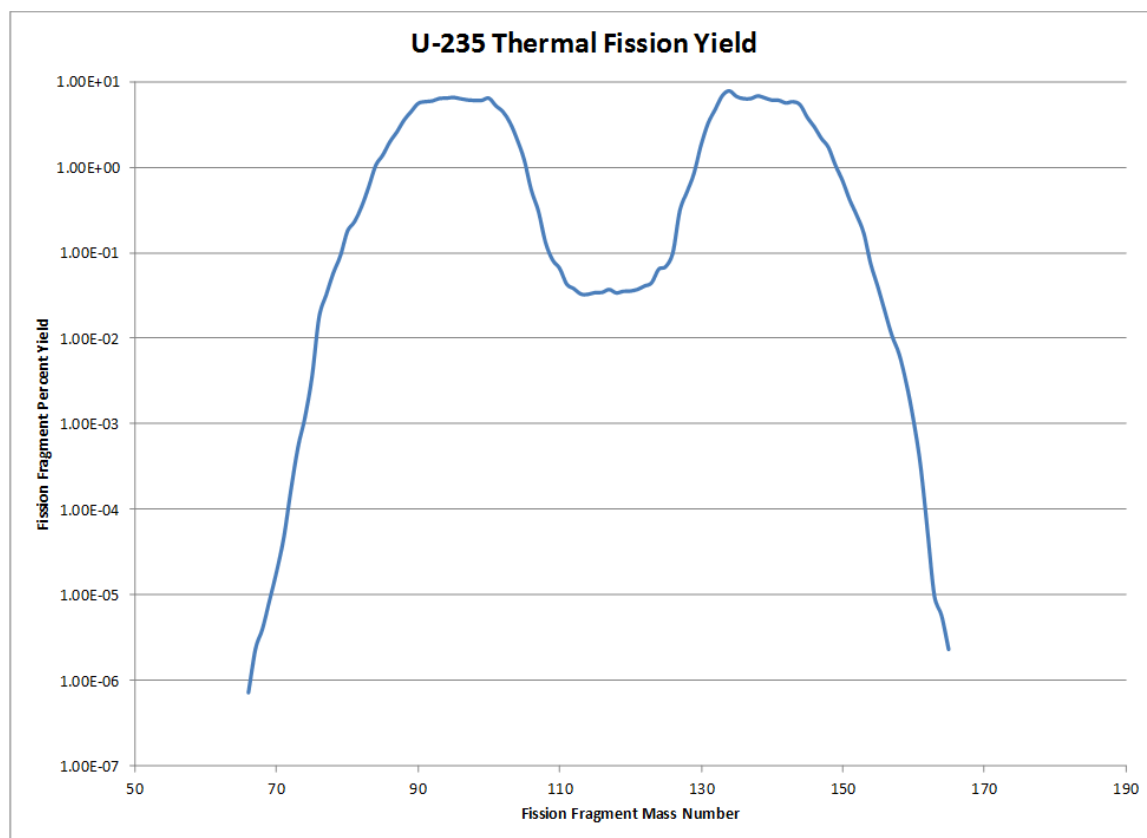
**Figure 2-1 Neutron fission of U-235**

There are many factors which must be considered when optimizing the production of Mo-99 in a reactor. The yield is a function of power level, flux distribution, target enrichment, irradiation time, energy of the incident neutron, target volume size, and position in the reactor. Other factors such as the thermal fission cross section of U-235 and the half-life of Mo-99 must also be taken into consideration. A study by the National Academy of Sciences in 2008 estimated that HEU targets are used to produce 95 to 98 % of the world's Mo-99. The transition to LEU targets will require a 5 to 6 fold increase in uranium to achieve comparable quantities of high SA Mo-99, but this will not affect the purity or yield. Other medical isotopes include the fission products I-131 and Xe-133, and fissioning U-235 produces these in equal

proportions to one other, and they can be recovered from both HEU and LEU targets (NAS 2009). Plutonium buildup will increase in the LEU targets, but this will not present a problem from a nonproliferation perspective due to the low burnup of U-235. After only about 3% burnup of U-235 is reached, the Mo-99 production saturates and the target would be removed (IAEA-TECDOC-515 1987). After irradiating the targets, they would need to be cooled for about one day.

### ***2.1.6 Other Production Methods***

Both Mo-99 and Tc-99m can be produced from other accelerator driven reactions, but the viability of these methods to yield sufficient quantities remains questionable. The most fitting reactions include  $^{100}\text{Mo} (p,pn) ^{99}\text{Mo}$ ,



$^{100}\text{Mo}$  (d,p2n)  $^{99}\text{Mo}$ ,  $^{100}\text{Mo}$  (p,2n)  $^{99\text{m}}\text{Tc}$ , and  $^{100}\text{Mo}$  (d,3n)  $^{99\text{m}}\text{Tc}$  (Takacs, et al. 2003). These researchers investigated these reactions because the prior work studying the nuclear data associated with these reactions does not have consistency. They found that the reaction  $^{100}\text{Mo}$  (p,pn)  $^{99}\text{Mo}$  could yield 3.86 mCi/ $\mu\text{Ah}$  (or 3.86 mCi per micro ampere hours of beam operation) when using a 100% enriched  $^{100}\text{Mo}$  target when the incident particle has an energy in the range of 11 to 40 MeV. The NAS study estimated that approximately 100 similar cyclotrons would be needed to meet the U. S. weekly demand. Additionally, Takacs et al. found that 20.6 mCi/ $\mu\text{Ah}$  could be produced from

a 100% enriched  $^{100}\text{Mo}$  target via the  $^{100}\text{Mo} (p,2n) ^{99\text{m}}\text{Tc}$  reaction given the incident particle energy lies in the range of 6 to 40 MeV. The most obvious problem associated with producing Tc-99m directly is that the short half-life would limit all aspects of the distribution chain. Thus, these methods are not deemed viable as possible substitutions for producing Mo-99, and the direct production route of Tc-99m is inherently problematic.

## 2.2 Target Designs

Fission product molybdenum can be produced with both HEU and LEU targets using uranium oxides, uranium metals, or a uranium alloy, typically with aluminum. These can exist in plate, pin, or cylindrical geometries. IAEA-TECDOC-515 sums up the three primary target geometries as: 1)  $\text{UO}_2$  or  $\text{UAl}_x$  film in between two stainless steel or aluminum cylinders, 2) a  $\text{UO}_2$  or U-Al alloy in stainless steel or aluminum clad rods, and 3) a uranium aluminum matrix sandwiched between two aluminum plates. Uranium metal targets boast several advantages over oxide targets in that they are more dense, they have a thermal conductivity an order of magnitude greater, and they can achieve a 100% plating efficiency compared to just 20% for  $\text{UO}_2$  (IAEA-TECDOC-515 1987). However, electrodepositing uranium metal on the inside walls of cylindrical targets requires high temperatures in an inert environment, and the resulting deposit morphology often branches. Work at Argonne

National Laboratory (ANL) in the 1980s showed that LEU uranium-oxide films can directly replace those using HEU, making the design and fabrication of new targets a relative non-issue. However, these LEU targets will probably not possess the necessary surface density of  $\text{UO}_2$  to yield comparable quantities of  $^{99}\text{Mo}$  (Vandegrift, Chaiko, et al. 1986). There is also the potential to use LEU uranium silicide fuels, namely  $\text{U}_3\text{Si}_2$  and  $\text{U}_3\text{Si}$ . The fabrication process proceeds in the same manner as current reactor fuels, making the licensing process much simpler. Work has been performed to develop targets that consist of uranium and  $\text{UO}_2$  dispersed in aluminum. One study carried out by CNEA in 2007 analyzed the production efficiency of HEU and LEU targets. The study compared the HEU targets used between 1998 and October 2002 to the LEU targets used from August 2002 to 2006 in the RA-3 reactor in Argentina (Cestau, Novello, et al., HEU and LEU Comparison in the Production of Molybdenum-99 2007). 103 HEU and 135 LEU batches from complete irradiation cycles were considered. The most productive batch from HEU targets in terms of specific activity produced was used as the standard. It was found that the latter three years using LEU targets proved to yield a greater production efficiency than this standard. Additionally, those years using LEU targets that did not achieve a similar efficiency can be attributed to the adaptation time of the LEU technology to large scale production.

Converting to LEU targets while maintaining similar  $^{99}\text{Mo}$  production yields can be achieved in three primary ways: 1) directly replace the HEU targets and simply increase the number of targets irradiated, 2) increase the target size and thereby the amount of U-235 in the target, or 3) change the composition of the target such as to increase the amount of U-235 (NAS 2009). An LEU target of the same geometry and uranium density would produce about 20% of the Mo-99 produced from an HEU target but would have almost identical chemical and physical properties. The disadvantage would be the associated waste with having more targets, and the reactor may have limited space for irradiation, which would also pose a problem and limitation on the target size. Thus, the most practical and popular solution has been to change the target composition. The main drawbacks of using LEU targets are the increase in irradiated-uranium by-product, the increase in chemicals and other processing equipment to extract the Mo-99, and the increase in cost and disposal due to the increase in plutonium and other transuranic elements (i.e. the waste would no longer be designated low-level but TRU) (Vandegrift, Chaiko, et al. 1986). Despite the additional by-products, there is no appreciable increase in gross alpha content in spent LEU targets, as was generally assumed, making the LEU fission product Mo-99 compliant with international requirements (Duran 2005). Table 2.5 lists general differences

between LEU and HEU targets. Although there is a shift away from HEU targets, three of the four large scale producers still use HEU while the fourth, NTP/SAFARI-I, is converting to LEU (IAEA 2010). The South African Nuclear Energy Cooperation (NECSA) reported that the SAFARI-I reactor had completed a full conversion to LEU fuel as of June 2009, and the NRU fully converted to LEU fuel in 1993 (NECSA 2009, Sears and Conlon 2006). The NAS study in 2009 claimed that LEU targets, “for large scale production of Mo-99 have been developed and demonstrated,” and they find, “no technical reasons that adequate quantities cannot be produced from LEU targets in the future (pg 2).” Thus, other producers slated for future construction will most likely have to operate with LEU, and many factors can dictate which type of target design to use. If a present infrastructure exists, the target fuel should be readily licensable and easily integrated into the system with little or no change in the core design. The fabrication cost of the targets, associated waste, and local <sup>99</sup>Mo demand will also influence the choice of fuel. From a safety standpoint, despite the target composition, all designs should have sufficient heat transfer properties to prevent overheating and ensure retention of fission fragments and gases. The following sections review the general target designs and the reactors that utilize them.

**Table 2.5 Comparison of LEU and HEU targets**

Target	HEU	LEU
<sup>235</sup> U enrichment (%)	93	19.75
<sup>235</sup> U (g)	15	18.5
Total U (g)	16.1	93.7
<sup>99</sup> Mo yield (Ci)	532	545
Total Mo (mg)	9.8	10.0
<sup>239</sup> Pu (μCi / mg)	30/0.44	720/12.0
<sup>234</sup> , <sup>235</sup> , <sup>238</sup> U (μCi)	1280	840
Total activity (μCi)	131	1560

Source (Vandegrift, Chaiko, et al. 1986)

### **2.2.1 Uranium Foil Cylindrical Targets**

Uranium foils can exist as either metals or oxides. A chemical process patented in the early 1970s showed that high purity, high SA Mo-99 could be extracted from uranium oxide foil targets, and the researchers further claimed this technique could be extended to uranium metal targets with little modification (Arino, Kramer, et al. 1974). Since the conversion to LEU requires a 5 to 6 fold increase in uranium content, uranium-metal targets have emerged as the most viable candidates due to their higher density. One of the first patents for uranium foil targets for production of Mo-99 was issued in 1976. The design consisted-, “of an enclosed, cylindrical, stainless steel vessel,

preferably having a thin, continuous, uniform layer of a fissionable material, integrally bonded to its inner walls” (Arino, Cosolito, et al. 1976). The uranium film is roughly one thousandth of an inch, amounting to roughly 20 milligrams per square centimeter for a total of 7 to 10 grams of uranium. The importance of binding the fissionable layer to the cylinders ensures good heat transfer properties. If the inner tube has a larger thermal expansion coefficient than the outer tube, it will increase the thermal contact between them (IAEA-TECDOC-1065 1999). Stainless steel cylinders were chosen in the patent design over aluminum cylinders due to the complexity associated with separating the uranium out of the aluminum matrix. This arises for two reasons. During irradiation diffusion bonding will occur between the uranium and the cylindrical tubes. Work done by Vandegrift et al showed that this bonding can be inhibited by spraying thin oxide layers on the inner and outer cylindrical tubes (Vandegrift, Snelgrove, et al. 1997). Using zirconium for the outer tube material and aluminum for the inner tube, zirconium and aluminum-oxides were sprayed on each one respectively. Metallography determined that the diffusion barrier prevented interaction of uranium with the zirconium, but the foil still could not be detached from the inner aluminum tube. Assuming the aluminum-oxide layer was insufficient, - researchers at ANL examined other oxides as well as other inner tube

materials such as magnesium and stainless steel. All of these materials except stainless steel have the added benefit of low absorption cross-sections. In the post-irradiation examination, the inner tubes could still not be separated from the uranium foil. Their explanation was that the high fission rate leads to high recoil atom fluxes, thus creating good atomic intermixing at the interface of the inner tube. The material or oxide used did not matter. Since the vast majority of thermal neutrons enter the targets from the outside moderator, the recoil atoms will tend toward the inner tube, making this a non-factor on the outer tube. However, advances in designs have since made this a relative non-issue. The same study proposed placing a 10-15  $\mu\text{m}$  metal barrier between the uranium foil and inner tube. The barrier thickness must be greater than the recoil range of the fission fragments, with the different candidate materials having a maximum range of  $\sim 7\mu\text{m}$  (Smaga, et al. 1997). An effective barrier should not inhibit the dissolution process, should not interfere with the molybdenum recovery or purity of Mo-99, should have a low thermal neutron absorption cross-section, and be readily manufactured into foils at low cost (Vandegrift, Snelgrove, et al. 1997). Therefore, copper, zinc, iron, and nickel were proposed as potential barrier materials. New post-irradiation tests using these produced mixed results but some combinations of materials did

demonstrate that it is possible to alleviate the atomic mixing and successfully remove the uranium foils from the inner tubes.

The above targets designed by ANL were all irradiated in the RSG-GAS reactor and processed in the Radioisotope and Radiopharmaceutical Production Centre at PUSPIPTEK in Serpong, Indonesia. This reactor was designed to accommodate the Cintichem process, which prior to 1989 generated almost half of the world's production of  $^{99}\text{Mo}$ . The original Cintichem targets consisted of stainless steel tubes coated with highly enriched  $\text{UO}_2$  (Vandegrift, Hofman, et al. 1999). With the onset of the RERTR program, the Indonesian National Nuclear Energy Agency (BATAN) collaborated with ANL to shift towards LEU targets. Using the experimental results described above, LEU targets using both nickel or zinc electroplated fission recoil barriers and LEU targets wrapped in Zn, Ni, and Al were irradiated in the RSG-GAS reactor. These newly designed LEU foil targets contained almost 30 grams of uranium-metal measuring  $\sim 130\mu\text{m}$  thick (Mutalib, et al. 1998). They are much shorter than the original targets and thus two LEU targets can be irradiated at the same time. The LEU target characteristics can be seen below. Mo-99 recovery yields were seen to be around 79 %, compared to about 65 % for the HEU  $\text{UO}_2$  targets and with

**Table 2.6 Characteristics of the LEU foil targets irradiated in the RSG-GAS reactor**

Target Number	Inner Wall <sup>a</sup>	Barrier Material	Barrier Thickness ( $\mu\text{m}$ )	Inner Tube Extractable	Foil Removed
1	304 SS	Zn foil	15	yes	yes
2	304 SS	Ni foil	15	yes	yes
3	304 SS	Zn plate	17 <sup>b</sup>	yes	yes
4	304 SS	Ni plate	11	yes	yes
5	304 SS	Al foil	23	yes	no
6	Al	Al foil	23	no	-
7	Zr	Zn foil	15	yes	yes
8	Zr	Zn foil	15	yes	no

<sup>a</sup>All outer cylinder walls were made of Zr.

<sup>b</sup>A greater thickness was observed with calipers, but this is common with plating.

Source (Mutalib, et al. 1998).

only moderate changes to the Cintichem process (Vandegrift, Hofman, et al. 1999).

Further analysis at ANL in 1999 focused on the development of an annular target design. The LEU metal foil would measure about 125-150  $\mu\text{m}$  thick and coolant could flow through the target, greatly increasing the heat transfer surface (Conner, et al. 1999). The end surface of the inner tube does not need to be as great since target disassembly does not require pushing. This allows for thinner tubes which leads to less fabrication costs, less neutron absorption in the tubes, and less overall waste. Both zirconium and aluminum tubes were irradiated in the RSG-GAS reactor with nickel or zinc as the fission-recoil barrier material. Zirconium tubes coated with either barrier

performed well as did the aluminum tubes coated with nickel. The aluminum tubes were preferred because the material is easier to work with than zirconium and cheaper (Conner, et al. 1999). With a moderating material at the center, annular designs such as this would require fission-barriers on both tubes. This study focused on the viability and durability of annular LEU targets under irradiation conditions, thus no information on  $^{99}\text{Mo}$  yield was given.

Reactors that operate with the cylindrical foil target design include the BR2 in Belgium and the Tajoura in Libya. The BR2 Materials Testing Reactor (MTR) began operation in 1963 and was updated between 1995 and 1997 to its current operating power of 100 MW<sup>th</sup> (Ponsard 2007). The original targets used at the BR2 facility had a uranium load of 0.5 grams, and this was later increased to 4 grams. The current design is an annular shape with U-Al metal sandwiched between two aluminum cylinders (Salacz 1985). The core is moderated with light water and beryllium. A total of 56 targets enriched to nearly 93 % can occupy the 6 irradiation devices (Ponsard 2007). Irradiating the targets for 150 hours in a thermal neutron flux of  $2.4 \times 10^{14}$  neutrons/cm<sup>2</sup>/s can yield up to 1000 Ci  $^{99}\text{Mo}$  / target, amounting to nearly 220 six day Ci (this does not take processing into account).

The Tajoura Reactor in Libya began operating in 1983 with 80 % enriched fuel. In 2006 the reactor completed conversion to a 19.7 % enriched  $\text{UO}_2$ -Al alloy containing 8 grams  $^{235}\text{U}$  clad in aluminum (Bsebsu, Abotweirat and Elwaer 2007). The uranium foil is covered with a nickel foil, and forced convection of water provides the moderation and cooling. The annular design consists of an aluminum plug at the center surrounded by the coolant, inner Al tube, Ni foil, U foil, Ni foil, outer Al tube, and coolant all within an Al irradiation cylinder. Thermal hydraulic analysis suggested an operating power of no more than 5 MW to remain under the necessary safety limits. With an irradiation time of 3 days under a thermal neutron flux of approximately  $10^{14}$  neutrons/cm<sup>2</sup>/s, an estimated 203 Ci  $^{99}\text{Mo}$  or 25 Ci  $^{99}\text{Mo}$  / g  $^{235}\text{U}$  can be produced (Bsebsu and Elwaer n.d.). Accounting for the molybdenum isotopes 97, 98, and 100, they calculate a SA of 199 Ci / mg Mo. The target under these conditions would generate 7.6 kW.

The Chilean Nuclear Energy Commission (CCHEN) operates the RECH-1 reactor at La Reina Nuclear Center. Chile, along with Libya and several other small countries, is a participant in the IAEA's Coordinated Research Project (CRP) which began in 2005 and aims to develop, "techniques for small scale, indigenous Mo-99 production using LEU fission or activation" (Bradley 2010). This 5 MW pool type reactor uses  $\text{U}_3\text{Si}_2$ -Al LEU fuel, and the

proposed target is again a 130 $\mu\text{m}$  thick LEU metallic uranium foil wrapped in a thin 15 $\mu\text{m}$  Ni foil that will be encased in two concentric Al cylinders (Medel and Torres n.d.). The reactor has thermal neutron fluxes on the order of  $8 \times 10^{13}$  and  $5 \times 10^{13}$  n/cm<sup>2</sup>/s at the two possible locations to be used for the targets. They analyzed a 13 gram LEU foil and found that after 48 hours irradiation time at the higher flux position, the maximum temperature in the target was too close to the safety limit, and it was subsequently deemed necessary to improve the cooling conditions. It was later found that the high temperature may have resulted from insufficient heat transfer due to an air gap between the inner Al tube and uranium foil (Schrader, et al. 2007). This was an unintentional result from the fabrication process, and if it cannot be improved the authors propose placing the target in a position in the reactor with a smaller flux. Both irradiation locations led to SA yields of roughly 116 Ci <sup>99</sup>Mo / mg Mo.

In order to reach large scale production levels of <sup>99</sup>Mo, the Korean Atomic Energy Research Institute (KAERI) has developed a new fabrication method for producing the needed LEU foils. This cooling-roll casting method can produce a wide continuous polycrystalline LEU foil ranging from 100 to 150  $\mu\text{m}$  thick (Kim, et al. 2004). The foils are 50 mm wide and over 5 m long in a single batch. This method alleviates the need for hot-rolling and a

subsequent heat-treatment and quenching, and the foils produced are of better quality. The NAS study defines hot rolling as rolling the metal after it has been heated above its recrystallization temperature and cold rolling as rolling the metal at room temperature. With standard hot or cold rolling techniques, only one side of the foil is in contact with the cooling roller making the other side rougher, and the direct-cast method developed at ANL can lead to gaps between the free side of the foil and the recoil barrier (Wienczek, et al. 2008). However, they do not believe the gap to be problematic.

### ***2.2.2 Uranium Foil Plate Targets***

The Ezeiza Atomic Centre in Argentina began producing  $^{99}\text{Mo}$  in 1985 from targets irradiated in the adjacent RA-3 reactor. The original targets were highly enriched U-Al mini-plates clad with aluminum (Cristini, et al. 2002). In 1990 the RA-3 core was converted to  $\text{U}_3\text{O}_8$  LEU fuel, and studies were subsequently carried out under the RERTR initiative to develop new LEU targets for molybdenum production (Adelfang, Alvarez and Pasqualini 2002). Since the core is designed for plate geometry fuel, the targets needed to be designed similarly to avoid licensing problems and to maintain similar fabrication procedures. In 2002 the RA-3 reactor became the first to produce  $^{99}\text{Mo}$  using solely LEU targets (CNEA November 4). These targets consist of a U-Al<sub>2</sub> compound dispersed in an Al matrix with approximately 3 g U / cc of

target surrounded in Al alloy clad (Kohut, et al. 2000). They are irradiated for approximately 108 hours in a neutron flux of approximately  $2 \times 10^{14}$  n/cm<sup>2</sup>/s (Cestau, Novello, et al. 2007). The target fabrication process is similar to that of LEU fuel plates. Uranium metal is melted in a furnace with powdered aluminum at a temperature  $\sim 1600$  °C. The resultant ingot then goes through a crushing, grinding, and sieving process to yield fine granules. Additional processing techniques yield a U-Al target nearly 74 % U-Al<sub>2</sub> and 26 % U-Al<sub>3</sub> and U-Al<sub>4</sub>. This study concluded that the LEU targets performed well during irradiation and post-processing and fabrication cost was comparable to the HEU targets.

The Australian Nuclear Science and Technology Organization (ANSTO) has produced <sup>99</sup>Mo for 25 years at the High Flux Australian Reactor (HIFAR) by irradiating 1.8 – 2.2 % UO<sub>2</sub> LEU pellets (Donlevy, et al. 2000). This reactor shut down operation in 2007 to convert to a production process that would use 19.75 % LEU targets (NAS 2009). ANSTO signed a contract with the Investigaciones Aplicadas Sociedad del Estado (INVAP) company in Argentina, and the new Open Pool Australian Lightwater (OPAL) reactor plans to scale up and use the LEU foil plate targets developed by CNEA. OPAL began operating in 2006. ANSTO actually reported to the NAS committee that the <sup>99</sup>Mo produced from both the HIFAR and in test batches

from OPAL had less impurities than that produced from HEU targets and met the limits set by the British Pharmacopeia for impurities (NAS 2009).

Additionally, a study published in 2005 by CNEA claimed that their LEU plate targets were as good or better than HEU targets with regard to radionuclide purity (Duran 2005). 28 batches of HEU and 46 batches of LEU targets were examined, and on average most of the contaminants ( $^{131}\text{I}$ ,  $^{103}\text{Ru}$ ,  $^{125}\text{Sb}$ ,  $^{137}\text{Cs}$ , and  $^{90}\text{Sr}$ ) were an order of magnitude greater in the HEU targets even though clinical trials that might be required by the FDA for an LEU produced  $^{99}\text{Mo}$  process would only detect gross undesirable drug effects rather than individual contaminants.

Since there are many contributing factors that affect  $^{99}\text{Mo}$  production, it is difficult to compare geometrically different target designs to one another, such as plates and cylinders. Factoring in different reactor design and operating specifications further complicates this. However, the Brazilian Multipurpose Reactor (RBM) is currently in the design phase, and several LEU targets have been examined with constant reactor operating conditions. The RBM will serve to supply the Brazilian market demand for  $^{99}\text{Mo}$  and plans are to use a  $\text{U}_3\text{Si}_2\text{-Al}$  fuel enriched to 19.75 %  $^{235}\text{U}$  (Domingos, et al. 2011). Using this fuel and the proposed core configuration, three different targets were simulated:  $\text{UAl}_x\text{-Al}$  dispersion plates, U-Al foil in plate geometry,

and U-Al foil in cylindrical geometry. Both foil designs use a Ni fission recoil barrier. All were modeled in the same peripheral location in the core in the same irradiation device for 7 days. With each target containing 20.1 g U enriched to 19.9 % wt  $^{235}\text{U}$ , the total  $^{99}\text{Mo}$  activities following irradiation were 5987 Ci, 3439 Ci, and 4607 Ci respectively. Further thermal hydraulic analysis determined that normal operating safety margins were not exceeded with any of the target designs. Assuming it takes 5 days post irradiation before utilization into a  $^{99\text{m}}\text{Tc}$  generator, the  $^{99}\text{Mo}$  activity will decrease in the dispersion target, the foil target in plate geometry, and the foil target in cylindrical geometry to roughly 1695 Ci, 974 Ci, and 1305 Ci respectively (Domingos, et al. 2011). With the IPEN/CNEN-SP processing facility expecting the future Brazilian demand for this radioisotope to reach 1000 Ci  $^{99}\text{Mo}$  / week, all 3 designs appear to be viable options. Choosing which target design to use may involve other factors such as fabrication and processing costs or the quantity of waste generated.

The Pakistan Research Reactor-I (PARR-1) has also analyzed the irradiation of U-Al<sub>x</sub> LEU foil plate targets with the goal of achieving 100 Ci  $^{99}\text{Mo}$  after irradiation, enough to meet the country's demand (A. Mushtaq, M. Iqbal and I. H. Bokhari, et al. 2009). The Pakistan Institute of Nuclear Science and Technology (PINSTECH) in Islamabad operates the PARR-1, and the

core was converted to  $U_3Si_2$ -Al LEU fuel in 1998 at an operational power of 10 MW. The uranium foil will measure roughly 125  $\mu\text{m}$  thick surrounded on both sides with a 15  $\mu\text{m}$  Ni foil. Two Al plates welded on all sides will sandwich the foils. The foil target is actually the same as that developed at ANL, and the annular design was first examined as the target candidate. It proved to work well, but for reasons not stated the plate design will be used (A. Mushtaq, M. Iqbal and I. Bokhari, et al. 2008). Initial neutronic and thermal hydraulic analyses have demonstrated that 100 Ci of  $^{99}\text{Mo}$  can be produced while maintaining all necessary safety limitations with both designs. One study did find that forced flow would be required with plate fuel to avoid the initiation of nucleate boiling in the target (Mohammad, Mahmood and Iqbal 2009). However, a follow up study did not mention this as a potential problem.

### ***2.2.3 Uranium Pin Targets***

Cylindrical pin targets can exist as high or low enriched uranium. One target analyzed by the Atomic Energy Organization of Iran utilized natural (0.7 %  $^{235}\text{U}$ )  $\text{UO}_2$  fuel. The Iranian demand for Mo-99 amounts to about 20 Ci / week, and the targets would be irradiated in the Tehran Research Reactor (Sayareh, Ghannadi Maragheh and Shamsaie 2003). The effect on fission rate between powdered, pressed, and sintered forms of  $\text{UO}_2$  was examined with MCNP4-A, and only minor fluctuations were noticed. Further analysis utilized

the pressed form, and a 100 gram target clad in aluminum yielded 37.5 Ci  $^{99}\text{Mo}$  / week, amounting to about 20 Ci / week following chemical processing and cooling. With the success of foil target designs over the last two decades, pin targets have slowly been replaced. This is in part due to the small amount of time it takes for the Mo-99 level to saturate. Once saturation is reached, the targets are taken out, and the remaining fuel is considered waste. Although foil and other designs may take longer to reach saturation because of the smaller uranium content, much less uranium and money are wasted.

#### ***2.2.4 Other Fuel Materials***

Although uranium silicide fuels, namely  $\text{U}_3\text{Si}_2$  and  $\text{U}_3\text{Si}$ , allow for a relatively easy transition to LEU, they present problems when trying to separate the Mo-99 (Sameh and Bertram-Berg 1992). When different LEU targets were examined for the conversion of the RA-3 reactor, the processing stages had to be drastically changed, and the  $^{99}\text{Mo}$  could still not be completely recovered after irradiation (Cols, Cristini and Manzini, Mo-99 from Low - Enriched Uranium 2000). Tests at Chalk River Nuclear Laboratories (CRNL) found that a silicate precipitate formed upon acid dissolution clogging the alumina column, and the precipitate also absorbs the molybdenum preventing elution (IAEA-TECDOC-515 1987). A study by ANL in the 1990s found that  $\text{U}_3\text{Si}_2$  targets do not easily dissolve in base (Buchholz and

Vandegrift 1995). Tests at CNEA analyzed non-irradiated natural uranium silicide mini-plates as targets and found that an oxidizing agent such as hydrogen peroxide could be used in conjunction with NaOH to dissolve the uranium silicide (Cols, Marques and Cristini 1994). When the team analyzed one of these mini-plates that had been irradiated for a short period of time in the RA-3 reactor they found the dissolution process to proceed more slowly (Cols, Marques and Cristini 1995). Also, a 20% enriched LEU uranium silicide target of  $U_3Si_2$  or  $U_3Si$  contains approximately 40% and 21.1 % respectively, less U-235 atoms per cubic centimeter than the typical LEU foil targets (Kolar and Wolterbeek 2004). They also point out that the primary advantage of this target lies in the ease of fabrication. Uranium and silicon are melted together and then ground into fine particles that are then mixed with aluminum powder. Uranium silicide has proven to be an efficient fuel, but as a target for producing Mo-99, more research and development are needed in the chemical processing stage.

Finally, one other material that has been examined to ease conversion to LEU fuel and possibly act as a target for Mo-99 production is uranium-molybdenum dispersed in aluminum. This composition allows for high uranium loading,  $\sim 8.3$  g/cc, and full sized fuel plates were irradiated in the OSIRIS reactor (Huet 2005). Follow up analyses showed that they maintained good

swelling behavior but that the initial design needed improvement due to the behavior of the fission products. Research has been carried out at the National Research Nuclear University MEPhI in Moscow, and the study showed that it would be feasible to convert the IRT MEPhI research reactor to 19.75 % UMo-Al LEU fuel (Alferov, Kryuchkov and Shchurovskaya 2011). This composition could potentially be used as a target material to produce Mo-99.

### **2.3 Post Cintichem U.S. <sup>99</sup>Mo Production**

Since the U.S. abandoned its Mo-99 production with the shutdown of Cintichem, Inc in 1989, there has been relatively little initiative to establish a national producer (of fission target produced Mo-99) that can supply part, if not all, of our domestic need. ANL had examined the possibility of using a 1 MW TRIGA Reactor to produce Mo-99 using LEU metal targets roughly two decades ago (Mo 1993). The core layout chosen was the Washington State University (WSU) TRIGA reactor. The annular target consisted of an LEU metal foil sandwiched between two aluminum cylinders with a reflector at the center. Air, beryllium, and water were analyzed for the reflector material and water was chosen because it yielded the greatest fission rate in the target. No fission-product barrier was used. The computer codes DIF3D and EPRI-CELL concluded that large amounts of <sup>99</sup>Mo could be produced in a TRIGA reactor using the LEU targets. A thermal neutron flux on the order of  $10^{12}$

neutrons/cm<sup>2</sup>/s can yield roughly  $10^4$  Ci <sup>99</sup>Mo / g Mo and 10 Ci <sup>99</sup>Mo / g <sup>235</sup>U.

Although ANL has been and continues to be at the forefront of the design of LEU targets, this work was not pursued further.

More recently, researchers at both the University of Missouri (UM) and Sandia National Laboratories (SNL) have been the two major groups seeking to produce <sup>99</sup>Mo. It is estimated that the U. S. would need to irradiate approximately 100 kg of LEU foil each year to meet its demand (Bakel, et al. 2008). Research at the University of Missouri is currently underway with the objective of supplying 50% of this demand, which would amount to irradiating roughly 2300 20g LEU foil targets a year at the University of Missouri Research Reactor (MURR) (Solbrekken, El-Gizawy and Allen 2008). Their primary goal is to develop and qualify an LEU-foil target, which was designed by ANL, such that the target could be utilized by independent producers (Jollay, et al. 2011). They estimated (as of 2011) that no more than fifty LEU foil targets had been irradiated, and there was no set of standards or specifications for manufacturing LEU foil targets. To comply with the MURR technical specifications set forth by the U.S.NRC, a 20 g target measuring 10 cm in length would require a coolant flow velocity of slightly more than 3 m/s. This can be achieved in MURR, which is a pressurized water reactor (PWR), but not the OSTR which is natural-convection cooled. MURR operates at a

maximum power of 10MW with a flux around  $4.0 \times 10^{14}$  n/cm<sup>2</sup>/s. However, the core is currently being converted to LEU which could potentially allow for a new operating license at a power of 12 MW (Foyto, et al. 2012). There have been no hot tests of the targets in MURR at this time.

SNL had originally performed test irradiations on HEU oxide fuel in the 1990s based on the Cintichem process and was the last U.S. site to do so on a full-production cycle (Parma, Coats and Dahl 2010). Targets were irradiated in the Annular Core Research Reactor (ACRR), but the original production program ceased in the wake of Canada's MAPLE reactors coming online, which had the potential to meet the global demand. However, with the failure of these reactors to operate as planned and their subsequent shutdown, there has been a renewed interest in the production of <sup>99</sup>Mo at SNL. They have proposed a medical isotope reactor concept using the ACRR as the design basis that could supply the entire U.S. demand using LEU targets as the fuel. This concept uses uranium oxide pins measuring approximately 1 cm in diameter with a height between 30 and 40 cm (Parma, Coats and Dahl 2010). They originally proposed irradiating 90 to 150 of these targets in a 1 to 2 MW open pool-type, passively safe reactor. With a pin power around 8 to 10 kW this would meet the U.S. demand. Control rods would be used to adjust the power level, and all reactivity coefficients appear to be strongly negative

although no values are given. The control rods would be located in the annulus of the core in order to flatten the flux. A later parametric study showed that there was a strong correlation between negative feedback and the target pitch (Dahl and Parma 2013). The Sandia Critical Experiment Facility (SCXF) will be used to allow them to compare grid plates of differing pitch as well as different reflector designs and moderator temperature feedback. They anticipate an average pin power of 10 kW with a maximum of 38 kW.

Another company seeking to produce  $^{99}\text{Mo}$  is Eden Radioisotopes. They plan on operating a single facility with a nuclear reactor no more than 2  $\text{MW}_{\text{th}}$ . Multiple fuel elements would be assembled into a single target, and this would allow for a chemical processing step with no damage to the fuel cladding (Vernon 2013). The reactor design would be heavily reflected and pool type, and the targets, as with the MURR design, would require forced water cooling. These hollow  $\text{UO}_2$  pellets would stack on top of one another for a fuel pin length of roughly 60 cm. This concept utilizes a driver assembly, though it doesn't require it, and it is virtually identical to the target assemblies. The major difference is the inclusion of an aluminum plug in the driver assembly to maintain the geometry of the  $\text{UO}_2$  pellets. Loading the core with a maximum number of 19 target assemblies (no driver) can yield 6650 six-day curies after one week of operation.



## CHAPTER 3

### OREGON STATE TRIGA REACTOR AND LEU TARGET DESIGN

#### 3.1 OSTR

According to the General Atomics website, there are currently 65 TRIGA (Test Research Isotope General Atomics) facilities in 22 countries around the world, by far the most of any type of research reactor. The first three were constructed and brought online in 1958 (Fouquet, Razvi and Whittemore 2003). The OSTR is an above ground Mark II design, 1-MW (licensed for 1.1) natural convection cooled pool-type reactor that can operate in square-wave or pulse mode. It is strictly a research reactor and therefore does not generate electricity. Unlike commercial power reactors, the OSTR does not operate continuously and is instead shut down at the end of each day. The core lies at the bottom of an aluminum tank roughly 6 ½ feet in diameter and 20 ½ feet deep, and contains three radial and one tangential beamports for irradiating samples. The tank contains approximately 4600 gallons of demineralized water at a temperature less than 49° C. The core volume is nearly 1/3 water by volume. Nearly 16 feet of water rests above the core to provide shielding at the top, and 1 ½ feet of water, 2 inches of lead, 10.2 inches of graphite, and 8 feet 2 inches of concrete shield in the radial

direction (Oregon State University n.d.). Criticality was first reached in 1967 with TRIGA standard fuel, but since 2008 the reactor has operated using LEU fuel. 66 fuel elements were used to take the LEU core critical. A 3 Curie americium beryllium neutron emitter provides the additional neutrons and acts as the startup source. Americium spontaneously decays via alpha emission, and these particles strike the beryllium to yield the supplementary neutrons.

Criticality is achieved by slowly withdrawing the control rods from the core until a steady state system is observed. A bridge atop the reactor has the drives for the regulating, shim, safety, and transient control rods. The aluminum clad transient control rod measures about 37 inches and contains 15 inches of borated graphite. Boron acts as a neutron poison due to its exceptionally large absorption cross section. Unlike the other three control rods which are motor-driven, the transient rod is pneumatically controlled. The safety, shim, and regulating rods are slightly longer at 43 inches, clad in stainless steel, and each have a nominal rod worth of about \$2.70. The transient rod has a worth of approximately \$4.00, and rod worth will be discussed in detail in the next chapter.

Six concentric rings hold the 126 spaces for the fuel rod elements, control rods, guide tubes, and pneumatic transfer tube as shown in Figure 3-3. Each measures 1.505 inches in diameter. A  $\frac{3}{4}$ -inch aluminum grid plate sits at

the bottom to support the core and receives the adaptor ends of the fuel-moderator elements and pneumatic transfer tube. Another aluminum plate sits at the top and allows for accurate positioning of the different core components. The current LEU fuel is a homogeneous mixture of uranium and zirconium hydride,  $\text{UZrH}_{1.6}$ , and measures approximately 15 inches long with a diameter of 1.5 inches. Erbium is also homogeneously mixed with the fuel as a burnable poison. 3.5 inches of graphite reflectors sandwich the fuel-moderator elements on both ends with 0.020 inches of stainless steel cladding on the outside. Each fuel element weighs approximately 7.0 pounds. The core consists of these fuel elements and dummy aluminum-clad graphite elements.

### **3.2 LEU Target**

The LEU target designed by Oregon State University and researchers from Pacific Northwest National Laboratory (PNNL) consists of 19.75%  $\text{UO}_2$  sandwiched between two cylinders of aluminum. The actual fuel targets are annular in design. This allows for the water moderator/coolant to flow through the center of the targets and greatly increases the thermalization of neutrons. This will have the benefit of reducing the self-shielding in the fuel which will ultimately lead to an increase in the utilization of the fuel. Also, the annulus almost doubles the surface area between the fuel target and coolant, leading to an increase in the heat transfer capabilities. Although the fabrication and

design specifics of this target are proprietary, the dimensions given in Table 3.1 are more than enough to model the target and perform the necessary analysis. Figures 3.1 shows an axial view of the target as it is modeled, and Figure 3.2 shows the axial view of the actual target. Figure 3.3 shows the target design. Figures 3.4 and 3.5 show cross section views of the OSTR facility and Figure 3.6 is an axial view of the general layout of the core.

**Table 3.1 Target specifications**

LEU Target Properties	
Central water radius	1.33096 cm
Inner aluminum clad outer radius	1.48844 cm
Fuel outer radius	1.71577 cm
Outer aluminum clad outer radius	1.87579 cm
Active fuel length	48.0065 cm
Top air follower region	5.3335 cm
Top aluminum cap	2.31 cm
UO <sub>2</sub> volume / target	109.857 cm <sup>3</sup>
<sup>235</sup> U mass / target	~ 158 grams

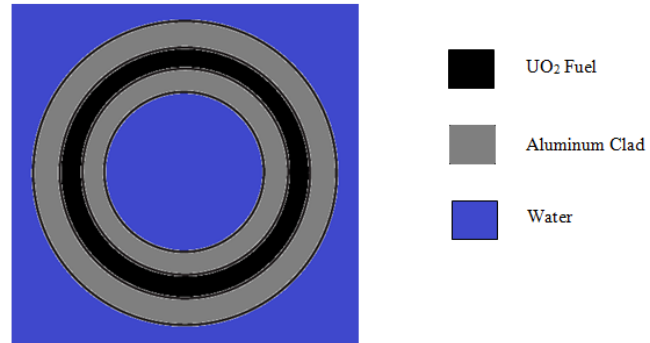


Figure 3-1 Axial view of modeled target

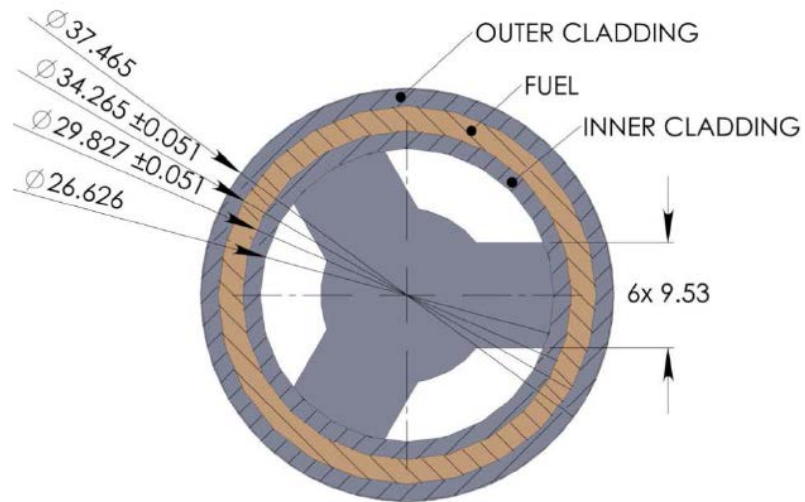


Figure 3-2 Axial view of actual target

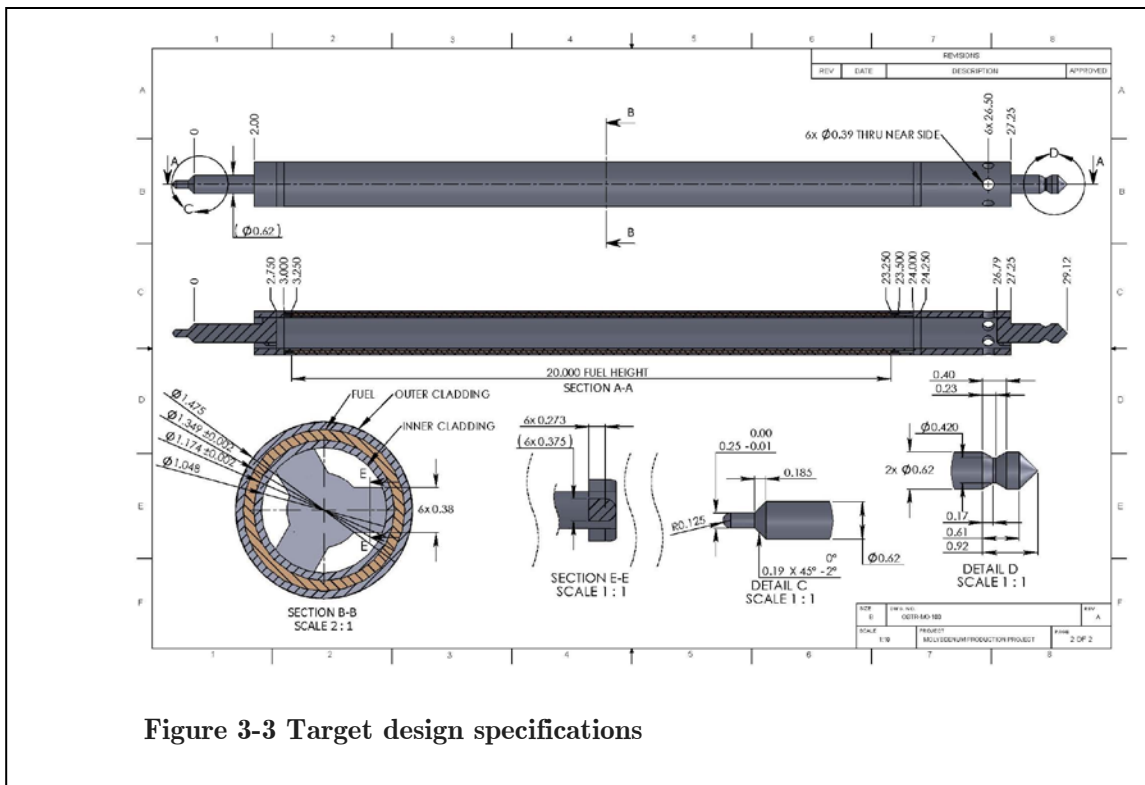


Figure 3-3 Target design specifications

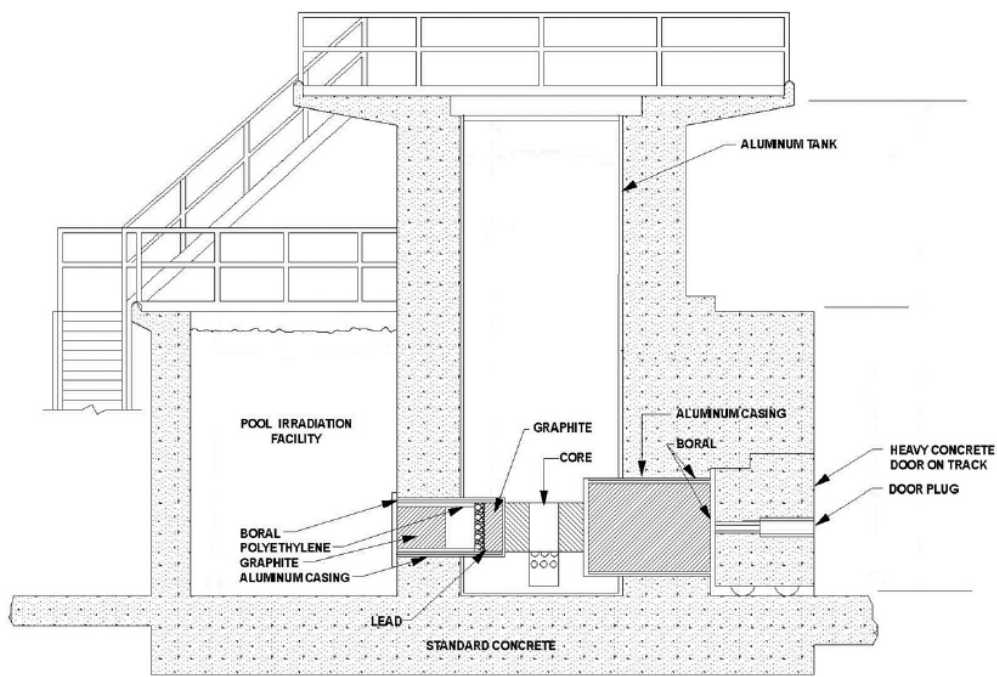


Figure 3-4 Vertical section of OSTR

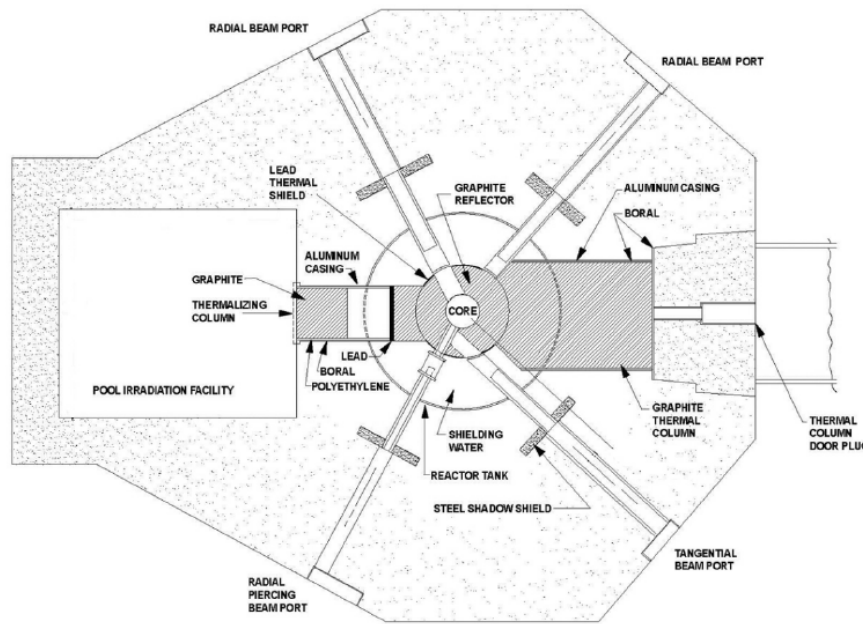


Figure 3-5 Horizontal section of OSTR

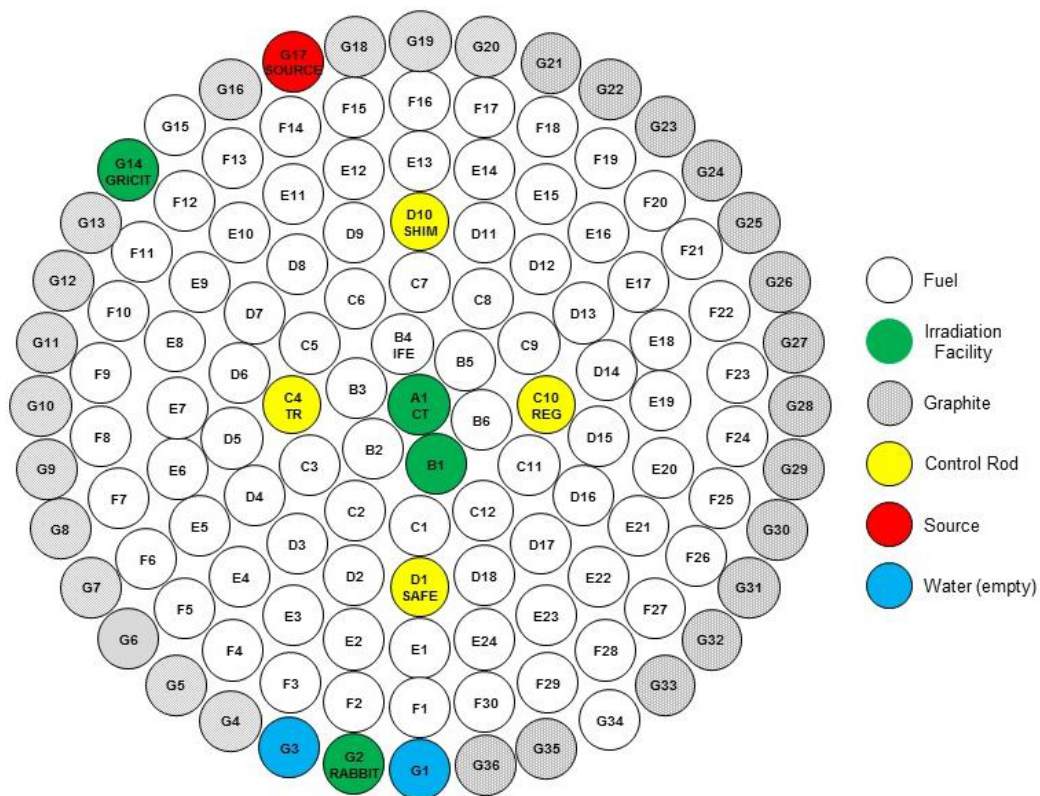


Figure 3-4 Axial view of OSTR core.

## CHAPTER 4

### REACTOR PHYSICS

The following section will examine the different reactor physics parameters analyzed in this research and will conclude with a brief discussion on the heat transfer properties of the targets. Quantifying these parameters will both demonstrate that the reactor system can be safely controlled under normal operating conditions and show that it possesses the necessary feedback mechanisms to counteract specific changes in the system when they do occur, such as an unexpected increase in the fuel temperature. In order to calculate these parameters we perform an eigenvalue calculation to determine the multiplication factor,  $k$ , of the system. The multiplication factor of the system is defined as:

$$k = \frac{\text{number of neutrons produced in one generation}}{\text{number of neutrons at the beginning of the generation}} .$$

If  $k = 1$ , the system is critical and can sustain a chain reaction. If  $k$  is greater than or less than one, the system is characterized as supercritical or subcritical respectively. The multiplication factor is calculated over a range of core conditions, and how it changes allows us to quantify the parameters of interest.

## 4.1 Reactivity Control

Nuclear reactors are initially loaded with much greater amounts of fuel than necessary to achieve criticality. This is due to the continual change in the isotopes of the fuel composition as fuel is burned and fission products are created, which results in an ever changing, though slowly, multiplication factor over time. Although commercial power reactors are built and designed to operate for much longer interrupted periods of time than a radioisotope production reactor, making the initial fuel loading quantity less of a longevity concern, there are still inherent negative reactivity feedback mechanisms that must be overcome to operate at steady state. The following sections focus on reactivity control in the core.

### 4.1.1 *Excess Reactivity*

Reactivity is the change in the neutron population from unity as represented below.

$$\rho = \frac{k - 1}{k}$$

Excess reactivity is merely the reactivity present if all the movable control poisons were instantly removed from the core (E. E. Lewis 2008). Because there must initially be a large amount of excess reactivity in the core, there are a variety of mechanisms that reactor operators can use to control the power, or more appropriately the fission rate, in a nuclear reactor, and hence

counteract the excess reactivity present. These include moveable control rods, burnable poisons in the fuel, chemical shims, adjusting the coolant flow rate, etc... The TRIGA LEU fuel currently present in the OSTR contains the burnable poison erbium-167, but no such poison will exist in the Mo-99 production targets. This can be attributed to the much shorter irradiation periods these targets will be subjected to and the fact that they will be chemically processed post-irradiation unlike traditional spent nuclear fuel (in the U.S.). A poison could interfere with this chemical process and is simply not needed. Flow rate adjustment is primarily used to control reactivity for Boiling Water Reactors (BWRs). Since the reactor design proposed for this work is based off the OSTR, the flow rate is natural and not controlled by the use of pumps. Also, there is no mechanism in place to administer or monitor a chemical shim that could possibly be used in this design. Again, with the irradiation time on the order of 1 to 2 weeks, there is simply no need for a chemical shim to be present in this design. This leaves the control rods as the only means of reactivity control. This parameter can be calculated by determining the multiplication factor of the core with all the control rods fully withdrawn.

#### *4.1.2 Shutdown Margin*

Another parameter that must be quantified is the shutdown margin. This is a measure of the negative reactivity in the core when all movable control elements are fully inserted (Duderstadt and Hamilton 1976). This leads to the minimum multiplication factor in the core, and it also represents how fast the power level will be reduced in an emergency shutdown. The shutdown margin will be positive for a reactor that is shutdown and represents the amount of reactivity needed to bring a reactor exactly critical. Like the excess reactivity, this parameter is also a function of time and temperature. Since the targets will be removed and processed after each irradiation time, they will always be “clean” or “cold”, and the shutdown margin will remain nearly constant throughout each irradiation cycle. Although the multiplication factor associated with all control rods fully inserted into the core dictates the shutdown margin, it is often instead calculated with the most reactive control rod fully withdrawn, representing the stuck-rod-scenario. Thus the multiplication factor is calculated with the regulating rod fully withdrawn and the others fully inserted. The Technical Specifications for the OSTR requires the LEU core to have a minimum shutdown margin of  $-0.55$  (Oregon State University n.d.).

### 4.1.3 Rod Worth

The core designs we have examined in this work rely on control rods alone to regulate the power level (fission rate) making it very important to know how much each rod is worth and how they interact with each other. The total rod worth is the difference in reactivity when all control elements are fully inserted and fully withdrawn. The relationship between total rod worth, excess reactivity, and shutdown margin is shown in Figure 4.1.

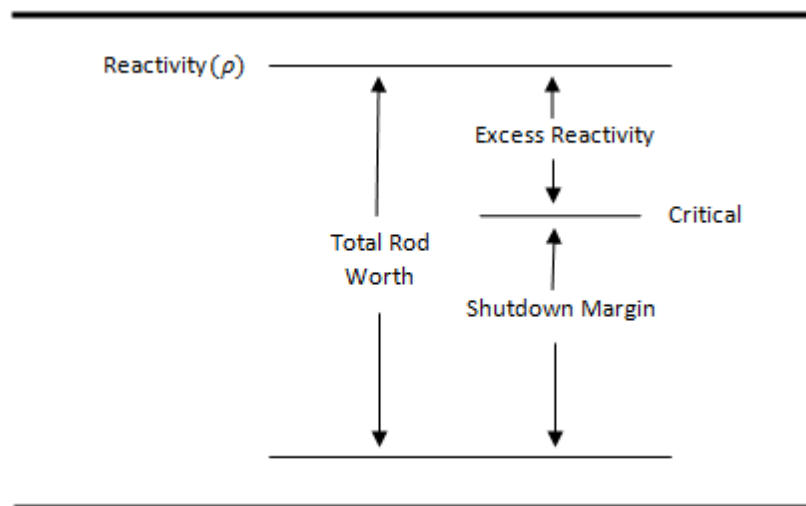


**Figure 4-1: Total rod worth, excess reactivity, and shutdown margin**

The individual rod worth is a measure of the reactivity change associated with full insertion of a single control rod. It is important to note that when examined simultaneously, the rods may be worth more or less than when they are examined individually and summed, an effect known as anti-shadowing or shadowing respectively, due to the perturbation in the flux each rod imposes

(Lamarsh 1975). This is more an issue for steady state operation, since control rods are used to flatten the flux across the core as much as possible, and moving one control rod slightly may yield an effect more or less than needed. In broad terms, control rods tend to have different “degrees of effectiveness: (1) a fine control by means of ‘regulating rods’; (2) a coarse or ‘shim’ control; and (3) an emergency or ‘scramming’ control,” that will immediately shut the reactor down (Liverhant 1960). One way to quantify these effects is to calculate the integral rod worth, or the reactivity change associated with incremental insertions/withdrawals of a single rod. This is typically done by fully withdrawing one of the rods and using the remaining control rods to bring the core critical. The withdrawn rod is then partially inserted, maybe 10%, and then a new multiplication factor calculated. The other control rods are then each partially withdrawn such that the core returns to a near critical state. This process continues until the rod being measured is fully inserted. An integrated rod worth curve is then constructed yielding the reactivity associated with a given percentage of the rod withdrawn. Thus if control rods need to be moved during steady state operation, reactor operators have a more accurate idea of how they will influence the system.

## **4.2 Reactivity Coefficients**

Although there are mechanisms in place to control the fission rate, there must also exist inherent feedback systems, arising from the core geometry and materials, should the fission rate, for whatever reason, no longer remain controllable. And even though no design is foolproof, these feedback systems enhance the level of safety should an accident occur, such as a stuck control rod, a pipe break, loss of power, etc. These feedback mechanisms are measured as reactivity coefficients. Every reactor under all plausible operating conditions should have a negative power coefficient of reactivity defined as

$$\alpha_P = \frac{d\rho}{dP} \quad ,$$

where an increase in power adversely affects the neutron population leading to a negative reactivity insertion. Because this quantity is dependent on neutronic and thermal-hydraulic phenomena, it is more convenient to examine temperature coefficients of reactivity (Duderstadt and Hamilton 1976).

Reactivity is often assumed as a function of time, but it is more accurately a function of the neutron flux and depends on macroscopic cross-sections, which themselves depend on the atomic number densities of the materials (Duderstadt and Hamilton 1976). Not only do the material densities change with temperature, which is directly dependent on the power distribution, i.e. neutron flux, but also, materials are constantly being burned and bred in the fuel due to neutron interactions which changes their relative concentrations.

This temperature induced reactivity feedback lends an inherent stability to nuclear reactors and can be broken into various reactor components such as fuel and moderator defined as

$$\alpha_T \equiv \frac{\partial \rho}{\partial T} \rightarrow \sum_i \frac{\partial \rho}{\partial T_i} = \sum_i \alpha_{T_i} \quad .$$

Thus it is very important to demonstrate that given a specific reactor design, if a transient occurs leading to an increase in temperature, the materials and core geometry will intrinsically lead to a reduction in the neutron population. There are three primary coefficients of reactivity associated with the core designs proposed: prompt temperature, moderator temperature, and void coefficient of reactivity (COR). These reactivity coefficients can be determined by observing the multiplication factor over a variety of different core configurations.

#### ***4.2.1 Prompt Temperature Coefficient of Reactivity***

The amount of time required to increase the reactor power by a factor of  $e$  is called the reactor period. During a transient where a large amount of positive reactivity is inserted in the core, the reactor period becomes very small and the power changes on such a short time scale that there is no appreciable heat transfer to the coolant (E. E. Lewis 2008). Thus, this COR is dictated by the fuel temperature alone and results from the phenomenon known as the Doppler effect, whereby increases in fuel temperature lead to

decreases in self-shielding which further causes increases in the resonance absorption (Duderstadt and Hamilton 1976). During normal operations, this feedback mechanism remains relatively small, but under extreme transients it becomes a factor. Neutron cross-sections are strongly dependent on the speed of the neutron relative to the background nuclei. Neutron speed is a function of temperature characterized by the Maxwell-Boltzmann distribution in an infinite, purely-scattering medium. Because the cross-sections are sharply peaked in the resonance region, the Breit-Wigner formulas that describe them must be averaged over the relative range of speeds (E. E. Lewis 2008). The net effect of this averaging widens the resonances, and increasing fuel temperature only further enhances this effect as shown in Figure 4.2. This COR is determined by observing the change in the multiplication factor as the fuel temperature changes.

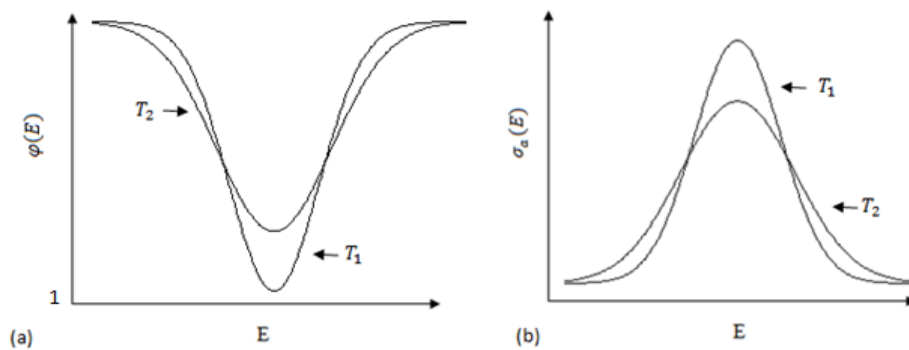


**Figure 4-2: Doppler broadening effect on self-shielding for  $T_2 > T_1$ . (a) neutron flux in fuel, (b) resonance absorption cross section.**

#### ***4.2.2 Moderator Temperature Coefficient of Reactivity***

If the temperature of the moderator increases while the density remains constant, the neutron spectrum will harden. A shift in the spectrum to higher energies will increase the resonance absorption, negatively affecting the reactivity. Also, the capture to fission cross-section ratio for  $^{235}\text{U}$  and  $^{239}\text{Pu}$  will increase, decreasing the thermal utilization (less neutrons created per neutron absorbed). However, for liquid moderated systems the feedback from increases in temperature is not the dominant mechanism. More important is the change in moderator density. A decrease in density will lead to a decrease in the number of hydrogen atoms per unit volume resulting in less thermalization. Since the effectiveness of slowing neutrons down decreases, there will be a corresponding increase in the resonance absorption. This negative reactivity insertion resulting from a decrease in moderator density arises because the core is under-moderated. For over-moderated cores this is not the case. This parameter is determined by analyzing the change in the multiplication factor over different moderator densities.

#### ***4.2.3 Void Coefficient of Reactivity***

This parameter essentially quantifies the same effects as the moderator temperature COR but assumes the density of the moderator is decreasing due to a buildup of air/boiling in the reactor. Thus the change in density is much

more significant. The density of the moderator throughout the core is not changed, only the density of the moderator in the innermost, or hottest, channel of the core. Because the core is under moderated there should be a negative response to a decrease in density. The void COR is determined in a similar manner to the moderator COR.

### 4.3 Delayed Neutron Fraction

Although reactivity control is the means by which nuclear reactors are controlled, delayed neutrons are what provide this ability. Greater than 99% of the neutrons in a reactor are prompt, meaning generated instantaneously from fission (E. E. Lewis 2008). The other remaining fraction is emitted from fission fragments created as a result of fission and are referred to as delayed. Different fissionable isotopes have different delayed neutron fractions, but  $^{235}\text{U}$  is the only isotope of concern since the short irradiation time makes the buildup of  $^{239}\text{Pu}$  negligible. The precursor neutron-emitters have half-lives ranging from hundreds of milliseconds to almost one minute and are placed into six groups accordingly. For  $^{235}\text{U}$  the total delayed neutron fraction,  $\beta$ , amounts to 0.00650. Despite this rather meager fraction, these neutrons have a far greater effect on the mean neutron lifetime, and because of this operators are capable of controlling the reactor period. Even if the multiplication factor of the system is known, without knowing the delayed neutron fraction it is

impossible to know when the reactor will go prompt critical or prompt super critical. The system is prompt critical when the delayed neutron fraction equals the reactivity.

#### **4.4 Prompt-Neutron Lifetime**

The neutron lifetime,  $l$ , is defined as the total number of neutrons in the reactor at a given time divided by the rate of neutrons lost through absorption and capture. The prompt-neutron lifetime refers to prompt neutrons alone. When prompt criticality is reached the chain reaction no longer requires delayed neutrons to sustain itself. If the system exceeds this and becomes prompt super critical, then the reactor period no longer relies on the delayed neutron half-lives (E. E. Lewis 2008). Instead the period will be dictated by the prompt-neutron lifetime.

#### **4.5 Approach to Criticality**

An approach to criticality analysis is used to predict the number of fuel elements/targets that will bring the core critical. Since all of the targets will be removed after a given irradiation cycle, the target loading strategy will be the same for each fresh core. With the core empty and control rods fully removed, targets are initially loaded in the six b-ring positions and a multiplication factor determined. Then the c-ring is filled with the allowable

ten targets and another multiplication factor determined. Targets are then placed in the d-ring one at a time until the core transitions from a subcritical to slightly supercritical state. Once the reactor has become supercritical, control rods must be inserted slightly to counter balance the excess reactivity now in the core. For the LEU core, a  $1/M$  plot was constructed to determine which target addition resulted in a critical core. A  $1/M$  plot involves measuring the count rate,  $M$ , at each different loading configuration and plotting  $1/M$  versus the number of fuel elements in the core. Normalizing the initial  $1/M$  quantity to unity, a linear extrapolation of the resulting plot will predict the critical fuel element.

#### **4.6 Minimum Critical Heat Flux Ratio**

It is very important that any reactor system has the necessary cooling capabilities such that the fuel and cladding temperatures stay well under their melting points, ensuring the integrity of the fuel pins and containment of fission products. One metric used to measure this safety limitation is the Minimum Critical Heat Flux Ratio (MCHFR). The critical heat flux (CHF) phenomenon, also termed departure from nuclear boiling (DNB), occurs when nucleate boiling transitions into the transition boiling regime in which a vapor film begins to coat the surface of the cladding causing degradation of the heat transfer coefficient. The resulting decrease in the heat transfer coefficient

results in a spike in the clad surface temperature in order to maintain the current heat flux (Todreas and Kazimi 1990). They further define the MCHFR as the minimum allowable ratio between the predicted critical heat flux and the operating heat flux (also called the MDNBR). The MCHFR represents a margin of safety. If the MCHFR is close to 1, then a slight increase in the heat flux might lead to DNB. Although the OSTR is a natural convection cooled research reactor, for which there is no regulatory limit on MCHFR, forced convection cooled research reactors must have a minimum value of 2.0 (Marcum, et al. 2009). This implies that the operating heat flux would have to double in order to reach the CHF. The MCHFR has not been directly examined in this work because a prior analysis at Oregon State University has already been completed. The conclusions of that study will be examined in the results section.

## **CHAPTER 5**

### **METHODOLOGY**

The following section will examine the methodology used to perform this research. A detailed MCNP5 model of the Oregon State TRIGA Reactor (OSTR) was developed during its conversion to LEU fuel, and its predictions have been verified by extensive measurements (Hartman, et al. 2013). This geometric model has been adapted and modified accordingly for this work. The simulation package will be discussed first, followed by a description of how the parameters needed in order to properly characterize the behavior of the reactor system are calculated using MCNP.

#### **5.1 MCNP and Monte Carlo Methods**

Monte Carlo Neutral Particle (MCNP) is a system code developed at Los Alamos National Laboratory that analyzes the transport of neutrons, gamma rays, and electrons (X-5 Monte Carlo Team 2003). MCNP5 is the version used for this work. MCNP5 is universally recognized as the standard for benchmarking other neutron transport codes because of several attractive features. Unlike deterministic methods, Monte Carlo methods have no discretization error. Energy, space, and angle can all be treated continuously (Lewis and Miller, Jr 1993). However, errors do arise from uncertainties in

cross-section data, but this affects all methods. Also, the code is constantly undergoing development, and this has led to the ability to model very detailed three dimensional geometries, something deterministic methods have only recently been capable of. The pitfall of Monte Carlo methods and MCNP5 lies in the computation time. The method is governed by statistics and therefore many particles must be tracked in order to achieve results with small uncertainty. However, there have been several variance reduction techniques developed over the last decade that help reduce the computation time and further enhance the capabilities of MCNP5.

MCNP5 was used to perform a k-eigenvalue calculation to determine the multiplication factor of the system. Both the materials and their geometrical arrangement will affect the multiplication factor. In order to determine  $k$ , a finite number of generations are simulated, and in each generation there are a finite number of particles, neutrons in this case, that are created. MCNP5 tracks the particle from 'birth' to 'death', and this tracking represents the particle's history.

MCNP5 carries out a simulation by using a pseudo-random number generator to sample from different cumulative probability density functions. The following is merely a generalized overview of the history flow of a particle from 'birth' to 'death' and the appropriate tally scoring. The source

distribution is first sampled to determine a particle's initial position, energy, and direction (Lewis and Miller, Jr 1993). Depending on the problem, other parameters can also be calculated. Then the particle is transported to the location of its next collision by sampling its track length distance. If the distance-to-surface equals the minimum track length, that particle moves to the boundary where it is treated according to the boundary type (reflective, periodic, etc.) along with other techniques if employed, such as variance reduction techniques. The track length tally is then incremented, and parameters such as energy and position are updated (X-5 Monte Carlo Team 2003). The previous steps are then repeated to continue the particle history. When the distance-to-collision is less than the distance-to-surface, MCNP5 determines the collision nuclide and then what type of interaction occurs. For general purposes, the neutron can either be captured, induce fission, or scatter. Upon capture or fission, the respective tallies are incremented and the particle history terminated (in the subsequent generation, the fission sites become the distribution for the source). If a scattering event occurs, a new direction and energy must be sampled. This process is repeated until all the particle histories have been completed. Quantities of interest are updated, and then the next generation of particle histories is tracked.

To demonstrate how random numbers are incorporated into the physics behind neutron transport, the track length estimator will be derived. With no external source, the neutron population at a distance  $x$  for a given volume, angle, and energy with a constant macroscopic total cross section is governed by the following:

$$\frac{\partial\psi(x)}{\partial x} + \Sigma_t(x)\psi(x) = 0 \quad .$$

The macroscopic total cross-section,  $\Sigma_t$ , represents the probability of interaction per unit length traveled and has units of  $\text{cm}^{-1}$  (E. E. Lewis 2008).

The angular flux,  $\psi$ , has the dimensions neutrons/ $\text{cm}^2$ /second. A simple rearrangement of this leads to

$$\frac{\partial\psi(x)}{\psi(x)} = -\Sigma_t(x)dx \quad ,$$

which can be readily solved with the condition  $\psi(0) = 1$  to yield the angular flux at a distance  $x$  to be

$$\psi(x) = e^{-\Sigma_t(x)x} \quad .$$

The probability that a collision occurs between  $x$  and  $x + dx$  along the flight path is

$$p(x)dx = \Sigma_t(x)\psi(x)dx \quad ,$$

and substituting the preceding expression for the angular flux yields

$$p(x)dx = \Sigma_t(x)e^{-\Sigma_t(x)x}dx \quad .$$

By integrating this equation from 0 to  $x$ , one can obtain the cumulative probability density function (CPDF)

$$CPDF = \int_0^x \Sigma_t(x) e^{-\Sigma_t(x)x} dx = \xi \quad ,$$

where  $\xi$  is a real number with values uniformly distributed between 0 and 1.

Solving this yields

$$\xi = 1 - e^{-\Sigma_t(x)x} \quad ,$$

and rearranging for  $x$  gives

$$x = -\frac{1}{\Sigma_t} \ln(1 - \xi) = -\frac{1}{\Sigma_t} \ln(\xi) \quad ,$$

where  $\xi$  has been substituted for  $(1 - \xi)$  because they obey the same distribution. Since the scalar flux can be defined as, “the total track length traversed by all particles per unit volume per unit time,” one can calculate this quantity after all histories have finished in a generation (E. E. Lewis 2008). For  $N$  particles in a given volume,  $V$ , the average track length becomes

$$\bar{x} = \frac{1}{N} \sum_n x_n \quad ,$$

where  $x_n$  represents the track length of the  $n^{th}$  particle. Therefore, the average scalar flux can be calculated as

$$\bar{\phi} = \frac{1}{V} \frac{1}{N} \sum_n x_n \quad .$$

The above example of incorporating random numbers and probability density functions to determine distance-to-collision can similarly be applied to other phenomena governing particle transport.

As stated earlier, many particle histories and generations must be executed in order to achieve meaningful results. The variance, or more accurately the standard deviation, measures the spread of values of a quantity about the mean of that quantity (Lewis and Miller, Jr 1993). An expression has been derived for the standard deviation,  $\sigma$ , and it is shown to be inversely proportional to the square root of the number of histories,

$$\sigma \propto \frac{1}{\sqrt{N}} \quad .$$

For instance, to reduce the variance by a factor of 10, a factor of 100 more particles must be tracked. This carries a heavy burden when millions of particles must be tracked in each generation and acts as one of the primary limiting factors for large scale Monte Carlo calculations. The variance can never actually be known, only the sample variance. A breakthrough in the precision of Monte Carlo results came about through the application of the Central Limit Theorem. It states that as  $N \rightarrow \infty$  and, “identically distributed random variables  $x_i$  with finite means and variances, the distribution of the  $\bar{x}$ ’s approaches a normal distribution (X-5 Monte Carlo Team 2003). Thus, if the sample variance is approximately equal to the actual variance, which is true for large values of  $N$ , this implies that confidence intervals from statistical tables can be used to determine the precision of the results.

## 5.2 MCNP Input Deck

The MCNP5 input deck consists of different user generated cards, or input parameters. Universally used cards include *cell*, *surface*, and *data* cards. For example, the user must define the geometry of the problem, the composition of the materials to be used, and how those materials fit into the desired geometry, and there are multiple ways to model the same system. The calculation of the eigenvalue is recognized by the use of a *kcode* card in the MCNP input deck. This card has at least four user supplied quantities that contain information necessary to perform the calculation. The user must supply the number of neutrons per generation, an initial guess for the multiplication factor, the number of skipped generations, and the total number of generations.

There are no specific guidelines to follow when choosing the number of neutrons per generation, but the user must be aware of the limitations by choosing a value too low or too high. Since the results are governed by statistics, too few neutrons per generation will render any solution meaningless. Too many neutrons and the statistical gain in accuracy will no longer outweigh the increase in computation time. Based off decades of experience and previous modeling of the OSTR, the number chosen for this work is 25,000 neutrons per generation. The initial guess for the multiplication

factor is generally chosen to be 1.0, which is based off predicated knowledge of how the system, i.e. reactor, will operate. A finite number of generations are skipped, or inactive, meaning the data generated in these cycles will not factor into the statistics associated with those cycles not skipped. These skipped cycles merely provide the necessary data for subsequent generations, such as an updated fission source distribution and multiplication factor. This allows the randomness associated with Monte Carlo methods to affect the entire system as equally as possible before statistics are applied to the results. The MCNP5 manual states that, “It is critical that the fission source points converge before  $k_{effs}$  and tallies are calculated to ensure proper mean  $k_{effs}$  and confidence intervals” (V. 2. X-5 Monte Carlo Team 2003). Fifty generations have been chosen to be inactive, and 300 active generations will follow for a total of 350 generations. The MCNP5 output file provides data for the user to use to determine whether an appropriate number of inactive cycles was chosen.

MCNP5 also employs the use of edit tallies which instruct MCNP5 to access different cross-section libraries in order to calculate specified quantities. These tallies are not problem specific but are user chosen to obtain whatever the desired information may be. This work requires that we determine the power profile across the core, from an operational and safety standpoint, as well as the amount of Mo-99 we can produce under such conditions. The track

length estimator is used to calculate the cell averaged flux over specified material regions and has units of particles/cm<sup>2</sup>/fission neutron. There are then subsequent flux multiplier tallies that calculate quantities of the form

$$C \int \varphi(E)R_m(E)dE \quad ,$$

where  $C$  is an arbitrary scalar constant used for normalization,  $\varphi(E)$  is the fluence, and  $R$  is a response function with an associated additive and/or multiplicative operator. Two different flux multipliers are used to acquire the necessary data. These numerical multipliers and their desired units are determined as follows:

$$\begin{aligned} Pin \ Power &\rightarrow \frac{neutrons}{cm^2 - fission \ neutron} * \frac{atms}{barn - cm} * \frac{barn - fission}{neutron - atoms} \\ &* \frac{2.43 \ fission \ neutrons}{fission} * \frac{fission}{200 \ MeV} * 1.1E6 \ Watts \\ &= 1.4189E4 \ Watts/cm^3 \end{aligned}$$

$$\begin{aligned} {}^{99}M \ atoms &\rightarrow \frac{neutrons}{cm^2 - fission \ neutron} * \frac{atms}{barn - cm} * \frac{barn - fission}{neutron - atoms} \\ &* \frac{2.43 \ fission \ neutrons}{fission} * \frac{fission}{200 \ MeV} * 1.1E6 \ Watts \\ &* \frac{MeV}{1.6E13 \ joules} * \frac{1 \ joule}{watt - second} * \frac{0.0612 \ {}^{99}Mo \ atoms}{fission} \\ &= 5.4273E16 \ {}^{99}Mo \ atoms/fission \end{aligned}$$

These tallies have been scaled to the maximum licensable operating power for the OSTR of 1.1 MW. Because eigenvalue calculations are steady

state, it is understood that all tallies will have the additional units of inverse time, or more specifically per second. Finally, it should be noted that eigenvalue calculations do not yield solution magnitude, only distribution, thus the quantities calculated are relative. Also, there are no driving terms, such as fixed sources or incident fluxes, thus the startup AmBe source is not included in the model (the source strength is orders of magnitude less than the flux due to fission and therefore insignificant).

### 5.3 Specific Activity

In order to determine the Specific Activity (SA) of the Mo-99, which has units of curies Mo-99/grams Mo, additional isotopes of molybdenum that are also fission products must be taken into consideration. Table 5.1 lists the different stable isotopes that would also be present in the targets and their fission yields. Also listed is a multiplier for each isotope which is simply the ratio of the yield of a given isotope to the yield of Mo-99 multiplied by the ratio of the mass of a given isotope to Mo-99. This multiplier is used to calculate the number of grams of each isotope using the single tally in MCNP that calculates the number of Mo-99 atoms (although each isotope could be tallied independently this would just increase the post processing time of the output file). With  $t_{irr}$  representing the irradiation time, the masses are

calculated as follows, and summing them will yield the total molybdenum in grams.

$$\frac{\text{atoms } ^{99}\text{Mo}}{\text{cm}^3 - \text{sec}} * V_{\text{target}} * t_{\text{irr}} * \frac{1 \text{ mol } ^{99}\text{Mo}}{6.022 * 10^{23} \text{ atoms } ^{99}\text{Mo}} * \frac{99 \text{g } ^{99}\text{Mo}}{1 \text{ mol } ^{99}\text{Mo}} * \text{Multiplier}$$

**Table 5.1: Molybdenum isotopes present in irradiated targets**

Isotope	Yield (%)	Multiplier
Mo-95	6.5	$(0.065/0.0612) * (95/99)$
Mo-96	6.3	$(0.063/0.0612) * (96/99)$
Mo-97	6.0	$(0.060/0.0612) * (97/99)$
Mo-98	5.79	$(0.0579/0.0612) * (98/99)$
Mo-99	6.12	1
Mo-100	6.29	$(0.0629/0.0612) * (100/99)$

The time dependent nature for producing Mo-99 in a reactor is governed by the rate equation

$$\frac{d}{dt} N(t) = PR - \lambda N(t) \quad ,$$

where the production rate (PR) is due to fission. This equation is readily solved by rearranging the terms and multiplying through by the integrating factor  $e^{\lambda t}$  as shown below.

$$\left[ \frac{d}{dt} N(t) + \lambda N(t) \right] e^{\lambda t} = PR e^{\lambda t}$$

This then becomes

$$\frac{d}{dt} [N(t)e^{\lambda t}] = PR e^{\lambda t} \quad ,$$

and if there is no Mo-99 present at time  $t = 0$  then  $N(0) = 0$ . Integrating between 0 and  $t$  then yields

$$\lambda N(t) = PR(1 - e^{-\lambda t}) \quad .$$

The production rate is simply the tally from MCNP, the decay constant,  $\lambda$ , is equal to  $0.25227 \text{ days}^{-1}$ , and  $t$  is the irradiation time, yielding the activity in disintegrations per second. To get the total activity simply multiply by the  $\text{UO}_2$  volume in each target, and dividing by the conversion  $3.7 \times 10^{10}$  disintegrations per second will yield the activity in curies.

#### 5.4 Calculation of Parameters

The fuel temperature coefficient of reactivity (COR) is determined by changing the cross-section libraries of the materials in MCNP5. The cross-section libraries contain the microscopic cross-sections (units of  $\text{cm}^{-2}$ ) evaluated at different temperatures, and the multiplication factor is calculated at these different temperatures. Two sets of libraries were used to determine the prompt fuel temperature COR. The first set is 60c, 12c, 14c, 15c, and 17c corresponding to temperatures of 293.6K, 400K, 600K, 800K, and 1200K respectively. This set was used so that a direct comparison could be drawn to

the prompt temperature COR given in the Safety and Analysis Report for the OSTR loaded with standard LEU TRIGA fuel. The second set of libraries are 70c, 71c, 72c, 73c and 74c corresponding to temperatures of 293.6K, 600K, 900K, 1200K, and 2500K, with these cross-section libraries being the most up to date.

The moderator COR is calculated by observing the change in the multiplication factor as the density of the moderator changes throughout the entire core. Water is both the coolant and the moderator, and the following densities were used: 1.0 g/cc, 0.9982 g/cc, 0.9922 g/cc, and 0.9832 g/cc. The void COR is also calculated by observing the change in the multiplication factor as the density of the moderator changes, but only in the innermost channel of the core. To determine the void COR the core was modeled with the following moderator densities for the innermost channel: 0.900 g/cc, 0.7500 g/cc, 0.500 g/cc, 0.250 g/cc, and 0.00129 g/cc corresponding respectively to voids of 10, 25, 50, 75, and 100% (the last of which is air).

The delayed neutron fraction is determined in MCNP5 by a built in function which is called through the use of a TOTNU NO card that determines the eigenvalue of the system using both prompt and delayed neutrons. Normally MCNP5 only calculates the eigenvalue on prompt neutrons alone since the problem solved is time-independent and the presence of delayed

neutrons does not change whether or not the system can reach a steady state.

The delayed neutron fraction is then determined by

$$\beta_{eff} = 1 - \frac{k_p}{k_{p+d}} ,$$

where p and d denote whether the eigenvalues associated with the systems were calculated solely with prompt neutrons or prompt and delayed neutrons together.

The prompt-neutron lifetime,  $l_p$ , is determined through the use of the  $1/v$  absorber method. This involves distributing a neutron poison, something with a high absorption cross-section, homogeneously throughout the coolant (Oregon State University n.d.). Boron-10 is used and  $l_p$  calculated as follows:

$$l_p = \frac{1}{N_B \sigma_{a,B} v} \frac{k - k_p}{k_p}$$

with:

$k$  is the eigenvalue with no absorber present

$k_p$  is the eigenvalue of the perturbed system containing boron

$N_B$  is the number density of boron (atoms / barn-cm)

$\sigma_{a,B}$  is the microscopic thermal absorption cross-section of  $^{10}\text{B}$  (3837 barns)

$v$  is the speed of a thermal neutron (220,000 cm / s)

Bretscher has determined that the prompt neutron lifetime can be more accurately represented as the limit as the boron number density approaches zero, shown below (Bretscher December 1997).

$$l_p = \lim_{N_B \rightarrow 0} \frac{1}{N_B \sigma_{a,B} \nu} \frac{\delta k}{k_p}$$

Two different boron concentrations are used to generate concentration-dependent data points. Given strict eigenvalue convergence criteria, indicative of the standard deviation in MCNP, and using very small concentrations of boron, a linear extrapolation of the two data points can then determine the prompt neutron lifetime with no boron atoms present. Boron concentrations of  $7.5 \times 10^{-8}$  and  $1.5 \times 10^{-7}$  atoms / barn-cm were chosen because they are small enough such that they will not perturb other reactor parameters. This changes the moderator (water) density to 0.100279965 and 0.10028004 atoms / barn-cm.

## CHAPTER 6

### RESULTS

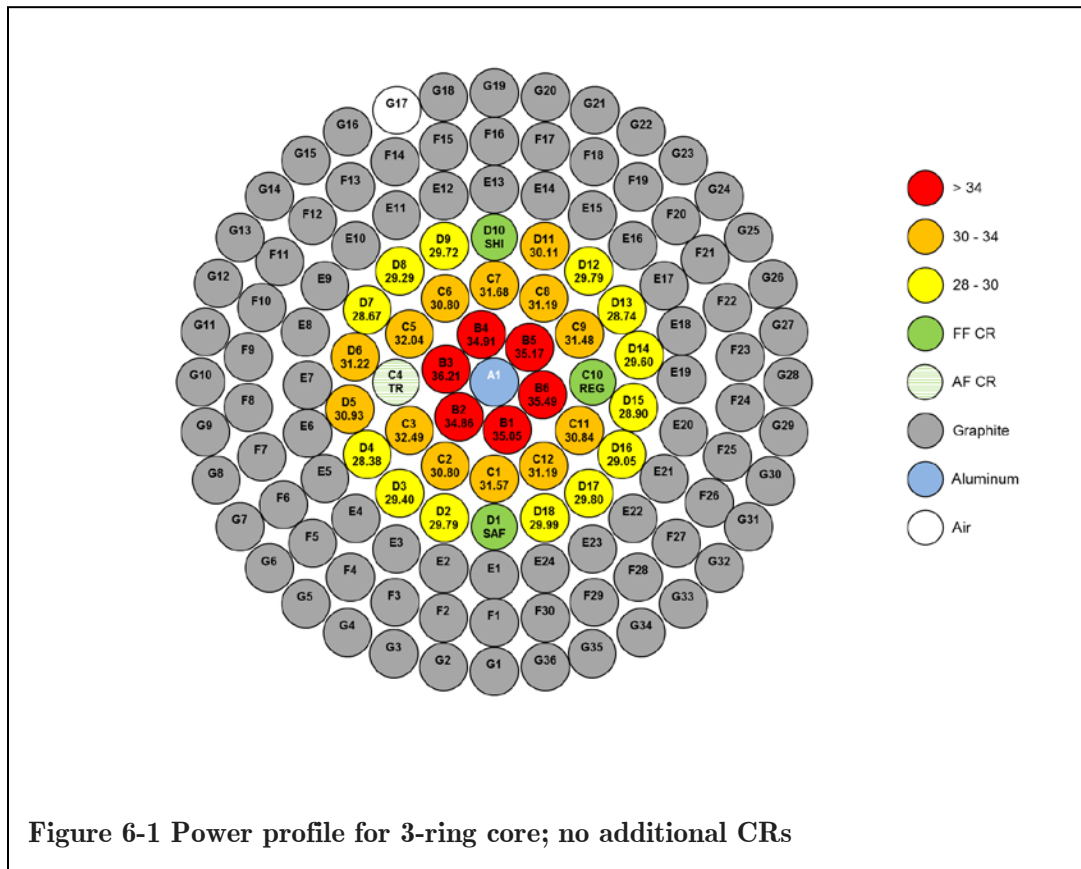
A variety of core designs were examined using MCNP5. Initial results suggested that we focus on small cores with no driver assemblies (non-target fuel). The two general core layouts analyzed were: 1) loading the inner B, C, and D rings with target elements (the 3-ring core) and 2) loading the inner B, C, D, and E rings with target elements (the 4-ring core). All non-target filled positions contain graphite reflector elements (except those which contain control rods and the source). As licensed, the OSTR can accommodate up to nine control rods, five more than are present in its current operational configuration, and these positions are fixed. With control rods being the lone mechanism of reactivity control, these two generalized cores were examined with and without the additional control rods in place. Also, the additional control rods were modeled as both fuel-followed and air-followed.

#### 6.1 3-Ring Core

Three variants of this core were analyzed, each with 32 LEU targets filling the B, C, and D ring. Position A1 can potentially contain a control rod, thus it was modeled as an aluminum slug (current design), a fuel followed control rod (FFCR), and an air followed control rod (AFCR). The FFCRs contain standard LEU TRIGA fuel ( $\text{UZrH}_{1.6}$ ) in the follower region.

**6.1.1 Power Profile and <sup>99</sup>Mo Production**

The following figures illustrate the power profile across the core in kW per pin followed by the Mo-99 produced per pin in curies. The total power is normalized to 1.1 MW, the highest licensable operating power of the OSTR.



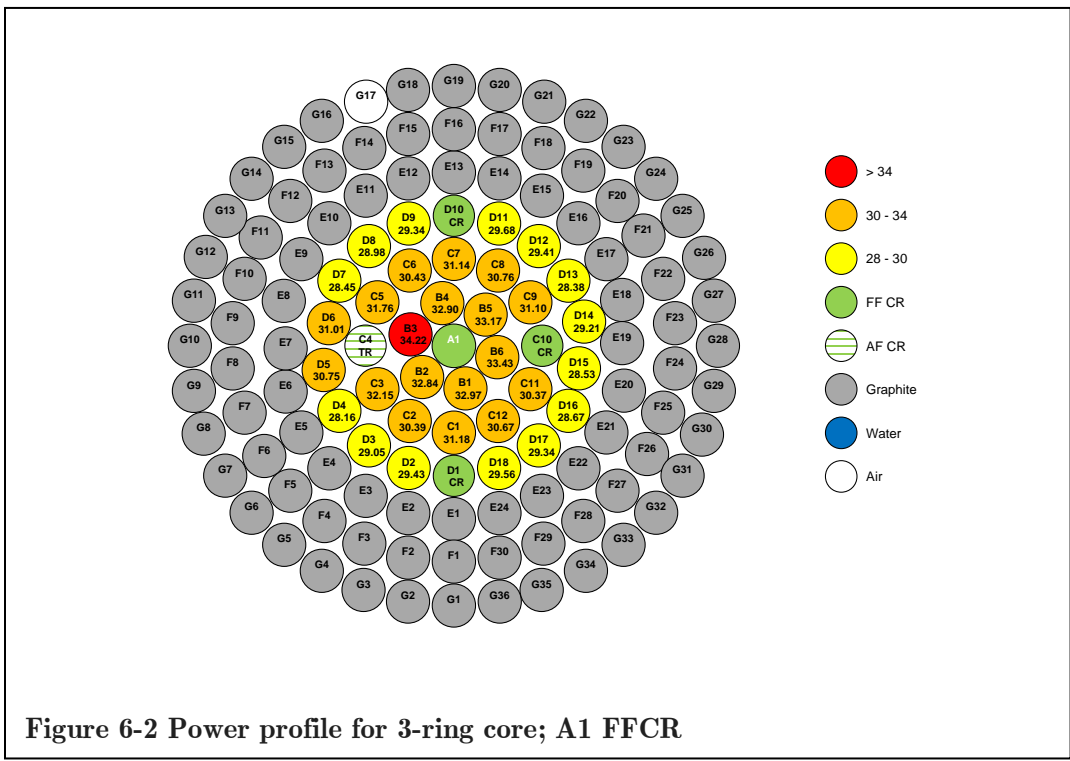


Figure 6-2 Power profile for 3-ring core; A1 FFCR

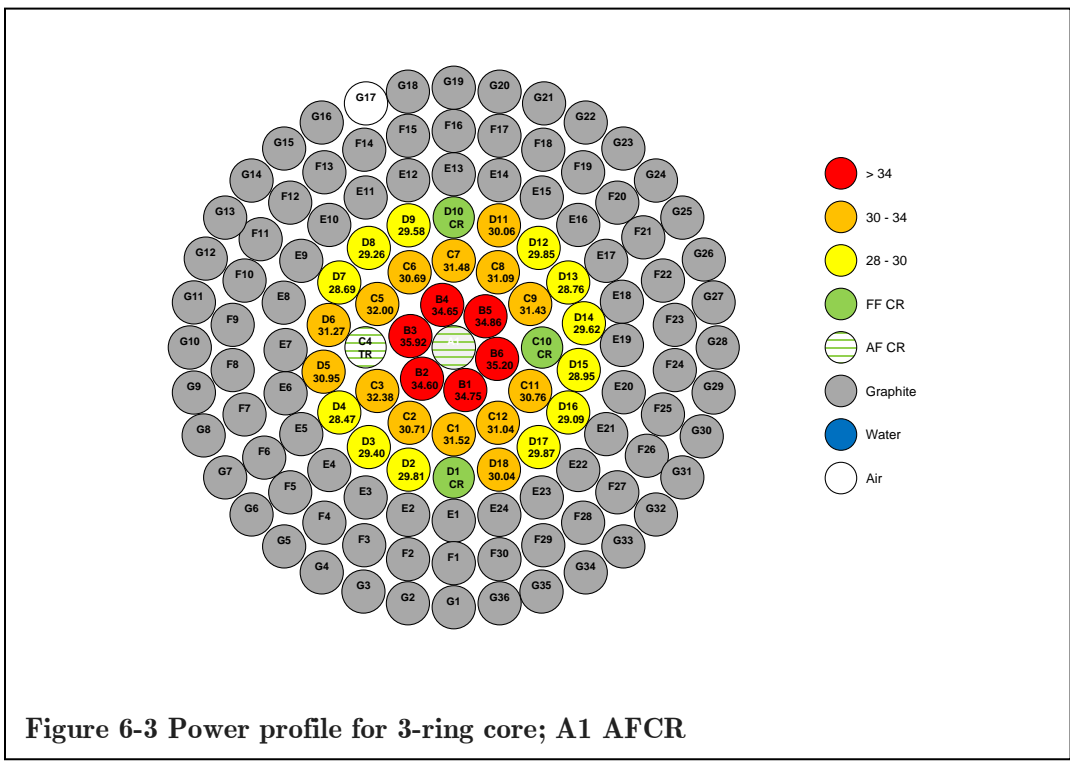


Figure 6-3 Power profile for 3-ring core; A1 AF CR

**Table 6.1 Molybdenum-99 production (Ci) per pin in different 3-ring cores after five days irradiation.**

Target Position	A1 Water-filled	A1 FFCR	A1 AFCR
B1	1435.6	1350.7	1423.3
B2	1428.0	1345.4	1417.3
<b>B3 (max/pin)</b>	<b>1483.0</b>	<b>1401.8</b>	<b>1471.3</b>
B4	1429.8	1347.2	1419.2
B5	1440.7	1358.9	1427.7
B6	1453.6	1369.5	1442.1
C1	1293.4	1277.1	1291.0
C2	1261.5	1244.7	1258.0
C3	1330.8	1316.7	1326.5
C5	1312.3	1301.1	1310.7
C6	1261.5	1246.4	1257.3
C7	1297.8	1275.6	1289.7
C8	1277.7	1260.2	1273.6
C9	1289.4	1273.9	1287.5
C11	1263.3	1244.1	1260.1
C12	1277.6	1256.4	1271.6
D2	1220.2	1205.4	1221.1
D3	1204.2	1189.9	1204.4
D4	1162.3	1153.5	1166.2
D5	1266.9	1259.6	1267.9
D6	1278.7	1270.3	1281.0
D7	1174.5	1165.4	1175.3
D8	1199.8	1187.1	1198.4
D9	1217.3	1201.8	1211.7
D11	1233.3	1215.9	1231.5
D12	1220.2	1204.6	1222.6
D13	1177.1	1162.4	1178.3
D14	1212.7	1196.6	1213.3
D15	1183.8	1168.7	1185.7
D16	1190.0	1174.6	1191.7
D17	1220.6	1201.8	1223.5
D18	1228.3	1210.7	1230.4
<b>Total</b>	<b>40,926.4</b>	<b>40,038.3</b>	<b>40,829.6</b>

**Table 6.2 Molybdenum-99 production in different 3-ring cores**

		Total				Average Per Target			
Core	Irradiation Time (days)	Mo-99 Activity (Ci)	Six-day Ci	Six-day SA (Ci Mo-99 / g Mo)	Total Mo(g)	Mo-99 Activity (Ci)	Six-day Ci	Six-day SA (Ci Mo-99 / g Mo)	Ci Mo-99 / g U-235
A1 slug	5	40926	9008	10085	0.893	1278	281	315	8.09
	7	47335	10419	8332	1.25	1479	325	260	9.36
A1 FFCR	5	40038	8812	10085	0.874	1251	275	315	7.92
	7	46308	10192	8332	1.22	1447	318	260	9.16
A1 AFCR	5	40829	8987	10085	0.891	1275	280	315	8.08
	7	47223	10394	8332	1.25	1475	324	260	9.34

The power decreases radially out from the center of the cores, and the hottest pin and greatest Mo-99 production occur at the B3 position. All control rods are withdrawn such that the center position is either aluminum, air, or  $\text{UZrH}_{1.6}$  fuel. Because the power is limited to a maximum of 1.1 MW and normalized over all fission (power) generating elements, the power generated per pin in the core with aluminum or air occupying the A1 position will be greater than in the core with a FFCR in the A1 position. Aluminum compared to air will lead to a slight increase in the thermalization in the center of the core since the neutrons basically stream unabated through air. However, the neutron absorption cross section of aluminum is much higher than that of air, and this should flatten the flux profile across the core. The peak to average power ratio for the cores with no additional CRs, a FFCR in position A1, and an AFCR in position A1 are

1.183, 1.147, and 1.177 respectively. This is expected since the addition of a CR, even when fully withdrawn, will slightly depress the flux in the center of the core. Additionally, power is generated in the fuel in the FFCR and the total power is thus normalized over one additional element.

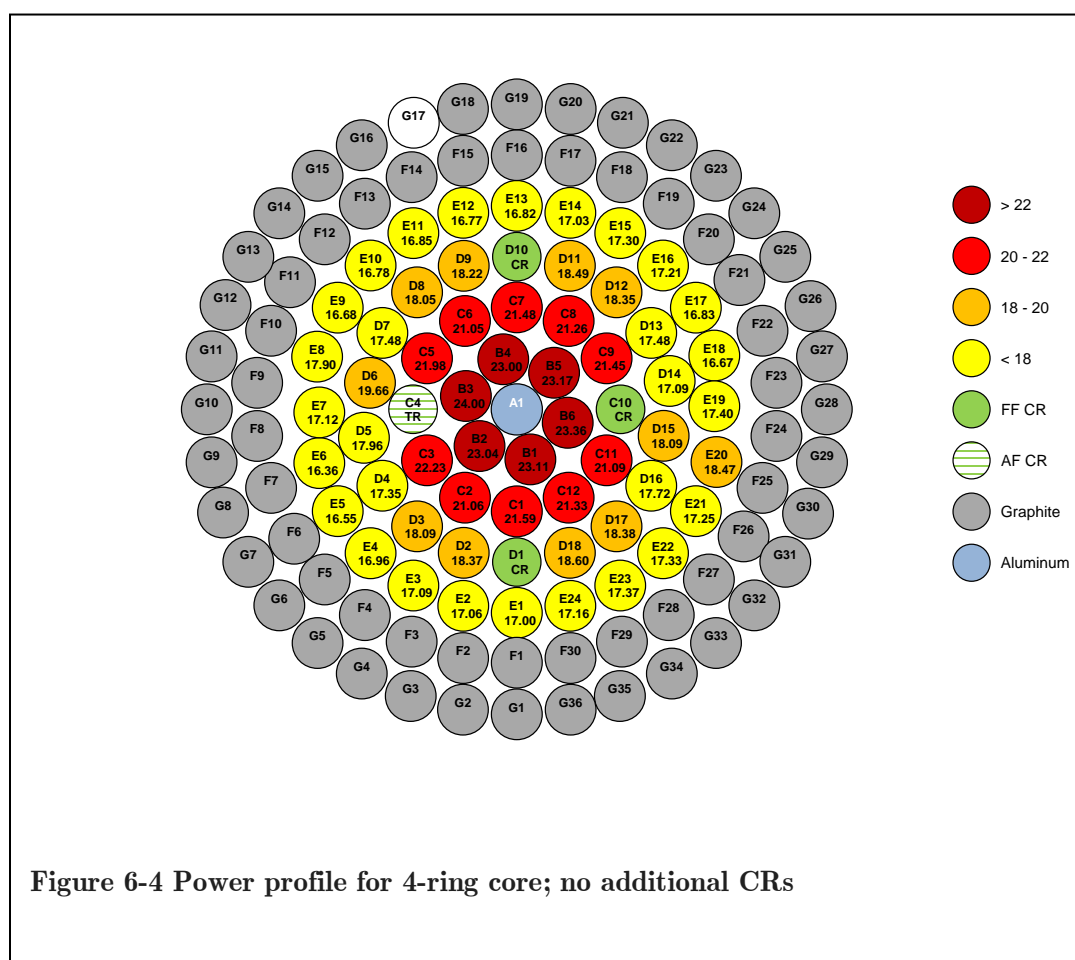
The core with aluminum occupying the A1 position yields a total of ~2.2 % more Mo-99 than the core with a FFCR in the A1 position and ~0.24 % more than the core with the AFCR in the A1 position after 5 days of irradiation. All three cores yield Mo-99 production activities that far exceed the U.S. weekly demand of ~6,000 six-day curies. The curies of Mo-99 produced as a function of Mo mass (SA) and U-235 mass for all three cases are virtually the same given the irradiation time. This is to be expected since the power is normalized to the same constant (1.1 MW), the molybdenum isotopes are bred into the reactor at a constant rate, and the isotope decays at a constant rate.

## **6.2 4-Ring Core**

This core was analyzed in seven different configurations with targets occupying the B, C, D, and E rings. The different cores modeled contain: (1) no additional CRs (the standard core), (2) a CR in the A1 position, (3) CRs in the A1, D12, and D17 positions, and (4) CRs in the A1, D12, D17, E4, and E9 positions. The CRs are examined both as fuel-followed and air-followed.

### 6.2.1 Power Profile and $^{99}\text{Mo}$ Production

The following figures illustrate the power profile across the core in kW per pin followed by the Mo-99 produced per pin in curies. Graphite reflector elements occupy the F and G rings and the power is normalized to 1.1 MW. The standard core contains 56 targets while the others contain either 54 or 52 targets depending on the number of additional control rods present in that specific core configuration.



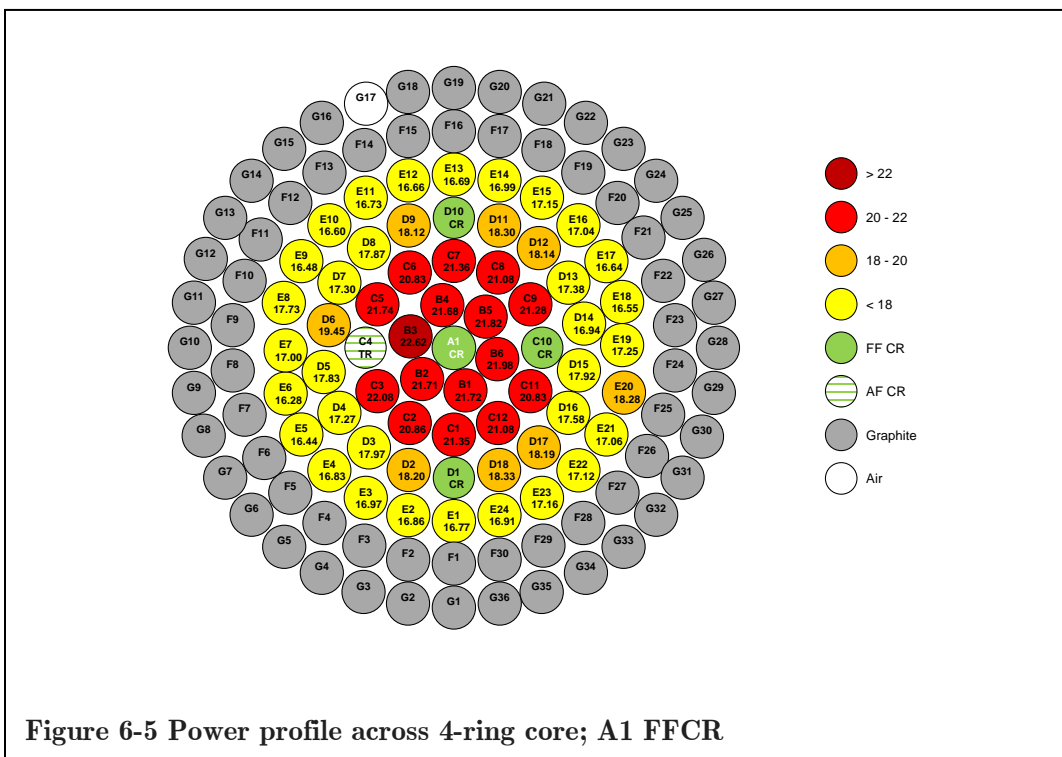


Figure 6-5 Power profile across 4-ring core; A1 FFCR

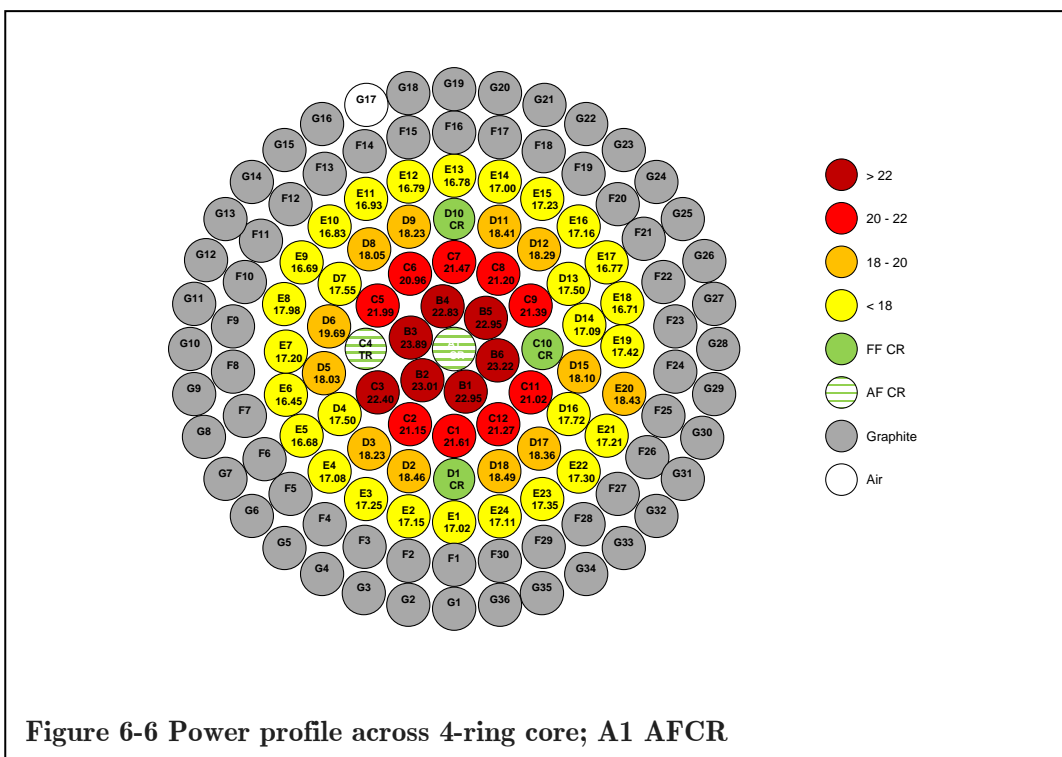


Figure 6-6 Power profile across 4-ring core; A1 AF CR

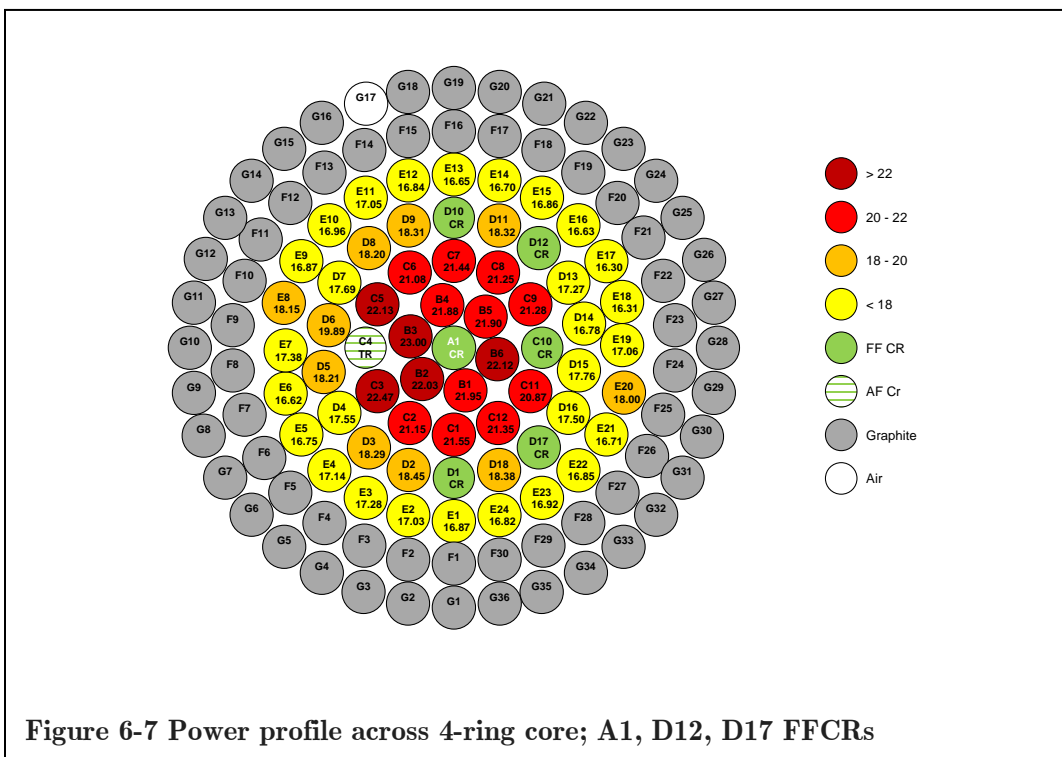


Figure 6-7 Power profile across 4-ring core; A1, D12, D17 FFCRs

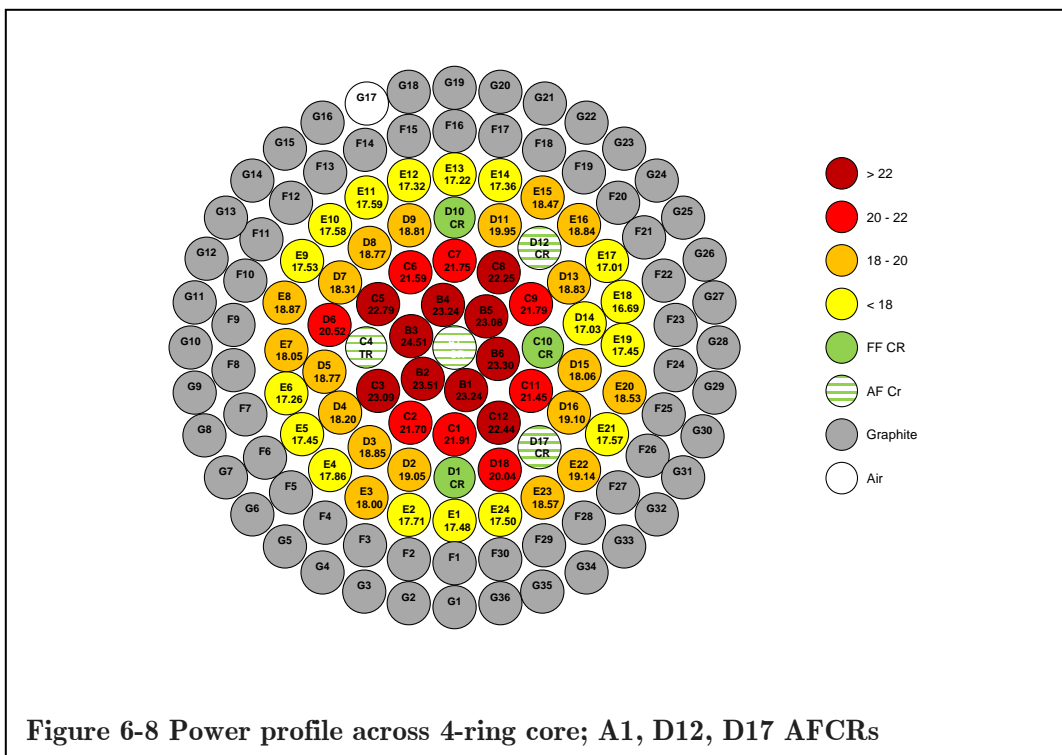


Figure 6-8 Power profile across 4-ring core; A1, D12, D17 AFCRs

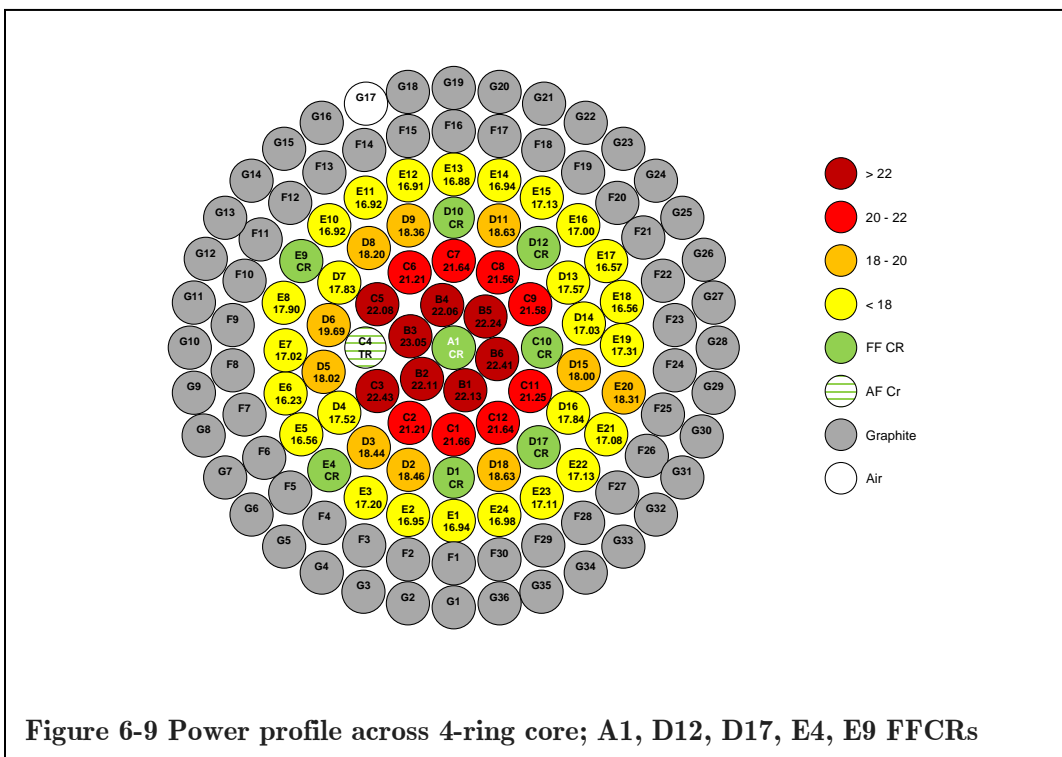


Figure 6-9 Power profile across 4-ring core; A1, D12, D17, E4, E9 FFCRs

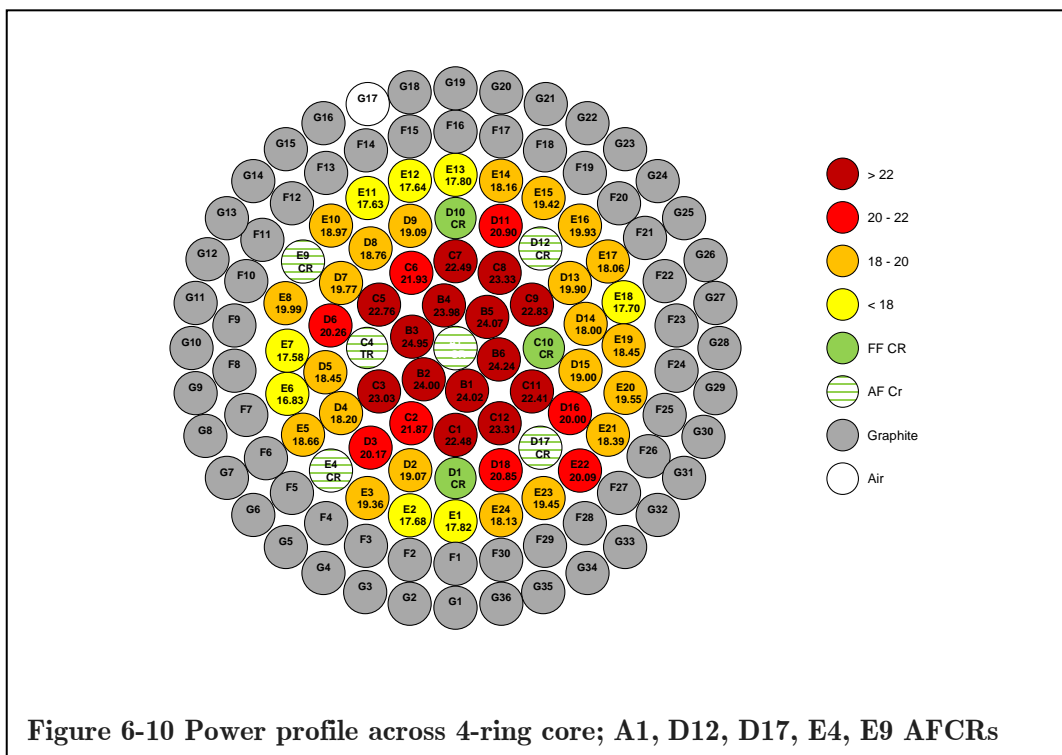


Figure 6-10 Power profile across 4-ring core; A1, D12, D17, E4, E9 AFCRs

**Table 6.3 Molybdenum-99 production (Ci) in different 4-ring cores after 5 days irradiation**

Target Position	A1 water filled	A1 FFCR	A1 AFCR	A1, D12, D17 FFCR	A1, D12, D17 AFCR	A1, D12, D17, E4, E9 FFCR	A1, D12, D17, E4, E9 AFCR
B1	946.59	889.74	939.92	899.20	951.88	906.42	984.07
B2	943.64	889.48	942.53	902.40	963.09	905.83	982.96
B3 (max)	982.90	926.67	978.61	942.13	1003.97	944.10	1022.2
B4	942.22	888.15	935.21	896.06	952.09	903.58	982.29
B5	948.98	893.81	940.23	897.17	945.44	911.05	986.00
B6	956.93	900.36	951.04	906.09	954.53	917.93	992.73
C1	884.57	874.34	885.13	882.93	897.42	887.27	920.88
C2	862.61	854.32	866.18	866.18	888.76	868.83	895.76
C3	910.71	904.27	917.36	920.34	945.76	918.77	943.28
C5	900.52	890.49	900.75	906.43	933.49	904.51	932.23
C6	862.35	853.13	858.71	863.35	884.19	868.81	898.30
C7	879.77	875.01	879.35	878.24	890.95	886.51	921.43
C8	870.91	863.38	868.55	870.38	911.49	883.23	955.69
C9	878.74	871.58	876.14	871.68	892.49	883.98	935.09
C11	864.05	853.28	861.16	854.68	878.49	870.28	917.91
C12	873.75	863.30	871.47	874.45	919.31	886.24	954.63
D2	752.38	745.62	756.26	755.84	780.21	756.02	781.09
D3	740.86	736.17	746.62	749.17	771.95	755.38	826.30
D4	710.54	707.36	716.91	718.74	745.49	717.82	745.38
D5	735.80	730.17	738.58	745.93	768.89	738.11	755.78
D6	805.20	796.85	806.42	814.55	840.37	806.67	830.03
D7	716.12	708.61	718.83	724.45	749.93	730.21	809.72
D8	739.49	732.14	739.18	745.53	769.00	745.47	768.35
D9	746.20	742.14	746.73	750.19	770.65	751.96	782.04
D11	757.32	749.74	754.19	750.58	817.17	763.05	856.30
D12	751.55	743.10	749.24	-	-	-	-
D13	715.98	711.99	716.89	707.57	771.42	719.54	815.13
D14	699.86	693.93	699.99	687.48	697.54	697.73	737.16
D15	740.88	734.07	741.26	727.44	739.96	737.41	778.23
D16	725.74	720.13	725.70	717.01	782.52	730.79	819.28
D17	752.68	745.07	751.94	-	-	-	-
D18	761.88	750.74	757.31	753.07	820.86	763.03	853.94

Target Position	A1 water filled	A1 FFCR	A1 AFCR	A1, D12, D17 FFCR	A1, D12, D17 AFCR	A1, D12, D17, E4, E9 FFCR	A1, D12, D17, E4, E9 AFCR
E1	696.47	686.80	697.17	690.84	715.99	693.96	729.74
E2	698.71	690.72	702.33	697.63	725.35	694.39	724.21
E3	700.22	694.93	706.63	707.74	737.13	704.61	792.95
E4	694.90	689.19	699.77	702.19	731.79	-	-
E5	678.02	673.31	683.42	686.26	714.92	678.35	764.17
E6	670.31	666.86	673.72	680.86	707.12	664.82	689.54
E7	701.11	696.48	704.69	711.75	739.26	697.33	719.97
E8	733.43	726.26	736.69	743.60	773.16	733.29	818.70
E9	683.16	674.96	683.67	691.16	717.96	-	-
E10	687.53	680.07	689.27	694.57	720.25	693.26	776.95
E11	690.14	685.37	6936.52	698.30	720.41	693.17	722.02
E12	687.10	682.23	687.77	689.94	709.33	692.82	722.66
E13	689.01	686.68	687.36	682.18	705.51	691.24	729.32
E14	697.47	695.91	696.50	683.87	711.05	693.73	743.75
E15	708.53	702.50	705.81	690.77	756.50	701.62	795.47
E16	704.78	698.18	702.78	681.39	771.92	696.17	816.18
E17	689.43	681.69	686.89	667.73	696.84	678.94	739.63
E18	682.99	677.91	684.63	668.22	683.64	678.17	724.96
E19	712.71	706.57	713.47	698.77	714.90	709.21	755.73
E20	756.66	748.71	755.03	737.42	759.07	750.18	800.77
E21	706.66	698.85	705.11	684.33	719.51	699.68	753.10
E22	709.92	701.41	708.57	690.33	783.89	701.78	822.87
E23	711.55	703.11	710.82	693.06	760.58	700.80	796.75
E24	703.10	692.60	700.77	688.83	716.87	695.61	742.52
<b>Total</b>	<b>43,155</b>	<b>42,247</b>	<b>43,155</b>	<b>41,241</b>	<b>43,132</b>	<b>40,104</b>	<b>43,066</b>

**Table 6.4 Molybdenum-99 production in different 4-ring cores**

		Total				Average Per Target			
Core	Irradiation Time (days)	Mo-99 Activity (Ci)	Six-day Ci	Six-day SA (Ci Mo-99 / g Mo)	Total Mo(g)	Mo-99 Activity (Ci)	Six-day Ci	Six-day SA (Ci Mo-99 / g Mo)	Ci Mo-99 / g U-235
A1 water (standard)	5	43156	9499	10085	0.942	771	170	180	4.88
	7	49914	10986	8332	1.32	891	196	149	5.64
A1 FFCR	5	42477	9349	10085	0.927	758	167	180	4.80
	7	49129	10813	8332	1.30	877	193	148	5.55
A1 AFCR	5	43154	9499	10085	0.942	771	170	180	4.88
	7	49912	10986	8332	1.32	891	196	149	5.64
A1,D12, D17 FFCR	5	41241	9078	10085	0.900	764	168	187	4.83
	7	47699	10499	8332	1.26	883	194	154	5.59
A1 D12, D17 AFCR	5	43132	9494	10085	0.941	799	176	187	5.06
	7	49886	10980	8332	1.32	924	203	154	5.85
A1, D12, D17, E4, E9 FFCR	5	40104	8827	10085	0.875	771	170	194	4.88
	7	46384	10209	8332	1.23	892	196	160	5.65
A1, D12, D17, E4, E9 AFCR	5	43066	9479	10085	0.940	828	182	194	5.24
	7	49810	10963	8332	1.32	958	211	160	6.06

The addition of a control rod in the A1 position leads to very similar behavior as that seen in the 3-ring core. Without any additional CRs (the standard core) the peak to average power ratio is 1.287, and with the FFCR and AFCR in A1 it is 1.234 and 1.281 respectively.

Replacing two target elements in the D-ring with CRs in addition to a CR at A1 leads to a slight increase in the pin power of the other target elements. In the case of the FFCRs, the fuel followers have a lower power density than the targets resulting in a higher peak to average power ratio of 1.255. This is lower

than the standard core (because of the additional fuel in A1) but higher than configurations with targets occupying the D12 and D17 positions. With the AFCRs, the total power is normalized over fewer elements resulting in a peak to average power ratio of 1.270. However, this ratio is decreasing and can be attributed to the decrease in thermalization. Water would typically occupy the annulus of the targets, and instead the air resembles a void that the neutrons just stream through.

If two additional targets are replaced with CRs in the E-ring, the peak to average power ratio in the AFCR core is now less than in the FFCR core, 1.248 compared to 1.257. These two cores have a total of nine control rods, and the trends for the fuel and air-followed cores remains similar to the two cores examined with seven control rods.

Both the standard core and the core with the AFCR in the A1 position yield the maximum amounts of Mo-99 at roughly 43,155 curies. These two cores have equal numbers of targets, and since the 4-ring core is larger, the decrease in thermalization due to the air present in the A1 position in the center of the core has little effect on the overall Mo-99 yield. The least amount of  $^{99}\text{Mo}$  is produced in the core with FFCRs in the A1, D12, D17, E4, and E9 positions. This difference is  $\sim 7\%$ . The six-day SA is virtually identical in all of the 4-ring and 3-ring cores. Operating at the licensed power of 1.1 MW, the per-target production is much smaller in the 4-ring cores.

### 6.3 Reactor Physics Parameters

The delayed neutron fraction, mean neutron lifetime, moderator coefficient of reactivity, and void coefficient of reactivity for the analyzed cores are shown in the table below. Also included are these quantities for the OSTR in Normal operation mode and the TRIGA at Reed College, both utilizing the standard LEU UZrH<sub>1.6</sub> fuel (Oregon State University n.d., Frantz 2011).

**Table 6.5 Delayed neutron fraction, mean neutron lifetime, moderator COR and void COR for different cores**

Core Configuration	Delayed Neutron Fraction	Mean Neutron Lifetime ( $\mu$ s)	Moderator Coefficient of Reactivity ( $\beta/^\circ\text{C}$ )	Void Coefficient of Reactivity ( $\beta/\%$ )
B_C_D_ring No additional CRs	0.00737	18.92	-1.822	-1.73
B_C_D_ring A1 FF	0.00742	38.49	-1.786	-1.74
B_C_D_ring A1 AF	0.00739	26.00	-1.889	-1.77
B_C_D_E_ring No additional CRs	0.00689	30.75	-1.374	-1.22
B_C_D_E_ring A1 FF	0.00690	26.01	-1.462	-1.24
B_C_D_E_ring A1 AF	0.00737	18.52	-1.511	-1.16
B_C_D_E_ring A1, D12, D17 FF	0.00729	31.93	-1.174	-1.18
B_C_D_E_ring A1 D12, D17 AF	0.00670	23.16	-1.747	-1.31
B_C_D_E_ring A1, D12, D17, E4, E9 FF	0.00717	32.25	-1.374	-1.24
B_C_D_E_ring A1, D12, D17, E4, E9, AF	0.00637	4.356	-1.577	-1.48
OSTR Normal mode BOL	0.0076	22.6	-0.72	-0.96
Reed TRIGA	0.00778	305.1	-0.5688	-0.8300

The delayed neutron fractions for the Mo-99 cores are lower than the normal OSTR core and the TRIGA at Reed. The mean neutron lifetime is longer for all the cores when they have FFCRs as opposed to AFCRs. Since the air basically represents a void, neutrons will stream through these regions, and if they are traveling in an axial direction they will much more likely escape from the core. The mean neutron lifetime is very short, 4.356  $\mu\text{s}$ , for the core with five additional AFCRs. This is most likely attributed to errors in the model, and a further analysis will be examined to discover the discrepancy.

All coefficients of reactivity (COR) should be negative and this is what is observed. The moderator COR becomes more negative as the size of the core is reduced. As the moderator temperature increases the neutron spectrum shifts to higher energies increasing the resonance absorption. The more profound effect results from the decrease in thermalization as the density of water decreases. Since the targets allow for water to flow through the annulus these cores are much more responsive to changes in the moderator density than standard TRIGA cores with solid  $\text{UZrH}_{1.6}$  fuel, providing a valuable negative feedback mechanism. The moderator COR for the 3- and 4-ring cores are roughly 2-2.5 times more negative than the Normal OSTR core and upwards of 3 times more negative than the Reed TRIGA. Figures 6.11 and 6.12 show the moderator COR for the 3 and 4-ring cores respectively over the temperature intervals from 20-40°C, 40-60°C, and 20-60°C. The COR was determined by varying the density of the moderator associated with these temperatures. This was done because evaluated nuclear cross section data is not directly available at these temperatures. The COR is plotted at the midpoint of these temperature ranges.

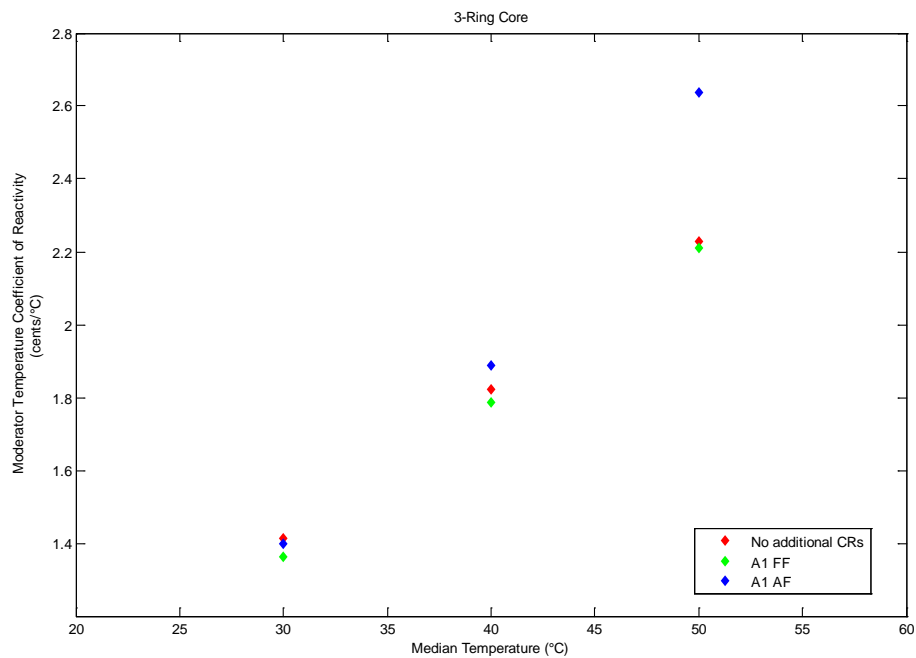


Figure 6-11 Moderator COR for 3-ring cores

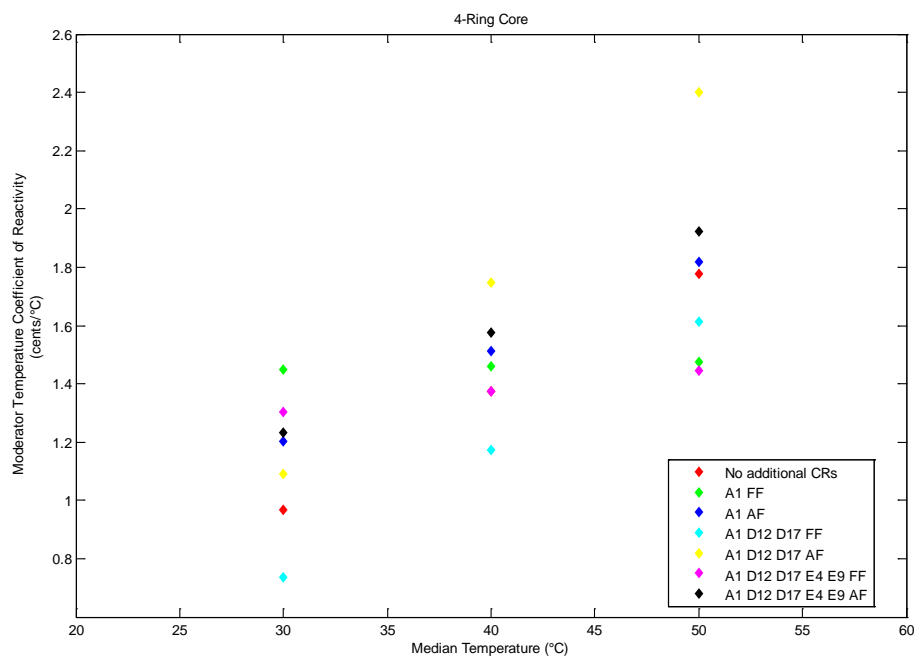


Figure 6-12 Moderator COR for 4-ring cores

A comparable analysis can be made for the void COR. This quantity is given in units of  $\$/\%$  of the core voided. The change of reactivity,  $\$$ , is calculated by comparing the core multiplication with the innermost channel in a completely voided state to that in which it is 10% voided. The volume of the moderator in the inner most channel of the core represents approximately 12.2%, 8.20%, 5.90%, and 8.20% for the 3-ring, 4-ring, Normal OSTR, and Reed TRIGA cores respectively. Although the voided region is a greater percentage by volume for the 3 and 4-ring cores, the loss in reactivity due to the void in the moderator outweighs the difference in volume, again providing a strong negative feedback mechanism. Figures 6.13 and 6.15 show the void COR as the void in the innermost channel incrementally increases from 10-25 %, 25-50 %, 50-75 %, and 75-100 % with the COR graphed at the high end of these ranges. Figures 6.14 and 6.16 show the void COR as the void range increases from 10-100 %, 25-100 %, 50-100 %, and 75-100 % and is graphed compared to the percent difference.

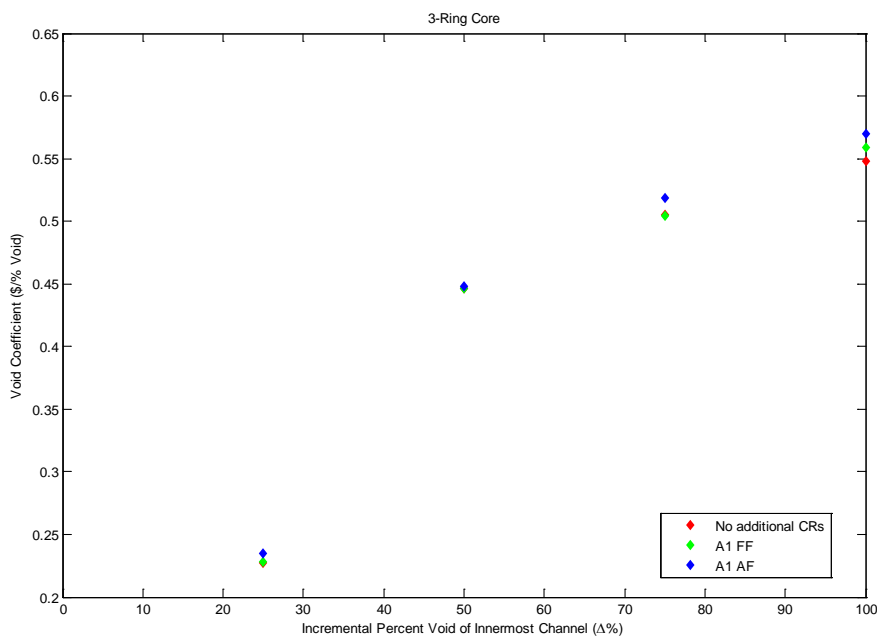


Figure 6-13 Void COR as the void increases incrementally for the different 3-ring cores

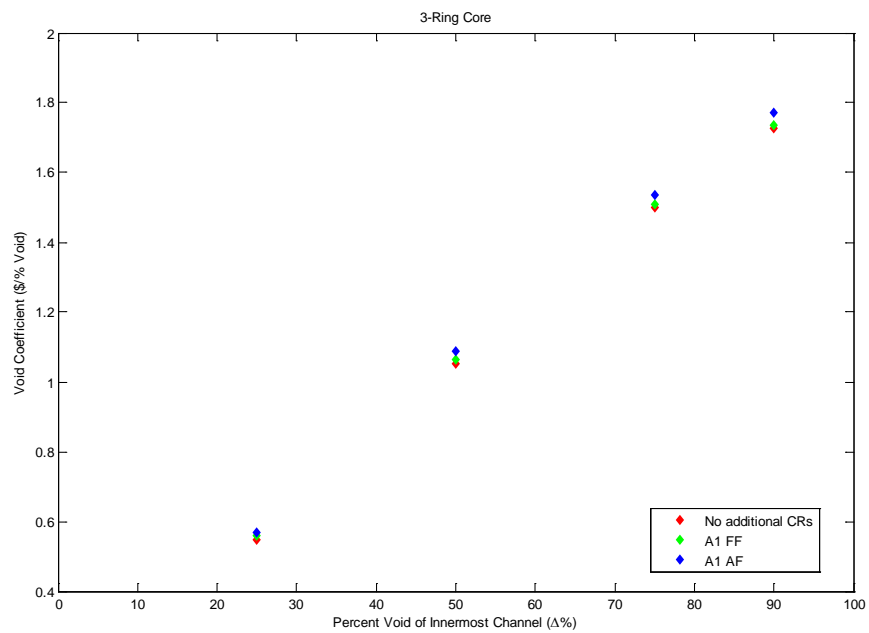


Figure 6-14 Void COR as the total void increases for the different 3-ring cores

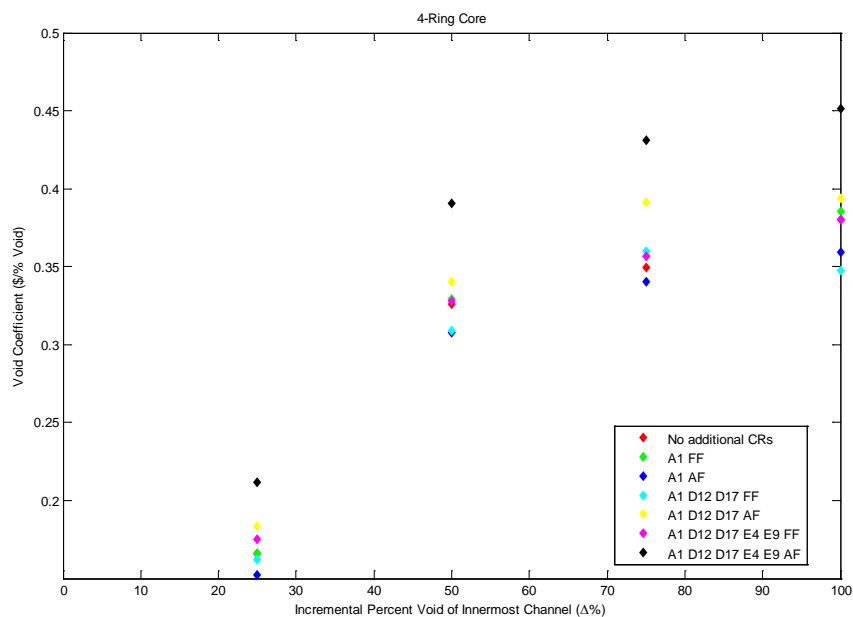


Figure 6-15 Void COR as the void increases incrementally for different 4-ring cores

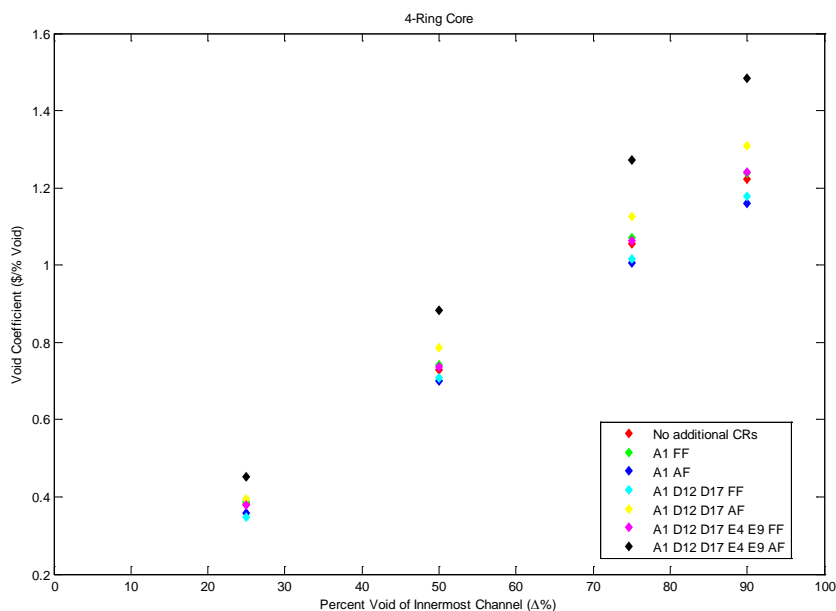


Figure 6-16 Void COR as the total void increases in different 4-ring cores

The prompt temperature COR was calculated using two different cross-section libraries. The older library was compiled in 1993 and was used so that a comparison could be made to previously published results from the Normal OSTR. The newer library contains cross section information evaluated primarily in 2006 and the temperature range is greater. Five temperatures for each library were simulated with all control rods out of the reactor. The prompt temperature COR was calculated over each temperature interval at the mid-point. The results using the old and new libraries are tabulated in Tables 6.6 and 6.7 respectively followed by graphical representations of the magnitudes (absolute values) of the CORs versus the median temperature between the data points.

Using the old cross section library, this COR is positive in two cases, both occurring at 77°C. When switching to the newer cross-section data, which has

been evaluated at slightly different temperatures and thus the temperature intervals are different, the COR is negative. In the Normal OSTR core with LEU fuel, the fuel temperature COR becomes more negative as the fuel temperature increases. This property of the UZrH fuel is one of the key inherent safety features of TRIGA reactors. In all of the cores examined, the prompt temperature COR generally becomes less negative as the temperature in the fuel increases, but it is nonetheless still negative. The fuel temperature COR for the cores examined here is roughly an order of magnitude less than the Normal OSTR core over the same temperature intervals. Figures 6.12 and 6.13 show the fuel temperature COR for the 3-ring cores using the old and new cross-section libraries respectively, and Figures 6.14 and 6.15 show the fuel temperature COR for the 4-ring cores using the old and new cross-section libraries respectively.

**Table 6.6 Prompt fuel temperature COR ( $(\Delta k/k)/^{\circ}\text{C}$ ) using old nuclear library**

Core configuration	77 °C	227 °C	427 °C	727 °C
B_C_D_ring No additional CRs	$-4.27 \times 10^{-4}$	$-1.12 \times 10^{-3}$	$-9.38 \times 10^{-4}$	$-8.24 \times 10^{-4}$
B_C_D_ring A1 FF	$-2.34 \times 10^{-4}$	$-1.04 \times 10^{-3}$	$-1.04 \times 10^{-3}$	$-9.42 \times 10^{-4}$
B_C_D_ring A1 AF	$-1.64 \times 10^{-4}$	$-9.19 \times 10^{-4}$	$-1.19 \times 10^{-3}$	$-9.24 \times 10^{-4}$
B_C_D_E_ring No additional CRs	$-7.18 \times 10^{-5}$	$-9.76 \times 10^{-4}$	$-1.01 \times 10^{-3}$	$-8.90 \times 10^{-4}$
B_C_D_E_ring A1 FF	$-4.30 \times 10^{-4}$	$-1.12 \times 10^{-3}$	$-9.03 \times 10^{-4}$	$-7.03 \times 10^{-4}$
B_C_D_E_ring A1 AF	$-3.02 \times 10^{-4}$	$-1.18 \times 10^{-3}$	$-9.34 \times 10^{-4}$	$-7.14 \times 10^{-4}$
B_C_D_E_ring A1, D12, D17 FF	$-5.36 \times 10^{-4}$	$-1.04 \times 10^{-3}$	$-8.54 \times 10^{-4}$	$-6.81 \times 10^{-4}$
B_C_D_E_ring A1, D12, D17 AF	$1.77 \times 10^{-4}$	$-1.10 \times 10^{-3}$	$-1.12 \times 10^{-3}$	$-7.89 \times 10^{-4}$
B_C_D_E_ring A1, D12, D17, E4, E9 FF	$-2.99 \times 10^{-4}$	$-1.07 \times 10^{-3}$	$-9.58 \times 10^{-4}$	$-6.19 \times 10^{-4}$
B_C_D_E_ring A1, D12, D17, E4, E9 AF	$1.28 \times 10^{-4}$	$-1.17 \times 10^{-3}$	$-7.23 \times 10^{-4}$	$-9.10 \times 10^{-4}$

**Table 4.7 Prompt fuel temperature COR ( $(\Delta k/k)/^{\circ}\text{C}$ ) using new nuclear library**

Core configuration	173.5 °C	477 °C	777 °C	1577 °C
B_C_D_ring No additional CRs	$-1.09 \times 10^{-3}$	$-9.38 \times 10^{-4}$	$-8.55 \times 10^{-4}$	$-6.90 \times 10^{-4}$
B_C_D_ring A1 FF	$-1.33 \times 10^{-3}$	$-7.86 \times 10^{-4}$	$-8.09 \times 10^{-4}$	$-6.50 \times 10^{-4}$
B_C_D_ring A1 AF	$-1.28 \times 10^{-3}$	$-1.12 \times 10^{-3}$	$-5.64 \times 10^{-4}$	$-6.55 \times 10^{-4}$
B_C_D_E_ring No additional CRs	$-1.13 \times 10^{-3}$	$-9.17 \times 10^{-4}$	$-8.45 \times 10^{-4}$	$-6.45 \times 10^{-4}$
B_C_D_E_ring A1 FF	$-1.12 \times 10^{-3}$	$-9.70 \times 10^{-4}$	$-6.99 \times 10^{-4}$	$-6.11 \times 10^{-4}$
B_C_D_E_ring A1 AF	$-1.19 \times 10^{-3}$	$-7.65 \times 10^{-4}$	$-8.47 \times 10^{-4}$	$-6.28 \times 10^{-4}$
B_C_D_E_ring A1, D12, D17 FF	$-1.12 \times 10^{-3}$	$-8.04 \times 10^{-4}$	$-9.20 \times 10^{-4}$	$-5.29 \times 10^{-4}$
B_C_D_E_ring A1, D12, D17 AF	$-1.16 \times 10^{-4}$	$-8.52 \times 10^{-4}$	$-9.02 \times 10^{-4}$	$-6.05 \times 10^{-4}$
B_C_D_E_ring A1, D12, D17, E4, E9 FF	$-1.25 \times 10^{-3}$	$-8.06 \times 10^{-4}$	$-8.42 \times 10^{-4}$	$-5.71 \times 10^{-4}$
B_C_D_E_ring A1, D12, D17, E4, E9 AF	$-1.40 \times 10^{-3}$	$-8.36 \times 10^{-4}$	$-7.00 \times 10^{-4}$	$-6.48 \times 10^{-4}$

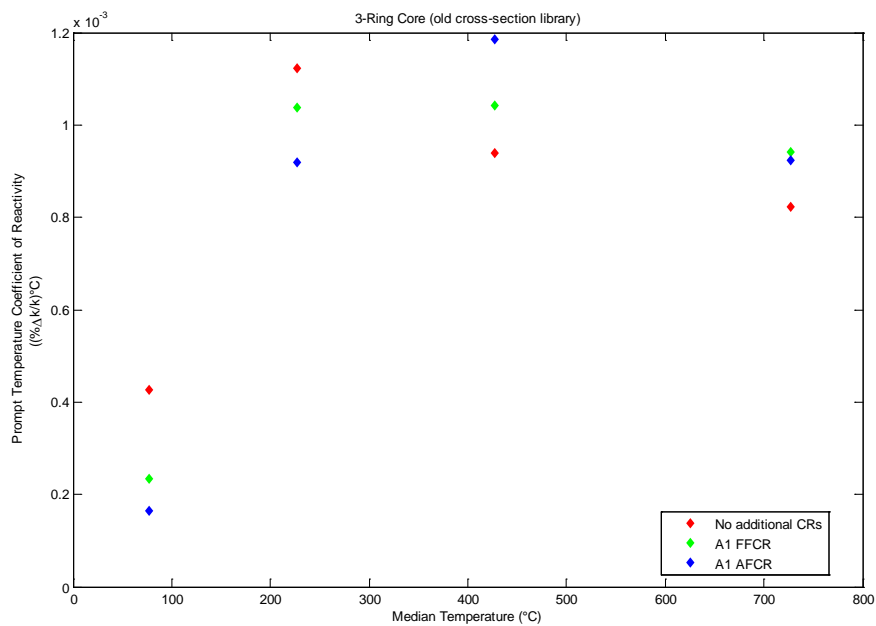


Figure 6-17 Prompt fuel temperature COR for 3-ring cores (old library)

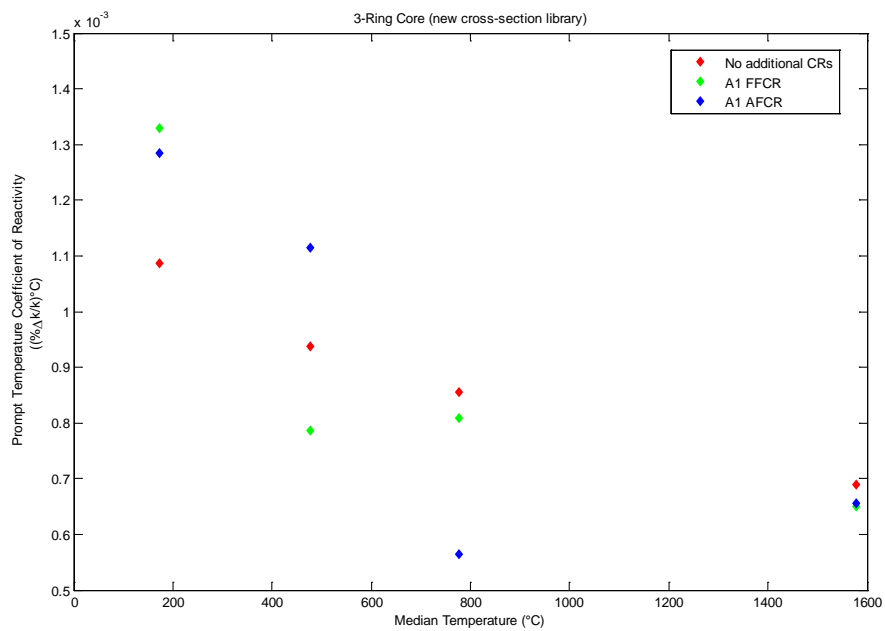


Figure 6-18 Prompt fuel temperature COR for 3-ring cores (new library)

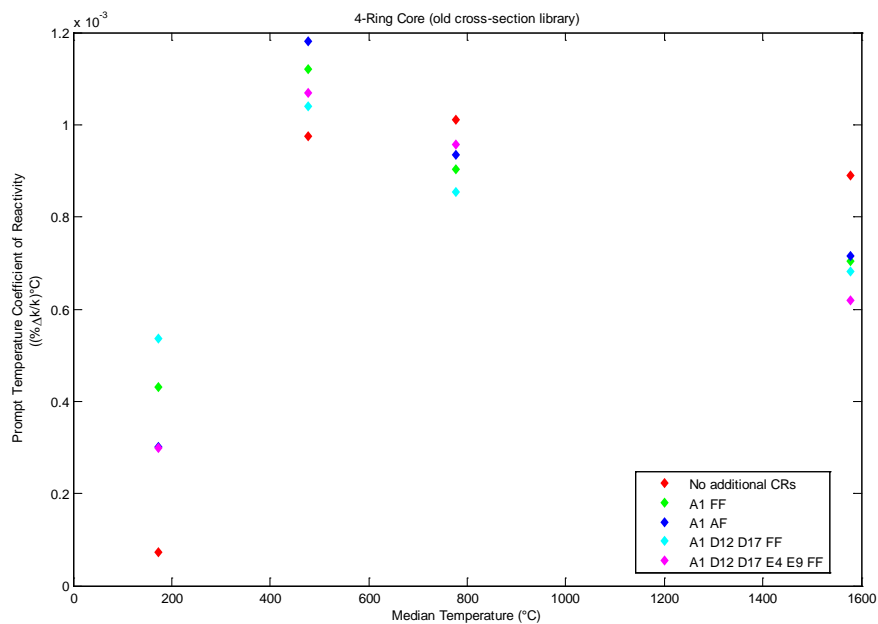


Figure 6-19 Prompt fuel temperature COR for 4-ring cores (old library)

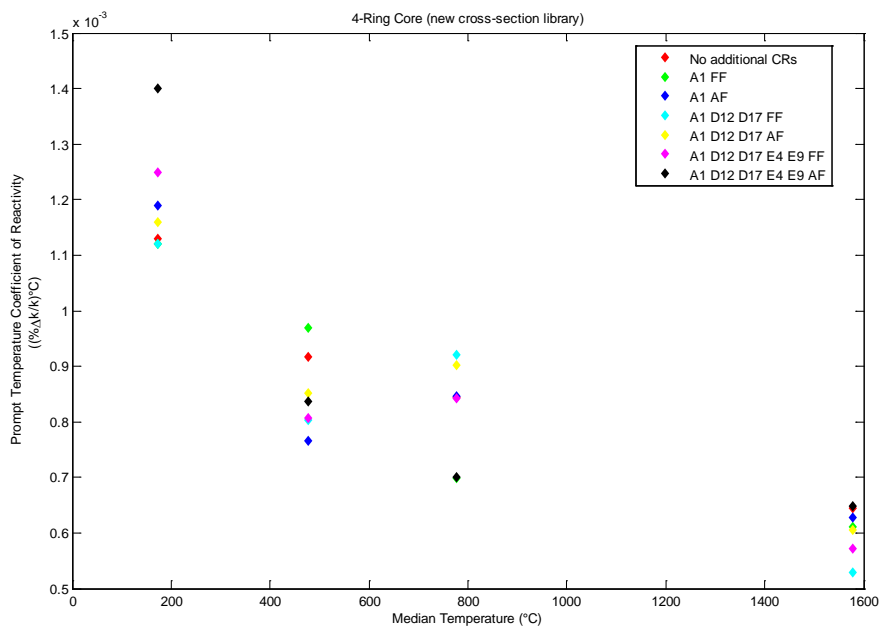


Figure 6-20 Prompt fuel temperature COR for 4-ring cores (new library)

The total rod worth, excess reactivity, and shutdown margin were calculated by comparing the core multiplication factors with the control rods completely withdrawn and fully inserted. In the case of an accident involving one of the control rods becoming stuck out of the core and no longer available for insertion, the shutdown margin was also calculated with the most reactive rod withdrawn. The regulatory rod is the most reactive rod and is modeled as withdrawn for each cores. These results are shown in Table 6.8.

**Table 6.8 Total rod worth, excess reactivity, and shutdown margin**

Core configuration	Total Rod Worth (\$)	Excess Reactivity (\$)	Shutdown Margin (\$)	Shutdown Margin with Reg rod out (\$)
B_C_D_ring No additional CRs	18.2	2.33	15.9	8.79
B_C_D_ring A1 FF	26.6	2.80	23.8	16.4
B_C_D_ring A1 AF	26.7	2.00	24.3	16.8
B_C_D_E_ring No additional CRs	12.5	16.8	-4.36	-10.2
B_C_D_E_ring A1 FF	16.7	16.9	-0.275	-5.00
B_C_D_E_ring A1 AF	16.6	16.6	-0.0586	-4.59
B_C_D_E_ring A1, D12, D17 FF	22.4	16.3	6.06	2.53
B_C_D_E_ring A1 D12, D17 AF	22.0	15.3	6.74	3.34
B_C_D_E_ring A1, D12, D17, E4, E9 FF	27.8	15.9	12.0	7.41
B_C_D_E_ring A1, D12, D17, E4, E9, AF	27.2	13.9	13.3	9.51

All of the 3-ring cores have sufficient negative reactivity to shut down even when the regulatory rod is fully withdrawn. However, the 4-ring cores with no additional control rods and a control rod in the A1 position do not have enough negative reactivity to shut down. The amount of positive reactivity in the 4-ring cores warrants the addition of at least three more control rods. The four configurations of the 4-ring core with seven and nine total control rods provide sufficient negative reactivity to shut down, and these along with all the 3-ring cores have greater than the \$0.55 requirement set forth in the Technical Specifications . The Safety and Analysis Report for the LEU core lists the shutdown margin as ~ \$1.21 at the beginning of core life (Oregon State University n.d.). The seven controllable cores are more than double this value.

#### **6.4 Minimum Critical Heat Flux Ratio**

A thermal hydraulic analysis of the OSTR core was carried out when the core was converted from HEU to LEU fuel. This analysis used RELAP5-3D to predict the MCHFR for a  $\text{UZrH}_{1.6}$  fuel element at various powers (Marcum, et al. 2009, RELAP5-3D Code Manual 2005). The maximum power examined for the  $\text{UZrH}_{1.6}$  fuel element was 35 kW. More recently, similar work has been done at Oregon State University to analyze the MCHFR associated with the  $\text{UO}_2$  Mo-99 targets. This analysis analyzed the Mo-99 targets at a maximum of 20 kW (Byfield 2013). At 10, 15, and 20 kW per  $\text{UZrH}_{1.6}$  fuel element, the MCHFRs are roughly 4.5, 3, and 2, respectively. At 10, 15, and 20 kW per Mo-99 target elements, the

MCHFRs are roughly 11.22, 7.27, and 5.28, respectively. At the same power per fuel element/target, the MCHFRs are 2.5, 2.4, and 2.6 times greater for the Mo-99 targets than for the  $\text{UZrH}_{1.6}$  fuel elements.

The maximum pin power observed in the Mo-99 cores was 36 kW in the 3-ring core with no additional control rods. At the maximum power of 35 kW per  $\text{UZrH}_{1.6}$  fuel element analyzed during the HEU to LEU conversion study, the MCHFR was found to be 1. It is reasonable to then assume that at a power of 36 kW for the Mo-99 targets that the MCHFR will more than double. This would put the MCHFR for the Mo-99 targets at a value greater than 2.

Because the power distribution varies axially along the target elements, the target located at the B3 position was partitioned into 20 different axial nodes to observe the change in power. The power per axial node is shown in Figure 6-21. The power takes the form of a cosine shape, and the peak power occurs in the center of the target where the flux is greatest. For a conservative estimate, if the maximum power observed of 2.35 kW in node 10 is taken to be the average power per node, then the total power in the target is approximately 47 kW. A correlation cannot be made between this pin power and those used in the prior studies and would require further analysis to better determine the MCHFR.

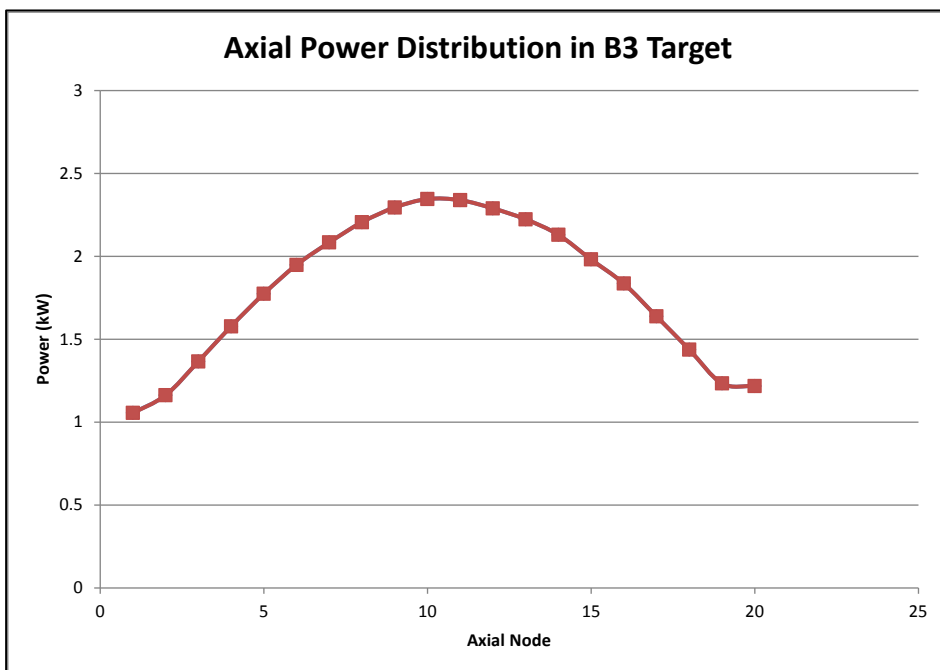


Figure 6-21 Axial power distribution in B3 target of standard 3-ring core

## CHAPTER 7

### DISCUSSION

The OSTR was used as the design basis for the Mo-99 cores examined, and the MCNP5 simulation package was utilized to perform this analysis. Both the Normal OSTR core and the Mo-99 cores examined are fueled with LEU. The two primary differences in the fuel and targets are the composition and design. The Normal OSTR core uses  $\text{UZrH}_{1.6}$  as the fuel material while the Mo-99 cores utilize  $\text{UO}_2$ , which acts as both the fuel and target material. The annular design of the targets allows for the coolant/moderator to flow through the center of the Mo-99 targets, whereas the  $\text{UZrH}_{1.6}$  fuel design does not. The Normal OSTR core contains 87 fuel elements that are designed to last for the operational life-time of the OSTR. The Mo-99 cores examined contain 32, 52, or 54 targets, making the Mo-99 cores much smaller than the Normal OSTR core, and these targets will be processed after a five to seven day irradiation cycle. Additional control rods were examined in the Mo-99 cores to control the reactivity present. The additional air-followed and fuel-followed control rods examined are identical in design to the current control rods in the core.

All seven viable designs (those that can shutdown) yield well over the roughly 6000 six-day curie weekly US demand after 5 days of irradiation. An analysis performed at Sandia National Laboratory (SNL) utilizing the Annular Core Research Reactor (ACRR) as the design basis and LEU  $\text{UO}_2$  pin targets

conservatively concluded that approximately 112 of their targets would need to be processed weekly to meet the US demand (Parma, Coats and Dahl 2010). This number assumes a core with 125 targets and an average pin power of 10 kW, and roughly 16 targets would be processed daily.

Current HEU targets used at the BR2 reactor yield up to 1000 Ci Mo-99 per target after 6.25 days of irradiation (Ponsard 2007). This amounts to roughly 220 six-day curies, which is slightly less than the per target production in the 3-ring core and slightly more than the per target production in the 4-ring core. The LEU foil targets analyzed for use in the Tajoura Reactor in Libya are projected to yield approximately 203 Ci Mo-99 per target (Bsebsu and Elwaer n.d.).

In this analysis the maximum pin power observed is 36.2 kW and occurs in the B3 position of the standard 3-ring core. Conclusions made off prior work at OSU validate the assumption that the MCHFR be greater than 2 at this operating power. Since coolant can flow through the center of the UO<sub>2</sub> targets, they have roughly two times the surface area in contact with the coolant. Although the OSTR is a natural convection cooled research reactor, for which there is no regulatory limit on MCHFR, forced convection cooled research reactors must have a minimum value of 2.0. Thus from both a regulatory and safety standpoint the pin power does not appear to be an issue.

The maximum power per pin in the 4-ring core also occurs at the B3 position and measures 24.95 kW. Since the seven viable cores (those with an

adequate shutdown margin) all produce more than enough Mo-99 to satisfy the United States' weekly demand of ~6000 curies, the structural integrity of the targets under these irradiation conditions becomes the primary limiting factor. There is no need to operate at a higher power since the isotope demand is clearly met operating at the licensable 1.1 MW, and increasing the power would only further stress the safety limitations of the targets. Operating at a lower power may be necessary, but again, this would depend on the structural integrity of the targets not being able to withstand the observed pin powers.

## **CHAPTER 8**

### **CONCLUSIONS AND FUTURE WORK**

#### **8.1 Conclusions**

This analysis has shown that a small low-power research reactor such as the OSTR can produce viable quantities of the medical radio-isotope Mo-99. The Mo-99 cores that were analyzed can all yield quantities of Mo-99 that would satisfy the US weekly demand. The reactor physics parameters of the different Mo-99 cores examined demonstrate that seven of the ten cores can operate safely. The moderator, void, and fuel temperature coefficients of reactivity are all negative, providing the necessary feedback during a departure from steady-state operation. For the larger 4-ring cores, additional control rods would be required in order to maintain the proper shutdown margin. As licensed, the OSTR can accommodate five additional control rods in conjunction with the regulatory, transient, shim, and safety rods it currently operates with. Based off this analysis, the Mo-99 cores examined would be readily licensable.

#### **8.2 Recommendations for Future Work**

The primary focus on future work should center on the operational cycle of the Mo-99 reactors. If the core is to be completely unloaded after a set irradiation time, then the targets will always be fresh, or 'clean'. However, it may be advantageous to unload and process some of the targets on a daily basis or

every few days. If a processing facility can only handle so many targets at once, then it would be fruitless to remove more targets from the core than needed. This would lead to cores having both fresh and irradiated targets. To optimize the Mo-99 production, a future analysis should determine how the fresh targets would be loaded into the core.

Additionally, not all of the control rods need to be inserted into the core to operate. It may prove optimal to limit which control rods are used to control the reactivity under steady-state operation. The control rods not used would only be employed in an emergency shutdown situation. Integral rod worth calculations should be performed for the moveable control rods.

Future work should include an in depth economic feasibility study. This will include the target fabrication costs, construction of a processing facility, transportation to the processing facility if there is no facility on site, and the costs associated with extracting the Mo-99 and constructing the necessary Tc-99m generators.

Finally, it may be necessary to perform additional thermal-hydraulic analyses of the targets. Although we believe the targets will remain above the minimum critical heat flux ratio of two, the targets were not actually analyzed at the high powers observed in this work.

## BIBLIOGRAPHY

- Adelfang, P., L. Alvarez, and E. Pasqualini. "RERTR Activities in Argentina." *24th International Meeting on RERTR*. Bariloche, Argentina, 2002.
- Alberman, Alain, et al. *Scenario for Sustainable Molybdenum-99 Production in Europe*. European Research Reactor Position Paper, CEA, IRN, NRG, RCR, SCK-CEN, POLATOM, and TUM, 2011.
- Alferov, V. P., E. F. Kryuchkov, and M. V. Shchurovskaya. "Feasibility Studies for LEU Conversion of the IRT MEFi Reactor Using U-Mo Tubular Fuel." *33rd International Meeting on RERTR*. Santiago, Chile, 2011.
- Anderson, T.V. *Oregon State TRIGA Reactor Training Manual Volume #1*. Corvallis, OR: Oregon State University, 2010.
- Arino, H., F. J. Cosolito, K. D. George, and A. K. Thornton. Preparation of a primary target for the production of fission products in a nuclear reactor. U.S. Patent US3940318 A. February 24, 1976.
- Arino, H., H. Kramer, J. McGovern, and A. Thornton. Production of high purity fission product molybdenum-99. U.S. Patent US3799883 A. March 26, 1974.
- Bakel, A., et al. "Overview of Progress Related to Implementation of the LEU-Modified CINTICHEM Process." *30th International Meeting on RERTR*. Washington D. C., 2008.
- Ball, R., V. Pavshook, and V. Y. Khvostionov. "Present Status of the Use of LEU in Aqueous Reactors to Produce Mo-99." *1998 International Meeting on Reduced Enrichment for Research and Test Reactors*. Sao Paulo, Brazil, 1998. 18-23.

- Banerjee, Sharmila, Maroor Raghavan Ambikalmajan Pillai, and Natesan Ramamoorthy. "Evolution of Tc-99m in Diagnostic Radiopharmaceuticals." *Seminars in Nuclear Medicine*, 2001: 260-277.
- Baranaev, Y. D., N. A. Nerozin, V. A. Pivovarov, and E. y. Smetanin. *Medical Complex for Radioisotope Production*. Obninsk, Russian Federation: Institute of Physics and Power Engineering (IPPE), 2008.
- Baum, E. M., H. D. Knox, and T. R. Miller. *Nuclides and Isotopes, Chart of the Nuclides*. Lockheed Martin, 2002.
- Bio-Tech Systems, Inc. *The U.S. market for diagnostic radiopharmaceuticals (No.250)*. Las Vegas: Bio-Tech Systems, Inc., 2006.
- Bradley, E. "IAEA activities to support the transition of Mo-99 production away from the use of HEU." *2010 Reduced Enrichment for Research and Test Reactors meeting*. Lisbon, Portugal, 2010.
- Bretscher, M. M. *Perturbation-Independent Methods for Calculating Research Reactor Kinetic Parameters*. Argonne: Argonne National Laboratory, December 1997.
- Bsebsu, F. M., and S. Elwaer. *Feasibility Study Part-II Theoretical Calculations of Fission Mo-99 Production by the Irradiation of LEU Metallic Uranium Foil at Tajoura Research Reactor*. Tripoli, Libya: Renewable Energies and Water Desalination Research Center, n.d.
- Bsebsu, F. M., F. Abotweirat, and S. Elwaer. "Feasibility Study Part-I Thermal Hydraulic Analysis of LEU target for Mo-99 Production in Tajoura Reactor." *2007 RERTR International Meeting*. Prague, Czech Republic, 2007.

- Buchholz, B. A., and G. F. Vandegrift. "Processing of LEU Targets for Mo-99 Production - Dissolution of U<sub>3</sub>Si<sub>2</sub> Targets by Alkaline Hydrogen Peroxide." *1995 International Meeting on RERTR*. Paris, France, 1995.
- Cacciapuoti, B. "Radioactive Isotopes of Element 43." *Physical Review*, 1939: 110.
- Caldwell, J. T., E. J. Dowdy, B. L. Berman, R. A. Alvarez, and P. Meyer. "Giant resonance for the actinide nuclei: Photoneutron and photofission cross sections for U-235, U-236, U-238, and Th-232." *Physical Review C*, 1980: 1215-1231.
- CEA. *The Jules Horowitz Reactor: General description*. 2009.  
<http://www.cad.cea.fr/rjh/general-description.html> (accessed February 20, 2012).
- Cestau, D., et al. "HEU and LEU Comparison in the Production of Molybdenum-99." *2007 International RERTR Meeting*. Prague, Czech Republic: Argonne National Laboratory, 2007.
- CNEA. "Argentina's Nuclear Panorama of Radioisotopes with LEU - History and Perspective." Buenos Aires, Argentina, November 4.
- Cols, H. J., P. R. Cristini, and A. C. Manzini. "Mo-99 from Low - Enriched Uranium." *2000 International Meeting on RERTR*. Las Vegas, Nevada, 2000.
- Cols, H. J., R. O. Marques, and P. R. Cristini. "Preliminary Investigations on the Use of Uranium Silicide Targets for Fission Mo-99 Production." *1994 International Meeting on RERTR*. Paris, France, 1994.
- Cols, H. J., Marques, R. O., Cristini, P. R.,. "Research on Behaviour of the Irradiated Uranium Silicide for Fission Mo-99 Production." *1995 International Meeting on RERTR*. Paris, France, 1995.

- Conner, C., et al. "Development of Annular Targets for Mo-99 Production." *International Meeting on Reduced Enrichment for Research and Test Reactors*. Budapest, Hungary, 1999.
- Cristini, P. R., H. J. Cols, R. Bavaro, M. Bronca, R. Centurion, and D. Cestau. "Production of Molybdenum-99 From Low Enriched Uranium Targets." *2002 International RERTR Meeting*. Bariloche, Argentina: Republica Argentina: Atomic Energy Commission of Argentina, 2002.
- Dahl, J. J., and E. J. Parma. "Validation and Optimization Testing of a Target Fueled Isotope Production Reactor." *2013 Topical Meeting on Molybdenum-99 Technological Development*. Chicago, Illinois, 2013.
- Diamond, W. T. "A radioactive ion beam facility using photofission." *Nuclear Instruments and Methods in Physics Research Section A: Accelerators, Spectrometers, Detectors and Associated Equipment*, 1999: 471-482.
- Domingos, D. B., et al. "Comparison of Low Enriched Uranium (UALx-Al and U-Ni) Targets with Different Geometries for the Production of Molybdenum-99 in the RMB." *2011 International Nuclear Atlantic Conference*. Belo Horizonte, MG, Brazil, 2011.
- Donlevy, T. M., et al. "Low Enrichment Mo-99 Target Development Program at ANSTO." *2000 International RERTR Meeting*. Las Vegas, Nevada, 2000.
- Duderstadt, James J., and Louis J. Hamilton. *Nuclear Reactor Analysis*. John Wiley & Sons, Inc., 1976.
- Duran, A. "Radionuclide Purity of Fission Mo-99 Produced from LEU and HEU - A Comparative Study." *2005 International RERTR Meeting*. Boston, MA: Argonne National Laboratory, 2005.

- England, T, and B Rider. *Evaluations and compilation of fission product yields*. Technical Report ENDF-349, Los Alamos, NM: Los Alamos National Laboratory, 1992.
- England, T. R., and B. F. Rider. *Evaluation and Compilation of Fission Product Yields*. Los Alamos National Laboratory, 1994.
- European Nuclear Society. "The Medical Isotope Crisis." *European Nuclear Society*, November 2009.
- Evans, R. W. *BWXT Services Medical Isotope Production System Status*. BWX Technologies, Inc., USA, 2008.
- Fouquet, D. M., J. Razvi, and W. Whittemore. "TRIGA research reactors: A pathway to the peaceful applications of nuclear energy." *Nuclear News*, 2003: 46-56.
- Foyto, L., et al. "The University of Missouri Research Reactor HEU to LEU Conversion Project Status." *2012 International Meetin on RERTR*. Warsaw, Poland, 2012.
- Frantz, Stephen G. "Reed College Research Reactor License No. R-112 Docket No. 50-288." Responses to the Request for Additional Information, 2011.
- Glenn, D., A. S. Heger, and W. B. Hladik III. "Comparison of characteristics of solution and conventional reactors for Mo-99 production." *Nuclear Technology*, 1997.
- Harris, D. C. *Quantitative Chemical Analysis (7th ed.)*. China Lake, california: W. H. Freeman and Company, New York, 2007.
- Hartman, M. R., et al. "Neutronic Analysis of the Oregon State TRIGA Reactor in Support of Conversion from HEU Fuel to LEU Fuel." *Nuclear Science and Engineering*, 2013: 135-149.

- Hetherington, E. L.R., and R. E. Boyd. *Targets for the Production of Neutron Activated Molybdenum-99*. IAEA-TECDOC-1065, Vienna: IAEA, 1999.
- Huet, F. "Post Irradiation Examination on UMo full-sized plates - IRIS 2 experiment." Budapest, Hungary, 2005.
- IAEA. *Compilation and Evaluation of Fission Yield Nuclear Data*. Vienna: International Atomic Energy Agency, 2000.
- IAEA. *Consultancy on Conversion Planning for Mo-99 Production Facilities from HEU to LEU*. Vienna, Austria: IAEA, 2010.
- IAEA. *Nuclear Safety Review For the Year 2009*. Vienna: International Atomic Energy Agency, 2010.
- IAEA-TECDOC-1065. "Production Technologies for Mo-99 and Tc-99m." 1999.
- IAEA-TECDOC-1601. *Homogeneous Aqueous Solution Nuclear Reactors for the Production of Mo-99 and other Short Lived Radioisotopes*. Vienna, Austria: International Atomic Energy Agency, 2008.
- IAEA-TECDOC-515. "Fission Molybdenum for Medical Use." *Technical Committee Meeting Organized by the International Atomic Energy Agency*. Karlsruhe: IAEA, 1987.
- Jollay, L., J. Creasy, C. Allen, and G. Solbrekken. "Development, Qualification, and Manufacturing of LEU-Foil Targetry for the Production of Mo-99." *33rd International Meeting on RERTR*. Santiago, Chile, 2011.
- Kim, K., et al. "Development of the Fabrication Technology of Wide Uranium Foils for Mo-99 Irradiation Target by Cooling-roll Casting Method." *26th International Meeting on RERTR*. Vienna, Austria, 2004.
- Knoll, G.F. *Radiation Detection and Measurement*. Ann Arbor, MI: John Wiley & Sons, Inc., 2000.

- Kohut, C., M. De La Fuente, Pl Echenique, and P. Adelfang. "Targets Development of Low Enrichment for the Production of Mo-99 Fission." *2000 International Meeting on Reduced Enrichment for Research and Test Reactors*. Las Vegas, Nevada, 2000.
- Kolar, Z. I., and H. T. Wolterbeek. "Making of Fission Mo-99 from LEU Silicides(s): A Radiochemists' View." *2004 International Meeting on RERTR*. Vienna, Austria, 2004.
- Lamarsh, John R. *Introduction to Nuclear Reactor Theory*. Addison-Wesley Publishing Company, 1975.
- Lewis, D. M. "Mo-99 Supply - the times they are a-changing. ." *European Journal of Nuclear Medicine and Molecular Imaging*, 2009: 1371-1374.
- Lewis, E. E. "Neutron Interactions." In *Fundamentals of Nuclear Reactor Physics*, 29-56. Boston, MA: Elsevier, 2008.
- Lewis, E. E., and W. F. Miller, Jr. *Computational Methods of Neutron Transport*. American Nuclear Society, Inc., 1993.
- Liverhant, S. E. *Elementary Introduction to Nuclear Reactor Physics*. London: Jonh Wiley & Sonc, Inc., 1960.
- Maoliang, L., C. Zuoyong, and D. Qimin. *The Progress Report of Aqueous Homogeneous Reactor for Isotope Production in China*. Chengdu, China: Nuclear Power Institute of China, 2008.
- Marck, S. C., A. J. Koning, and K. E. Charlton. "The options for the future production of the medical isotope 99Mo." *European Journal of Nuclear Medicine and Molecular Imaging*, 2010: 1817-1820.
- Marcum, W. R., B. G. Woods, M. R. Hartman, S. R. Reese, T. S. Palmer, and S. T. Keller. "Steady-State Thermal-Hydraulic Analysis of the Oregon State

- University TRIGA Reactor Using RELAP5-3D." *Nuclear Science and Engineering*, 2009: 261-274.
- Medel, J., and G. Torres. *Neutronic Analysis for the Fission Mo-99 Production by Irradiation of a LEU Target at RECH-1 Reactor*. Santiago, Chile: Chilean Nuclear Energy Commission, n.d.
- Mirzadeh, S., R. E. Schenter, A. P. Callahan, and F. F. (Russ) Knapp, Jr. "Production Capabilities in U.S. Nuclear Reactors for Medical Radioisotopes." Oak Ridge National Laboratory, 1992.
- Mo, S. C. "Production of Mo-99 Using LEU and Molybdenum Targets in a 1 MW TRIGA Reactor." *1993 International Meeting on Reduced Enrichment for Research and Test Reactors*. Oarai, Ibaraki, Japan: Argonne National Laboratory, 1993.
- Mohammad, A., T. Mahmood, and M. Iqbal. "Fission MOLY production at PARR-1 using LEU plate type target." *Nuclear Engineering and Design*, 2009: 521-525.
- Mushtaq, A., M. Iqbal, I. H. Bokhari, and T. Mahmood. "Low enriched uranium foil plate target for the production of fission Molybdenum-99 in Pakistan Research Reactor-1." *Nuclear Instruments and Methods in Physics Research Section B: Beam Interactions with Materials and Atoms*, 2009: 1109-1114.
- Mushtaq, A., M. Iqbal, I. H. Bokhari, T. Mahmood, Z. Ahmad, and Q. Zaman. "Neutronic and thermal hydraulic analysis for production of fission molybdenum-99 at Pakistan Research Reactor-1." *Annals of Nuclear Energy*, 2008: 345-352.
- Mutalib, A., et al. "Full-Scale Demonstration of the Cintichem Process for the Production of Mo-99 Using a Low-Enriched Target." *1998 International*

*Meeting on Reduced Enrichment for Research and Test Reactors.* Sao Paulo, Brazil, 1998.

NAS. *Medical Isotope Production Without Highly Enriched Uranium.* The National Academy of Sciences, Committee on Medical Isotope Production Without Highly Enriched Uranium, 2009.

Natural Resources Defense Council. *Nuclear Facts.* Washington, D.C.: Natural Resources Defense Council, 2007.

NECSA. *Media Release: Nuclear Reactor Uses Only Low Enriched Uranium (LEU) for the First Time.* Pelindaba, South Africa: NECSA, 2009.

NNDC. "Evaluated Nuclear Structure Data File (ENSDF)." National Nuclear Data Center, n.d.

NNSA. "International Safeguards: Challenges and Opportunities for the 21st Century." *National Nuclear Security Administration.* September 9, 2008. [http://nnsa.energy.gov/sites/default/files/nnsa/inlinefiles/NGSI\\_Report.pdf](http://nnsa.energy.gov/sites/default/files/nnsa/inlinefiles/NGSI_Report.pdf) (accessed August 30, 2011).

NNSA, and ANSTO. "Global initiative to combat nuclear terrorism: Workshop on the production of Mo-99 using low enriched uranium." Sydney, Australia, 2007.

Oregon State University. *OSTR Safety and Analysis Report Chapter 4.* Oregon State University, n.d.

Ottinger, C. L., and E. D. Collins. *Assessment of Potential ORNL Contributions to Supply of Molybdenum-99.* ORNL/TM-13184, Oak Ridge: Oak Ridge National Laboratory, 1996.

Parma, Edward J., Richard L. Coats, and James J. Dahl. *Sandia National Laboratories Medical Isotope Reactor Concept.* Albuquerque, New Mexico: SNL, 2010.

- Pavshook, V. *Effective Method of Mo-99 and Sr-89 Production Using Liquid Fuel Reactor*. Russian Federation: Russian Research Center, Kurchatov Institute, 2008.
- Ponsard, B. "Production of radioisotopes in the BR2 high-flux reactor for applications in nuclear medicine and industry." *Journal of Labelled Compounds and Radiopharmaceuticas*, 2007: 333-337.
- Salacz, J. *Production of fission Mo-99, I-131, and Xe-133*. Fleurus, Belgium: The National Institute for Radioelements, 1985.
- Salikhbaev, U. S., S. Khujaev, S. A. Baytelesov, F. R. Kungurov, and A. Boltabaev. "Possibility of Production of Molybdenum-99 Using Neutron Activation at the WWR-SM Research Reactor with LEU Fuel." *33rd International Meeting on RERTR*. Santiago, Chile, 2011.
- Sameh, A. A., and A. Bertram-Berg. "HEU and LEU MTR Fuel Elements as Target Materials for the Production of Fission Molybdenum." *1992 International Meeting on RERTR*. Roskilde, Denmark, 1992. 313-333.
- Sayareh, R., M. Ghannadi Maragheh, and M. Shamsaie. "Theoretical calculations for the production of Mo-99 using natural uranium in Iran." *Annals of Nuclear Energy*, 2003: 883-895.
- Schrader, R., et al. "Progress in Chile in the development of the fission Mo-99 production using modified CINTICHEM." *2007 International RERTR Meeting*. Prague, Czech Republic, 2007.
- Sears, D., and K. Conlon. *Development of LEU Fuel to Convert Research Reactors: NRU, MAPLE, and SLOWPOKE*. Atomic Energy of Canada Limited (AECL), 2006.
- Segre, E., and C. S. Wu. "Some Fission Products of Uranium." *Physical Review*, 1939: 552.

- Shultis, J. K., and R. E. Faw. *An MNCP Primer*. Manhattan: Department of Mechanical and Nuclear Engineering, Kansas State University , 2004.
- Smaga, J. A., et al. "Electroplating Fission-Recoil Barriers onto LEU-Metal Foils for Mo-99 Production Targets." *XXth International Meeting on Reduced Enrichment for Research and Test Reactors*. Argonne National Laboratory, 1997.
- Solbrekken, G. L., A. S. El-Gizawy, and C. Allen. "Engineering Design of LEU Foil Based Target for High Volume Production of Mo-99." *30th International Meeting on RERTR*. Washington D.C., 2008.
- Song, X., and W. Niu. *Optimization of 200 kW Medical Isotope Production Reactor Design*. Nuclear Power Institute of China, Sichuan Nuclear Society, 2008.
- Takacs, S., Z. Szucs, F. Tarkanyi, A. Hermanne, and M. Sonck. "Evaluation of proton induced reactions on Mo-100: New cross sections for production of Tc-99m and Mo-99." *Journal of Radioanalytical and Nuclear Chemistry*, 2003: 195-201.
- Todreas, Neil E., and Mujid S. Kazimi. *Nuclear Systems I*. New York: Taylor & Francis Group, 1990.
- TRIUMF. *Making Medical Isotopes: Report of the Task Force on Alternatives for Medical-Isotope Production*. Vancouver: University of British Columbia, Advanced Applied Physics Solutions, Inc., 2008.
- Van der Schaaf, B, and P.G.T De Jong. "PALLAS: the new nuclear research reactor in the Netherlands." *Nucleaire Geneeskunde*, 2010: 624-628.
- Van Sonnenberg, Clint. "FDA clears Covidiens low-enriched uranium based isotope production." *Health Imaging*, March 11, 2011.

- Vandegrift, G. F., et al. *Converting Targets and Processes for Fission-Product Mo-99 From High- to Low-Enriched Uranium*. Chapter for IAEA TECDOC, IAEA, 1997.
- Vandegrift, G. F., Conner, C., Hofman, G. L., Snelgrove, J. L., Mutalib, A., Purwadi, B. Adang, H. G., Hotman, L., Kadarisman, Sukmana, A., Dicky, T. J., Sriyono, Suropto, A., Lutfi, D., Amin, D. L., Basiran, A., Gogo, A., Sarwani, Taryo, T. "Demonstration of Mo-99 Production Using LEU Metal-Foil Targets in the Cintichem Process." *1999 International Meeting on Reduced Enrichment for Research and Test Reactors*. Budapest, Hungary, 1999.
- Vandegrift, G. F., Chaiko, D. J., Heinrich, R. R., Kucera, E. T., Jensen, K. J., Poa, D. S., Varma, R., Vissers, D. R. . "Preliminary Investigations for Technoogy Assessment of Mo-99 Production From LEU Targets." *1986 International Meeting on Reduced Enrichment for Research and Test Reactors*. Gatlinburg, Tennessee: Argonne National Laboratory, 1986.
- Verbeek, Pierre. *Report on Molybdenum 99 Production for Nuclear Medicine 2010 - 2020*. Association of Imaging Producers & Equipment Suppliers (European Industrial Association for Nuclear Medicine and Molecular Healthcare), 2008.
- Vernon, Milton E. "Mo-99 Production Utilizing Target-only Reactor Design." *2013 Topical Meeting on Molybdenum-99 Technological Development*. Chicago, Illinois, 2013.
- Wienczek, T. C., G. F. Vandegrift, A. Bakel, A. Leyva, and A. S. Hebden. "Status and Progress of Foil and Target Fabrication Activities for the Production of Mo-99 from LEU." *30th International meeting on Reduced Enrichment for Research and Test Reactors*. Washington D. C., 2008.

X-5 Monte Carlo Team. *MCNP - A General Monte Carlo N-Particle Transport Code, Version 5, Volume 1: Overview and Theory*. Los Alamos National Security, LLC, 2003.

X-5 Monte Carlo Team, Vol 2. *MCNP - A General Monte Carlo N-Particle Transport Code, Version 5, Volume 2: User's Guide*. Los Alamos National Security, LLC, 2003.

Zuoyong, C., L. Maoliang, D. Qimin, and Z. Jinsong. *Preliminary Study of Mo-99 Extraction Process from Uranyl-Nitrate Fuel Solution of Medical Isotope Production Reactor*. Chengdu, China: Nuclear Power Institute of China, 2008.